



Norwegian University of
Science and Technology

Applications of the Goldstone equivalence theorem to scattering and decay processes

Petter Taule

MSc in Physics

Submission date: June 2018

Supervisor: Michael Kachelriess, IFY

Norwegian University of Science and Technology
Department of Physics

Abstract

We study applications of the Goldstone boson equivalence theorem to decay and scattering processes, exemplifying the broken gauge theory structure of electroweak interactions. Apart from interest on theoretical grounds, we are motivated by the problem of the dark matter identity, and the importance of electroweak bremsstrahlung contributions to dark matter annihilation. Higgs decay into charged gauge bosons is approached using four separate methods, including the utilisation of the equivalence theorem, and we show that the results of all approaches agree. Furthermore, the equivalence theorem is applied to electroweak bremsstrahlung corrections in the specific process of quark production from electron-positron annihilation. We find that the emission of the Goldstone boson intrinsically has the appropriate high-energy behaviour, in contrast to the longitudinal component of the massive gauge boson. Thus, the equivalence theorem necessitate a cancellation of the longitudinal contributions from all sub-processes at a given order in perturbation theory.

Sammendrag

Vi ser på anvendelser av Goldstone-boson-ekvivalensteoremet på desintegrasjon- og spredningsprosesser, som eksemplifiserer den brutte, justerinvariante strukturen til elektrosvak teori. Utover teoretisk interesse, motiveres vi av det ubesvarte spørsmålet om mørk materie, samt betydningen av elektrosvak bremsestråling i mørk-materie-annihilasjon. Desintegrasjon av Higgs-bosonet til ladede justerbosoner studeres ved hjelp av fire forskjellige metoder, deriblant ved hjelp av ekvivalensteoremet, og vi viser hvordan resultatene fra de forskjellige metodene samsvarer med hverandre. I tillegg anvender vi ekvivalensteoremet på elektrosvake bremsestrålingskorreksjoner til kvark-produksjon fra elektron-positron-annihilasjon. Vi finner at emisjonen av Goldstone-bosonet har iboende akseptabel høyenergiopptørrelse, i motsetning til den longitudinale komponenten til det massive justerbosonet. Dermed nødvendiggjør ekvivalensteoremet kanselleringen av longitudinale bidrag fra alle delprosesser i en gitt orden i perturbasjonsteori.

Preface

This thesis is the product of research conducted during the final semesters of the two-year Master Program in Physics at the Norwegian University of Science and Technology (NTNU). I would like to thank my supervisor Prof. Michael Kachelrieß for his profound insight and invaluable guidance throughout the duration of the project. Gratitudes are also extended to Ole Martin Kringlebotn for proofreading and valuable feedback. I am grateful to my fellow students, in particular Håvard, Haakon, Oda, Frode and Lars, for great companionship both at and outside the University. Finally, many thanks go to my family for support and encouragement.

A handwritten signature in black ink, reading "Petter Taule". The signature is written in a cursive style with a large, sweeping initial 'P'.

Petter Taule
Trondheim, Norway
June 2018

Contents

Abstract	i
Sammendrag	iii
Preface	v
Abbreviations	ix
1 Introduction	1
2 Dark matter	3
2.1 Evidence	3
2.2 Candidates	6
2.3 Detection	9
2.4 Bremsstrahlung processes	10
3 Theoretical preliminaries	13
3.1 Quantum chromodynamics	13
3.2 Glashow-Salam-Weinberg model	15
3.3 Goldstone boson equivalence theorem	22
3.4 Polarisation sums	24
4 Electron-positron annihilation	29
4.1 Hadronisation	29
4.2 Leading order process	30
4.3 Real gluon emission	35
4.4 Virtual gluon exchange	39
4.5 Combined $\mathcal{O}(\alpha_s)$ correction	43
5 Four approaches to Higgs decay	45
5.1 Unitary gauge	45
5.2 Goldstone boson equivalence theorem	47
5.3 Feynman-'t Hooft gauge	48
5.4 Charged boson loop	50

6 Electroweak bremsstrahlung corrections	57
6.1 Explicit calculations	57
6.2 Discussion	63
7 Summary and outlook	65
A Mathematical conventions and formulae	67
B Feynman rules	71
C Kinematics of scattering and decay	75

Abbreviations

- CMB** cosmic microwave background. 5, 8
- CoM** center-of-momentum. 38, 46, 47, 75–78
- DM** dark matter. i, vii, 1–12, 65, 66
- DR** dimensional regularization. 29, 30, 34, 35, 40, 41, 52, 65, 68, 69, 75
- EQT** Goldstone boson equivalence theorem. i, vii, 2, 22, 23, 45, 47, 48, 57, 61–63, 65
- GSW** Glashow-Salam-Weinberg. vii, 2, 15, 17, 19, 21, 22, 25, 64
- IR** infrared. 2, 29, 30, 35, 37, 40, 43, 44, 63, 65
- KLN** Kinoshita-Lee-Nauenberg. 44, 65
- LSP** lightest supersymmetric particle. 8
- MACHO** massive compact halo object. 6
- MSSM** minimal supersymmetric standard model. 11
- QCD** quantum chromodynamics. vii, 2, 8, 13–15, 29, 32, 35, 44, 64, 65, 72
- QED** quantum electrodynamics. 15, 31–33
- QFT** quantum field theory. 1, 33, 44, 51, 65, 67
- SM** Standard Model. 1, 7–10, 15, 18, 19, 66, 71
- SSB** spontaneous symmetry breaking. 1, 2, 15–17, 20–22
- SUSY** supersymmetry. 7, 8, 66
- UV** ultraviolet. 40, 43, 50, 52, 54, 55
- vev** vacuum expectation value. 9, 16, 17, 20
- WIMP** weakly interacting massive particle. 6, 7, 9

1 Introduction

The Standard Model of particle physics currently represents the best framework for describing nature at its fundamental level [1]. It categorises all known elementary particles and describe their interactions via three of the four known fundamental forces.

On the theory side, the Standard Model is a quantum field theory, exhibiting interesting physics such as local gauge invariance, spontaneous symmetry breaking, anomalies and asymptotic freedom. Nevertheless, the applicability of a theory is not established by how interesting it is, but rather on its explanatory and, perhaps most important, predictive power. Fortunately, theoretical predictions from the Standard Model have resulted in perhaps the best agreement between prediction and experiment in the history of science [2]. Examples of predictions which have been experimentally verified to a high degree of accuracy are: (i) the value of the electron magnetic moment, which agrees with the value measured experimentally to eight significant figures [3, 4], (ii) the existence of the massive weak gauge bosons W and Z and their properties [5, 6], and (iii) the existence of the Higgs boson [7].

On the other hand, it is apparent that the Standard Model is not the full story in terms of a complete theory of fundamental interactions. Indeed, it only accounts for about 5% of the content of the universe, according to the Λ CDM (Lambda Cold Dark Matter)-model of cosmology [8]. The rest of the universe consists of dark matter ($\sim 26\%$) and dark energy ($\sim 68\%$), whose identities remain great unresolved mysteries of cosmology [9–13]. In addition, the model does not incorporate a description of gravity, since there are no consistent quantum theory of gravity yet. Other issues which presumably require physics beyond the Standard Model include observed neutrino oscillations [14, 15] and the hierarchy problem [16].

The model describes the electromagnetic, weak and strong interactions by gauge groups, where the force carriers are gauge fields. In 1954, C. Yang and R. Mills generalised the gauge invariance of electromagnetism to construct a non-abelian gauge theory [17], which motivated the search for non-abelian gauge theories describing the weak and strong interactions. In light of this, S. Glashow, A. Salam and J. Ward combined electromagnetism and weak interactions using a $SU(2) \otimes U(1)$ group structure in the early 1960s [18, 19]. In 1967, S. Weinberg incorporated the Higgs mechanism to explain the masses of the gauge fields W and Z , giving electroweak theory its present-day form [20]. The Higgs mechanism is the description of how gauge bosons acquire mass by absorbing (“eating”) the Goldstone bosons from spontaneous symmetry breaking [21–23].

The fact that the theory of electroweak interactions is a broken gauge theory, has interesting consequences, which we investigate in this thesis. In particular, we study the Goldstone boson equivalence theorem and applications of it. The theorem was first proven by Cornwall et al. [24], and essentially states that at energies much higher than the scale set by spontaneous symmetry breaking, the unbroken theory becomes an accurate description. The longitudinal degree of freedom of the massive gauge boson, which was obtained through the Higgs mechanism, becomes distinct and equivalent with the Goldstone boson from which it originated.

In addition to the equivalence theorem being interesting in its own right, our motivation for studying it is the question of the dark matter identity. An important probe for dark matter properties is indirect searches, where one uses observations of radiation (presumably) coming from dark matter annihilation to construct and constrain theoretical models of potential dark matter particles [11]. The significance of electroweak corrections to such models has been studied and acknowledged by several publications [25–36], and remain to be of interest. For a dark matter candidate considerably heavier than the weak scale, the equivalence theorem becomes applicable for those kinds of radiative corrections, and can simplify calculations to a great extent in many cases.

Structure of thesis

The thesis consists of seven chapters including this introduction and the conclusion, as well as three appendices. Below, we outline the contents of each chapter.

In Chapter 2, we review the current understanding of dark matter including cosmological evidence and proposed candidates. Also, the importance of electroweak bremsstrahlung to dark matter annihilation is discussed. Chapter 3 lays the fundamental theoretical groundwork for this research, introducing quantum chromodynamics, the Glashow-Salam-Weinberg model and finally, the equivalence theorem. Moving on to concrete calculations, Chapter 4 revisits the standard computation of electron-positron annihilation to hadrons at next-to-leading order in quantum chromodynamics. We show how the arising infrared divergences cancel at that order, and introduce a convenient formalism for computing s-channel processes which is also used later in the thesis. In Chapter 5, we consider Higgs decay to charged gauge bosons, and compute the decay rate using several methods including the equivalence theorem. The various approaches to the calculation illustrate multiple features of electroweak theory. Finally, in Chapter 6, we apply the equivalence theorem to a W bremsstrahlung diagram and compare the total cross section to that from a “standard” calculation.

In Chapter 7, we conclude. Mathematical conventions used in the thesis as well as relevant mathematical formulae are presented in Appendix A. In Appendix B we list the relevant Feynman rules used in our calculations, and Appendix C derives kinematics for scattering and decay processes.

2 Dark matter

The identity of dark matter (DM) is one of the great unresolved problems in particle physics and cosmology [9–12]. Despite great amount of cosmological evidence pointing to its existence, the nature of the DM particle has yet to be determined. In this chapter, we give a brief review of the current knowledge about DM, including the cosmological indications, the most promising candidates, methods of detection, and finally, the importance of electroweak corrections to DM annihilation.

2.1 Evidence

Rotation curves

Observations of rotation curves of nearby galaxies provides some of the most direct and convincing evidence for DM. Rotation curves are graphs of rotational velocities of stars and gas as a function of distance to the galaxy center. From Newtonian dynamics we expect that the rotational velocity is given by

$$v(r) = \sqrt{\frac{GM(r)}{r}} \quad (2.1)$$

where G is the gravitational constant and $M(r)$ is the total mass enclosed within radius r . In particular, we expect a $1/\sqrt{r}$ -dependence beyond the bulk of the luminous matter. However, observed rotation curves show a flat behaviour at large distances, suggesting a non-luminous component with $M(r) \propto r$. Figure 2.1 from Ref. [37] shows a rotation curve for a collection of galaxies that fall into a luminosity interval centered around $\langle M_I \rangle = -20.9$. The horizontal axis is normalised against an appropriate length scale R_{opt} , defined as the radius containing the bulk of the optical disk. Correspondingly, the vertical axis is scaled in terms of the measured velocity at R_{opt} . Indeed, we see an approximately constant velocity beyond R_{opt} . The dashed line shows the required contribution of the dark component to account for the measured rotation velocities.

Gravitational lensing

According to general relativity, light propagates along geodesics of spacetime, and gets bent when passing a massive object. Therefore, large concentrations of mass act

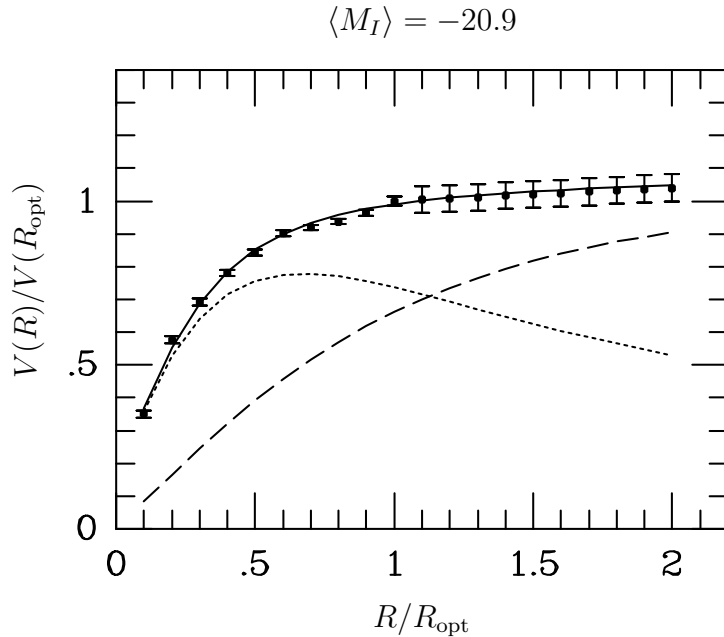


Figure 2.1: Universal rotation curve for galaxies associated with a luminosity bin centered around $\langle M_I \rangle = -20.9$ from Ref. [37]. The dotted line shows the contribution from the luminous disk, while the dashed line shows the dark halo.

as lenses deflecting passing light. The angle of deflection is proportional to the mass of the structure responsible for the lensing [38]. We divide the gravitational lensing effects into three classes [39]:

- 1) *Strong lensing*. The images of distant objects are clearly visibly distorted, we observe for instance multiple images, arcs or Einstein rings.
- 2) *Weak lensing*. The distortion of an object is hard to distinguish from the intrinsic shape of the object (e.g. subtle stretching of an elliptic galaxy). However, taking an average over large ensembles of galaxies, the lensing effect shows up statistically.
- 3) *Galactic microlensing*. No distortion is observed or statistically inferred, but the light from a background object changes in time. A transient lensing object passes in-between source and observer, and gives a characteristic light curve.

We can use gravitational lensing of a distant object to make a map of the mass distribution between the object and the observer. Comparing this to the mass distribution of observed luminous objects provides sound indications of the presence of non-luminous matter. Perhaps the best evidence for DM is the observations of the

collision of the galaxy clusters 1E0657-558 [40]. X-ray observations of the collision show that intergalactic gas collided and interacted, while observations by visible light show that the stars of the galaxies were insignificantly affected, although slowed down by gravity. The intergalactic gas make up most of the baryonic matter, but the mass distribution derived from gravitational lensing demonstrates that the dominant mass component follows the stars throughout the collision, not the gas. This suggests that the dominant component is non-luminous and non-interacting, which, by definition, is DM.

Galaxy clusters

The signature of DM becomes eminent at distance scales of galaxies and clusters of galaxies, as we have seen above. One of the first indications for DM came from an estimation of the mass-to-light ratio of the Coma cluster, by F. Zwicky in 1933 [41]. Using the virial theorem in combination with measurements of the dispersion of radial velocities, he inferred a mass-to-light ratio of around 400 solar masses per solar luminosity. Today, we have additional methods for measuring the mass of a cluster, including gravitational lensing and the examination of X-ray profiles from hot gas in the cluster. These methods are generally in agreement that visible matter constitute around 20–30 % of the total mass on cluster scales [11].

Cosmic microwave background

The evidence for DM we have presented so far, do not let us determine the total amount of DM in the universe. This information can be obtained from observations of the cosmic microwave background (CMB). The CMB is radiation from the last-scattering-surface of the early universe. When electrons and protons combined into hydrogen, photons decoupled from matter and have been propagating freely throughout the universe ever since. These photons are the CMB radiation. The spectrum is very close to a black-body with temperature 2.726 K and isotropic at the 10^{-5} level. However, density fluctuations on the last-scattering-surface leads to anisotropies in the CMB. These anisotropies are usually expanded in the spherical harmonics, and the variance of the coefficients are plotted against the angular scale defined by the expansion. The form of this power spectrum provides a good testing mechanism for cosmological models, and it puts rigid constraints on the cosmological parameters. We do not present the justification of this statement here; an introduction to the subject can be found in e.g. Ref. [42].

Measurements of the CMB performed by the Planck satellite constrain the various

energy density parameters of the universe to be [8]:

$$\Omega_b h^2 = 0.022\,25 \pm 0.000\,16, \quad (2.2a)$$

$$\Omega_{\text{DM}} h^2 = 0.1198 \pm 0.0015, \quad (2.2b)$$

$$\Omega_\Lambda = 0.6844 \pm 0.0091, \quad (2.2c)$$

where $\Omega_i = \rho_i/\rho_c$ is the abundance in units of the critical density ρ_c . The critical density corresponds to a flat universe, and the fact that the data sums up to $\Omega_{\text{tot}} \simeq 1$ suggests that our universe is indeed flat or nearly flat. The reduced Hubble parameter is defined as $h = H_0/(100 \text{ km s}^{-1} \text{ Mpc}^{-1}) = 0.6727 \pm 0.0066$ [8]. Finally, the abundances Ω_b , Ω_{DM} and Ω_Λ are defined for the baryonic matter, dark matter, and dark energy, respectively. We see that the baryonic matter only contributes $\sim 19\%$ of the total matter in the universe, implying that the dark component is dominating.

2.2 Candidates

A vast number of possible DM particle candidates have been proposed.¹ The candidates can firstly be divided into baryonic and non-baryonic. The main baryonic candidate is the massive compact halo objects (MACHOs), which are small astrophysical objects that emit little or no light, e.g. dead stars. These MACHOs are mostly ruled out as potential DM candidates, however: Searches for microlensing events of the Large Magellanic Cloud constrain the MACHO abundances to a tiny fraction of the DM [44, 45].

Among the non-baryonic candidates, an important distinction is that between *hot* or *cold* candidates [9]. Hot DM candidates were moving relativistically in the early universe, while cold candidates moved non-relativistically. The distinction has decisive consequences for models of structure formation.

In this section, we present some of the most promising non-baryonic DM candidates.

Weakly interacting massive particles

The weakly interacting massive particles (WIMPs) constitute a class of hypothetical particles with mass in the 10 GeV–TeV range that only interact with the weak gauge bosons, and not gluons or photons. WIMPs are non-baryonic and cold, and they are perhaps the most studied DM candidates. In addition to being a DM candidate, the gauge hierarchy problem (essentially why the Higgs mass is much smaller than the

¹There are also models which attempt to explain the cosmological phenomena attributed to DM without the introduction of one or more new particles, e.g. Modified Newtonian Dynamics (MOND) [43]. We do not discuss them in this text.

Planck mass) is a noteworthy motivation for the WIMPs, because typical attempts to alleviate the problem involve new particles at the weak scale [12].

The formation history of the WIMPs is well understood, if it was produced as a thermal relic of the Big Bang. In the beginning, the universe is dense and hot. In particular, the temperature is larger than the WIMP mass, $T > m_\chi$, and the annihilation rate is large compared to the expansion rate of the universe. The WIMPs remain in equilibrium. Subsequently, the universe cools to temperatures below m_χ , and the abundance of the DM particle becomes Boltzmann suppressed; it drops by a factor proportional to $\exp(-m_\chi/T)$. This would lead to a vanishing abundance, if it were not for the simultaneous expansion of the universe. The WIMP annihilation drops dramatically because the particles are more and more dilute, thus stabilising the abundance. This is known as *freeze-out*.

The process is described quantitatively by the Boltzmann equation,

$$\frac{dn}{dt} = -3Hn - \langle\sigma_{Av}\rangle (n^2 - n_{\text{eq}}^2), \quad (2.3)$$

which express the time evolution of the number density n of WIMPs. The first term on the right hand side accounts for the expansion of the universe, where $H = \dot{a}/a$ is the Hubble expansion rate. If there were no interactions, this would be the only term and the solution would be $n \propto a^{-3}$, as expected. In the second term, the n^2 -term arises from WIMP annihilation processes, while n_{eq}^2 accounts for the reverse processes. The $\langle\sigma_{Av}\rangle$ -factor is the thermally averaged total cross section for annihilation of WIMPs. At early times, the expansion term is negligible compared to the creation and destruction terms, so the density is at equilibrium. Freeze-out is defined by $H = n\langle\sigma_{Av}\rangle$. Using an analytic approximation to the Boltzmann equation, as well as entropy considerations, the relic density of DM today is found to be [9]

$$\Omega_{\text{DM}}h^2 \approx \frac{3 \times 10^{-27} \text{ cm}^3\text{s}^{-1}}{\langle\sigma_{Av}\rangle}. \quad (2.4)$$

From Eq. (2.2) we have $\Omega_{\text{DM}}h^2 \approx 0.11$ which requires a thermally averaged cross section

$$\langle\sigma_{Av}\rangle \approx 3 \times 10^{-26} \text{ cm}^3\text{s}^{-1}. \quad (2.5)$$

Nevertheless, this result arose from a rough analysis, and there are several effects that could lead to thermal relic DM having a higher or lower cross section. Moreover, it is not certain that DM is indeed a thermal relic.

One of the well-motivated theoretical frameworks for beyond the Standard Model (SM) physics is supersymmetry (SUSY). SUSY theories typically provide elegant solutions to the gauge hierarchy problem, because new weak-scale physics is introduced [12]. In SUSY extensions of the SM, all fermions of the SM have a new (as of now undiscovered) bosonic partner particle, and vice versa. Thus, several DM candidates arise in this framework. We do not discuss details of supersymmetry here,

reviews can be found in e.g. [9, 11, 46]. Many SUSY theories feature a symmetry called R -parity, defined as $R = (-1)^{3B+L+2s}$, where B , L and s are baryon number, lepton number and spin, respectively. SM particles have $R = 1$ while SUSY particles have $R = -1$, so if R -parity is conserved, the lightest supersymmetric particle (LSP) must be stable and can only annihilate into SM particles. Hence, the LSP is a good DM candidate.

In the larger parts of most SUSY models' parameter spaces, the LSP is the neutralino. It is a linear combination of the supersymmetric partners of the electroweak gauge bosons and the Higgs bosons (for technical reasons, there are two Higgs bosons in SUSY models). It is a spin-1/2 Majorana fermion, and its Majorana nature leads to helicity suppression for annihilation into SM fermions, which we discuss in Section 2.4.

Sterile neutrinos

SM neutrinos have decidedly been ruled out as DM candidates, because of their light mass and low abundance. CMB data from the Planck satellite strongly constrain the SM neutrino abundance to $\Omega_\nu h^2 < 0.0063$ [8], which is less than 6% of the total DM abundance.

Sterile neutrinos are right-handed neutrinos which do not interact through the SM apart from mixing. In the SM, neutrinos are massless, but observation of neutrino oscillations imply neutrino masses [14, 15]. Adding sterile neutrinos lets neutrinos acquire mass through Yukawa couplings similar to the other fermions, which may be the explanation of neutrino masses. Additionally, a gauge-invariant, so-called Majorana mass term involving only sterile neutrinos can be added to the SM Lagrangian. Then, the mass eigenstates follows from diagonalizing the resultant mass matrix. Assuming neutrino Yukawa couplings of order $y \sim \mathcal{O}(1)$, one obtains the desired light neutrino masses if the sterile neutrino masses are large, typically $M \sim 10^{14}$ GeV. This is called the see-saw mechanism. Sterile neutrinos at this scale seem unlikely DM candidates [12]. Nonetheless, there is no compelling reason to assume a Yukawa coupling of order $\mathcal{O}(1)$, so a possible DM candidate might be light sterile neutrinos.

There are a number of ways sterile neutrinos may have been produced. Possibilities include production through neutrino oscillations [47], or from decays of heavier particles [48]. Furthermore, the abundance may be enhanced if the universe has a non-zero lepton asymmetry [49].

Axions

Axions are particles postulated as a potential solution to the strong CP problem in quantum chromodynamics (QCD). In the QCD Lagrangian, there is a charge-parity violating term proportional to a parameter θ . This term gives a large contribution to the electric dipole moment of the neutron, $d_e \sim 10^{-16} e$ cm, but measurements

constrain the dipole moment to be $d_e < 10^{-26} e \text{ cm}$ [50]. It follows that the parameter must be remarkably small. The axion solution to this problem is to add fields to the SM yielding an anomalous U(1) symmetry. The symmetry is spontaneously broken, and the associated Goldstone boson is called the axion [51–53]. This leads to a small value of θ .

Axions have interactions with gluons, fermions, and photons. It may decay into a pair of photons, and the lifetime of this process constrains the axion mass to $m_a \lesssim 20 \text{ eV}$ if the axions are to live longer than the universe. Further limits from cosmological observations imply $m_a \lesssim 10 \text{ meV}$ [54].

Axion DM also has several possible production mechanisms. Thermal production implies a relic density of $\Omega_a \sim 0.22(m_a/80 \text{ eV})$, but the lifetime constraint mentioned above implies that this mechanism cannot produce axion abundance corresponding to the observed DM abundance [12]. Nevertheless, there are non-thermal production mechanisms, for example through spontaneous symmetry breaking when the temperature is of the same order as the vacuum expectation value (vev). This is called a Peccei-Quinn phase transition, and whether this transition happened before or after inflation gives different constraints on the axion parameters [55]. The allowed parameters typically imply that axions are light and weakly-interacting, making them a viable DM candidate.

2.3 Detection

Efforts to detect DM can primarily be divided into indirect and direct detection methods.

Indirect detection attempts to probe DM by observable flux of SM particles produced in its annihilation or decay. Regions where presumably large amounts of DM accumulate seem like reasonable places to look at, since the annihilation rate is probably high. Such regions are for example the center of the galaxy, or even near smaller objects like the Sun or the Earth, where DM particles lose energy due to scattering [11]. The indirect detection methods can be used to constrain the DM annihilation cross section, and if we assume that DM is the lightest beyond-the-SM particle, it will exclusively annihilate into SM particles. If an observed signal is to be attributed to DM annihilation, there should be no astrophysical explanation, and a specific DM model should be able to reproduce the correct annihilation rate. Examples of such signals which may be ascribed directly or indirectly to DM annihilation are: (i) observation of positron excess compared to conventional production models by the Fermi and PAMELA satellites [56, 57] and (ii) detection of high-energy (PeV) neutrinos by the IceCube telescope [58].

If WIMPs constitute DM and our galaxy is filled with them, numerous amounts should be passing through the Earth. Direct detection methods aim to observe recoils of nuclei induced by interactions with DM. The event rate is expected to be

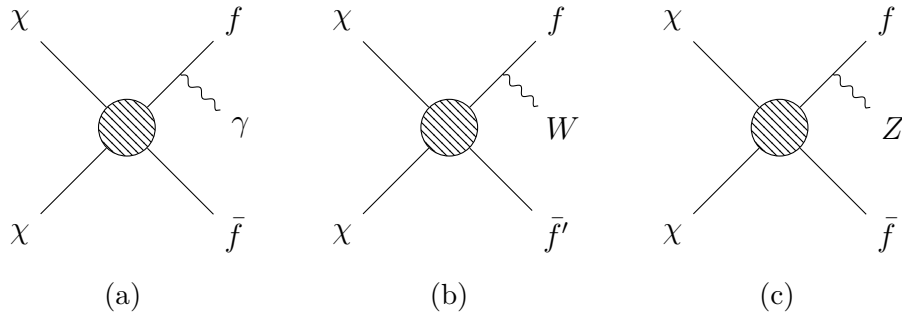


Figure 2.2: Bremsstrahlung corrections to DM annihilation into SM particles.

low, so to do this effectively it is essential to minimize background noise. Therefore the experiments operate deep underground to avoid interference from cosmic rays. Furthermore, a possible signal can be distinguished from the background by looking for an annual variation due to Earth’s motion around the Sun, since the velocity and orientation of the detector relative to the DM halo in our galaxy will vary [59]. Ongoing experiments include XENON [60], EDELWEISS [61], SuperCDMS [62] and DAMA/LIBRA [63].

Other detection methods include collider searches. In a collider experiment a DM signal would be missing energy, since the particle will (presumably) escape the detector. As of yet, no evidence for DM production at a collider have appeared.

2.4 Bremsstrahlung processes

Annihilation of DM to SM particles will necessarily be accompanied by radiative corrections on the form of *bremstrahlung* (brake radiation), where a gauge boson is emitted from intermediate (internal *bremstrahlung*) or final (external *bremstrahlung*) state particles, see Fig. 2.2. Photon *bremstrahlung* from DM annihilation have important consequences since the observed gamma ray flux imposes constraints on the model in question [64–66]. For example, so-called *leptophilic* models where DM mainly annihilates into leptons have been proposed to explain the observed positron excess mentioned in Section 2.3, see e.g. Ref. [67]. These models typically require boost factors [68], but the accompanying production of photons might violate observational constraints on the gamma ray flux.

Another class of *bremstrahlung* corrections to DM annihilation is *electroweak bremstrahlung*, where massive W or Z bosons are radiated from the intermediate or final state. Its importance has been recognised and investigated in several publications: Ref. [25] calculates neutralino annihilation into three massive particles, and Ref. [26] considers superheavy DM annihilation and consequences of the following electroweak cascade. External *bremstrahlung* from leptonic final states are studied in Refs. [27–31], while internal *bremstrahlung* is the topic of Refs. [32–34]. Finally,

Ref. [35] considers final state radiation of weak gauge bosons or Higgs bosons in the minimal supersymmetric standard model (MSSM). Electroweak bremsstrahlung has noteworthy phenomenological consequences since the decay of W or Z leads to production of photons, hadrons or leptons, regardless of the direct DM couplings [36]. Thus, even if for instance the DM particle only annihilates to neutrinos, gamma rays and hadrons will be produced.

Helicity suppression

Photon and electroweak bremsstrahlung play major roles in certain DM models. If the annihilation into a light fermion pair is *helicity suppressed*, this suppression is often lifted by photon or electroweak bremsstrahlung and these channels become the dominant ones. We discuss shortly the origin of this suppression in the following; a thorough analysis can be found in e.g. Ref. [35].

The thermal averaged cross section for a non-relativistic species can be expanded in even powers of the Møller velocity [69],

$$\langle\sigma v\rangle = a + bv^2 + \dots . \quad (2.6)$$

It can further be shown that the a arises from s -wave annihilation, while b corresponds to both s - and p -wave channels. For a dark matter halo today, we have $v \sim 10^{-3}c$ so the second term is strongly suppressed. Thus, the s -wave is the only unsuppressed contribution to the annihilation rate today.

Consider a pair of Majorana DM particles (e.g. the neutralino mentioned in Section 2.2) annihilating into a Dirac fermion pair. An initial state of two identical Majorana fermions must be antisymmetric, and since the spacial wave function is symmetric for an s -wave contribution ($L = 0$), the spin wave function must be antisymmetric. Hence, the spin wave function is the antisymmetric singlet $S = 0$. Moreover, for a fermion pair we have the following general expressions for charge conjugation and parity:

$$C = (-1)^{L+S} \quad \text{and} \quad P = (-1)^{L+1}. \quad (2.7)$$

It follows that the initial state has $C = 1$ (as required for a Majorana pair) and $P = -1$. Assuming CP invariance, the final state must necessarily have $J_{CP} = 0_-$. Since $CP = (-1)^{L+S}(-1)^{L+1} = (-1)^{S+1}$, the final state fermion pair must therefore also be in the singlet state $S = 0$. Combined with the fact that the fermions are produced back-to-back, we conclude that they have the same helicity.

A theory of massless fermions exhibits chiral symmetry, where left-handed and right-handed fermions transform independently, and chirality and helicity are equivalent quantities. Accordingly, a fermion-antifermion pair has the same chirality and opposite helicity. From the discussion above, it follows that the annihilation of DM Majorana particles into Dirac fermions is only possible if chiral symmetry is broken, for example

through a Dirac mass term in the Lagrangian. Therefore, we can conclude that the annihilation rate is proportional to the fermion mass squared, and becomes suppressed for light fermions.

The helicity suppression may be lifted by adding a vector boson in the final state [70]. Thus, radiative “corrections” like this might in fact give the dominant contributions to the annihilation rate.

3 Theoretical preliminaries

3.1 Quantum chromodynamics

QCD is the theory of strong interactions of quarks and gluons. We will in this section discuss the Lagrangian of QCD, through which the Feynman rules we use in Chapter 4 are defined. Furthermore, we review a noteworthy feature of the theory: asymptotic freedom.

QCD Lagrangian

QCD is a non-abelian gauge theory, with gauge group $SU(3)$ [71–73]. The associated charge with the symmetry group is called *colour*, and fermions which carry colour are the *quarks*. We denote the quark fields by ψ_i^q , where $i = 1, 2, 3$ is the colour index and $q = u, d, \dots$ is the flavour label. There are eight gauge bosons called *gluons*, with fields A_μ^a , $a = 1, \dots, 8$.¹ The QCD Lagrangian is

$$\mathcal{L}_{\text{QCD}} = -\frac{1}{4}F_{\mu\nu}^a F^{a\mu\nu} + \sum_q \bar{\psi}_i^q (i\not{D}_{ij} - m_q \delta_{ij}) \psi_j^q \quad (3.1)$$

where a summation of repeated colour indices is understood. The gluon field-strength tensor is

$$F_{\mu\nu}^a = \partial_\mu F_\nu^a - \partial_\nu F_\mu^a - g_s f^{abc} F_\mu^b F_\nu^c. \quad (3.2)$$

Here, g_s is the $SU(3)$ gauge coupling constant and f^{abc} are structure constants of the fundamental representation of $SU(3)$. The covariant derivative acting on quarks is given by

$$(D_\mu)_{ij} = \delta_{ij} \partial_\mu + ig_s A_\mu^a T_{ij}^a \quad (3.3)$$

where T^a are the group generators in the fundamental representation. These definitions leave the Lagrangian invariant under $SU(3)$ transformations, where the quarks, antiquarks and gauge bosons transform under the fundamental, antifundamental and adjoint representations, respectively.

The generators T^a obey the commutation relations $[T^a, T^b] = if^{abc}T^c$, which define their Lie algebra $\mathfrak{su}(3)$. We conventionally normalise the generators in a given

¹We use $a, b, c, d = 1, \dots, 8$ for gluon colour indices and $i, j = 1, 2, 3$ for quark colour indices in this section.

representation so that

$$\text{Tr}(T^a T^b) = \frac{1}{2} \delta^{ab}. \quad (3.4)$$

Furthermore, it is very useful to label representation in a basis independent manner, such labels are called *Casimir invariants*. We define for example the quadratic Casimir C_2 by

$$\sum_a T^a T^a = C_2 \mathbf{1}, \quad (3.5)$$

which is basis independent. (To show that this operator is proportional to the identity, one can use Schur's Lemma, see e.g. Ref. [2, sec. 25.1].) To evaluate the quadratic Casimir C_F in the fundamental representation of $\text{SU}(N)$, we set $a = b$ and sum over a in Eq. (3.4). Using that $\text{Tr} \mathbf{1} = N$ and $\delta^{aa} = N^2 - 1$, it follows that

$$C_F = \frac{N^2 - 1}{2N} = \frac{4}{3} \quad (3.6)$$

where we in the last equality set $N = 3$.

As it stands, the functional integral

$$\int \mathcal{D}A \exp \left(i \int d^4x \mathcal{L}_{\text{QCD}} \right)$$

with the Lagrangian from Eq. (3.1) is ill-defined: Because of gauge invariance the functional integral will sum over an infinite set of physically equivalent configurations. The issue must be fixed by an appropriate gauge-fixing procedure before we can develop the QCD Feynman rules. If we insist on a Lorentz covariant gauge-fixing, additional, unphysical Faddeev-Popov ghosts must be added to the Lagrangian to compensate for the unphysical degrees of freedom that are not eliminated by the gauge-fixing [74]. No ghosts appear in the QCD processes considered in this text (they appear in higher order corrections however), therefore we do not discuss the dynamics of the QCD ghosts here.

Some selected QCD Feynman rules used in the text are presented in Appendix B.

Asymptotic freedom

A significant property of QCD is the asymptotic freedom [72], which implies that we only can legitimately apply perturbative methods in the short-distance limit. Asymptotic freedom is a general feature of pure Yang-Mill theories, stating that the coupling constant decreases as the renormalisation scale increases. This behaviour can be derived from the beta function of the running coupling, which describes its variation under the renormalisation group. One can show that the one-loop beta function of QCD is

$$\beta(\alpha_s) = \mu^2 \frac{\partial \alpha_s}{\partial \mu^2} = -\alpha_s^2 \left(\frac{11}{3} N_C - \frac{2}{3} n_f \right) \equiv -\alpha_s^2 b_1, \quad (3.7)$$

where $\alpha_s = g_s^2/(4\pi)$, N_C is the number of colours and n_f is the number of active quark flavours. The renormalisation scale is μ . Thus, for a world with six flavours, $n_f = 6$, the sign of the leading term of the beta function is negative. Consequently, the coupling α_s decreases as $\mu \rightarrow \infty$.

This effect can be understood qualitatively by the action of virtual particles polarising the vacuum. In quantum electrodynamics (QED), virtual fermion-antifermion pairs in the vicinity of a charge act as a dielectric medium and screen the charge. Thus, the effective charge decreases at larger distances. The QCD vacuum behaves the same way, but the effects from virtual quark-antiquark pairs are small compared to contributions from virtual gluons. Virtual gluons work in the other direction and augment the charge field. In consequence, the effective charge increases with increasing distance.

The solution of Eq. (3.7) is

$$\frac{1}{\alpha_s(\mu^2)} = \frac{1}{\alpha_s(\mu_0^2)} + b_1 \ln \left(\frac{\mu^2}{\mu_0^2} \right), \quad (3.8)$$

from which we see that the coupling constant diverges for a finite value of μ . We call this scale the QCD scale, defined by $\alpha_s^{-1}(\Lambda_{\text{QCD}}^2) = 0$. Writing the coupling constant in terms of this scale, we have

$$\alpha_s(Q^2) = \frac{1}{b_1 \ln(Q^2/\Lambda_{\text{QCD}}^2)}. \quad (3.9)$$

Perturbation theory is only valid when $\alpha_s \ll 1$, thus we must require $Q^2 \gg \Lambda_{\text{QCD}}^2$. For low-energy processes alternative approaches must be used, we return to this issue in Section 4.1.

3.2 Glashow-Salam-Weinberg model

In this section, we introduce the Glashow-Salam-Weinberg (GSW) model of electroweak interactions. We describe how the $SU(2)_L \otimes U(1)_Y$ gauge symmetry is broken down to $U(1)_{\text{em}}$ through spontaneous symmetry breaking (SSB), and how the weak gauge bosons acquire masses through the Higgs mechanism. After a brief discussion of the fermion sector, we end the section by considering the GSW model in the general R_ξ gauge.

Electroweak Lagrangian

In the SM, electroweak interactions are the combined description of the electromagnetic and weak interactions [18–20]. This unification of two of the fundamental interactions is described mathematically by the $SU(2)_L \otimes U(1)_Y$ gauge group, where Y

stands for *hypercharge*. The $SU(2)_L$ group is called weak isospin, and the L indicates that only left-handed fermions take part in the gauge interaction, an experimental fact [75].

The unbroken theory contains four massless gauge bosons, of which three should acquire mass through the Higgs mechanism in SSB. We add therefore a scalar, complex $SU(2)$ doublet called the *Higgs multiplet*, supplying four additional degrees of freedom. Three of these will become the longitudinal degrees of freedom of the massive gauge bosons. We write the complex doublet as follows:

$$\Phi = \frac{1}{\sqrt{2}} \begin{pmatrix} \varphi_1 + i\varphi_2 \\ \varphi_3 + i\varphi_4 \end{pmatrix} \equiv \begin{pmatrix} \varphi^+ \\ \varphi^0 \end{pmatrix}. \quad (3.10)$$

In the last equality, we introduced notation which will be convenient later: Following convention, we will choose the vev of SSB in the lower component of Φ . Then the upper component will obtain $U(1)_{\text{em}}$ charge $Q(\varphi^+) = +1$, and similarly $Q(\varphi^0) = 0$. Moreover, we will frequently use $\varphi^Z \equiv \varphi_4$ since this field is eaten by the Z boson in the unitary gauge.

The complete electroweak Lagrangian consists of the following pieces,

$$\mathcal{L} = \mathcal{L}_{\text{Higgs}} + \mathcal{L}_{\text{Gauge}} + \mathcal{L}_{\text{Fermion}} + \mathcal{L}_{\text{Yukawa}} + \mathcal{L}_{\text{GF}} + \mathcal{L}_{\text{Ghost}}. \quad (3.11)$$

We will investigate the various terms in the coming sections: First, we consider the gauge and Higgs Lagrangians, and then we will go on to the fermion sector with the fermion and Yukawa Lagrangians. We will initially use the unitary gauge, where there are no gauge-fixing (GF) or ghost terms. Subsequently, we proceed to the general R_ξ gauge, where contrastingly gauge-fixing and ghost terms must be included.

Gauge sector

The Higgs term contains the kinetics of the Higgs multiplet and the Higgs potential,

$$\mathcal{L}_{\text{Higgs}} = (D_\mu \Phi)^\dagger (D^\mu \Phi) + \mu^2 \Phi^\dagger \Phi - \lambda (\Phi^\dagger \Phi)^2 \quad (3.12)$$

where the covariant derivative is

$$D_\mu = \partial_\mu + \frac{ig}{2} \tau^a W_\mu^a + \frac{ig'}{2} B_\mu. \quad (3.13)$$

We define g and g' as the $SU(2)_L$ and $U(1)_Y$ couplings, respectively. Furthermore, we have labeled the hypercharge boson B and the three weak isospin gauge bosons W^a , $a = 1, 2, 3$. Finally, we use the Pauli matrices τ^a as the generators for the fundamental representation of $SU(2)$, while we have chosen the hypercharge of the Higgs multiplet to be 1, $Y(\Phi) = 1$. The factors $1/2$ are added by convention.

Secondly, the gauge term contains the kinetic terms of the gauge bosons,

$$\mathcal{L}_{\text{Gauge}} = -\frac{1}{4}W_{\mu\nu}^a W^{a\mu\nu} - \frac{1}{4}B_{\mu\nu}B^{\mu\nu} \quad (3.14)$$

where $W_{\mu\nu}^a$ and $B_{\mu\nu}$ are the field-strengths

$$W_{\mu\nu}^a = \partial_\mu W_\nu^a - \partial_\nu W_\mu^a - g\epsilon^{abc}W_\mu^b W_\nu^c, \quad (3.15a)$$

$$B_{\mu\nu} = \partial_\mu B_\nu - \partial_\nu B_\mu. \quad (3.15b)$$

Here, ϵ^{abc} are the structure constants in the fundamental representation of SU(2), i.e. the completely antisymmetric tensor.

The Higgs potential in Eq. (3.12) induces a vev for Φ , $\langle \Phi^\dagger \Phi \rangle = \mu^2/\lambda \equiv v^2$. We choose the vev to be in the lower, real component of the Higgs multiplet,

$$\Phi = \frac{1}{\sqrt{2}} \begin{pmatrix} \varphi^+ \\ v + h(x) + i\varphi^Z \end{pmatrix}. \quad (3.16)$$

where $h(x)$ is the fluctuation around the vev which is the physical Higgs field. In the unitary gauge we remove the φ -fields by a gauge transformation, hence

$$\Phi = \frac{v + h(x)}{\sqrt{2}} \begin{pmatrix} 0 \\ 1 \end{pmatrix}. \quad (3.17)$$

Consequently, after SSB, the Higgs field has a mass term $m_h = \sqrt{2}\mu$ as well as cubic and quartic self-interactions. Moreover, the part containing v in the kinetic term in Eq. (3.12) gives the mass terms

$$\begin{aligned} \mathcal{L}_m &= \frac{v^2}{2} \begin{pmatrix} 0 & 1 \end{pmatrix} \begin{pmatrix} \frac{g}{2}\tau^a W_\mu^a + \frac{g'}{2}B_\mu \\ \frac{g}{2}\tau^a W^{a\mu} + \frac{g'}{2}B^\mu \end{pmatrix} \begin{pmatrix} 0 \\ 1 \end{pmatrix} \\ &= \frac{v^2 g^2}{8} \begin{pmatrix} 0 & 1 \end{pmatrix} \begin{pmatrix} \frac{g'}{g}B_\mu + W_\mu^3 & W_\mu^1 - iW_\mu^2 \\ W_\mu^1 + iW_\mu^2 & \frac{g'}{g}B_\mu - W_\mu^3 \end{pmatrix} \begin{pmatrix} \frac{g'}{g}B_\mu + W_\mu^3 & W_\mu^1 - iW_\mu^2 \\ W_\mu^1 + iW_\mu^2 & \frac{g'}{g}B_\mu - W_\mu^3 \end{pmatrix} \begin{pmatrix} 0 \\ 1 \end{pmatrix} \\ &= \frac{v^2 g^2}{8} \left[(W_\mu^1)^2 + (W_\mu^2)^2 + \left(\frac{g'}{g}B_\mu + W_\mu^3 \right)^2 \right]. \end{aligned} \quad (3.18)$$

Next, we diagonalize these mass terms to get rid of the cross term. We rotate the B_μ and W_μ^3 fields as follows,

$$Z_\mu \equiv \cos \theta_W W_\mu^3 - \sin \theta_W B_\mu, \quad (3.19a)$$

$$A_\mu \equiv \sin \theta_W W_\mu^3 + \cos \theta_W B_\mu, \quad (3.19b)$$

which preserve the normalisation of the kinetic terms in Eq. (3.14). We defined the weak mixing angle θ_W by

$$\tan \theta_W = \frac{g'}{g}. \quad (3.20)$$

Furthermore, the coupling of A_μ with W_μ^a is determined by the commutator

$$g [A_\mu, W_\mu^a] = g \sin \theta_W W_\mu^3 W_\mu^a [\tau^3, \tau^a].$$

We identify the electromagnetic charge $e = g \sin \theta_W = g' \cos \theta_W$, and define

$$\tau^\pm = \frac{1}{\sqrt{2}}(\tau^1 \pm i\tau^2) \quad \text{and} \quad W_\mu^\pm = \frac{1}{\sqrt{2}}(W_\mu^1 \mp iW_\mu^2), \quad (3.21)$$

which satisfy $[\tau^3, \tau^\pm] = \pm\tau^\pm$ and $W_\mu^a \tau^a = W_\mu^+ \tau^+ + W_\mu^- \tau^- + W_\mu^3 \tau^3$. Thus, the W_μ^\pm combinations have charges $\pm e$, and appear in charged current interactions. The mass terms of the physical gauge bosons become

$$\mathcal{L}_m = \frac{1}{2}m_W^2 W_\mu^+ W_\mu^- + \frac{1}{2}m_Z^2 Z_\mu Z^\mu, \quad (3.22)$$

where we read off the masses $m_W = gv/2$, $m_Z = (gv/2) \cos \theta_W = m_W \cos \theta_W$ and $m_A = 0$.

Inserting the physical fields in the covariant derivative, Eq. (3.13), we have

$$\begin{aligned} D_\mu &= \partial_\mu + \frac{ig}{2}\tau^a W_\mu^a + \frac{ig'}{2}B_\mu \mathbf{1} \\ &= \partial_\mu + \frac{ig}{2}(\tau^+ W_\mu^+ + \tau^- W_\mu^-) \\ &\quad + \frac{ig}{2}(\cos \theta_W Z_\mu + \sin \theta_W A_\mu) \tau^3 + \frac{ig'}{2}(-\sin \theta_W Z_\mu + \cos \theta_W A_\mu) \mathbf{1} \\ &= \partial_\mu + \frac{ig}{2}(\tau^+ W_\mu^+ + \tau^- W_\mu^-) \\ &\quad + \frac{i}{2}e(\tau^3 + \mathbf{1})A_\mu + \frac{ig}{2\cos \theta_W}[\tau^3 - \sin^2 \theta_W(\tau^3 + \mathbf{1})] Z_\mu. \end{aligned} \quad (3.23)$$

Here, we used Eq. (3.20) as well as $e = g \sin \theta_W$. We recognise $(\tau^3 + \mathbf{1})/2$ as the electromagnetic charge generator, and observing that the hypercharge generator is the identity, we obtain the Gell-Mann-Nishijima relation $Q = T^3 + Y/2$ where $T^3 = \tau^3/2$ [76, 77]. Using this operator on the Higgs multiplet shows that our initial notation for its components is consistent.

Fermion sector

Next, we consider the kinematics and mass terms of the SM fermions, and their coupling to the electroweak gauge bosons. Weak interactions are maximally parity-violating: only left-handed fermions couple to the charged, weak gauge bosons. In mathematical terms, the left-handed fermions transform in the fundamental representation of SU(2), while the right-handed fermions are unaffected by SU(2)

Table 3.1: Values of T^3 , Y and Q for scalars and fermions in the SM. The quantum numbers are repeated for the second and third generations.

Field	ϕ^+	ϕ^0	ν_{eL}	e_L	e_R	u_L	d_L	u_R	d_R
T^3	1/2	-1/2	1/2	-1/2	0	1/2	-1/2	0	0
Y	1	1	-1	-1	-2	1/3	1/3	4/3	-2/3
Q	1	0	0	-1	-1	2/3	-1/3	2/3	-1/3

transformations, i.e. they are singlets. Thus we pair each generation of left-handed leptons and quarks in doublets the following way:

$$L^i = \left\{ \begin{pmatrix} \nu_{eL} \\ e_L \end{pmatrix}, \begin{pmatrix} \nu_{\mu L} \\ \mu_L \end{pmatrix}, \begin{pmatrix} \nu_{\tau L} \\ \tau_L \end{pmatrix} \right\} \quad \text{and} \quad Q^i = \left\{ \begin{pmatrix} u_L \\ d_L \end{pmatrix}, \begin{pmatrix} c_L \\ s_L \end{pmatrix}, \begin{pmatrix} t_L \\ b_L \end{pmatrix} \right\}, \quad (3.24)$$

where $i = 1, 2, 3$ labels the generation. Similarly, we denote the right-handed singlets as

$$\begin{aligned} e_R^i &= \{e_R, \mu_R, \tau_R\}, & u_R^i &= \{u_R, c_R, t_R\}, \\ \nu_R^i &= \{\nu_{eR}, \nu_{\mu R}, \nu_{\tau R}\}, & d_R^i &= \{d_R, s_R, b_R\}. \end{aligned} \quad (3.25)$$

Right-handed neutrinos have not yet been observed, but we include them here for completeness.

The kinetic terms for the SM fermions are

$$\begin{aligned} \mathcal{L}_{\text{Fermion}} &= \sum_i \left(i\bar{L}^i \gamma^\mu D_\mu L^i + i\bar{Q}^i \gamma^\mu D_\mu Q^i \right. \\ &\quad \left. + i\bar{e}_R^i \gamma^\mu D_\mu e_R^i + i\bar{\nu}_R^i \gamma^\mu D_\mu \nu_R^i + i\bar{d}_R^i \gamma^\mu D_\mu u_R^i + i\bar{d}_R^i \gamma^\mu D_\mu d_R^i \right), \end{aligned} \quad (3.26)$$

where the covariant derivatives are given by

$$\begin{aligned} D_\mu \psi_L &= \left[\partial_\mu + \frac{ig}{2} (\tau^+ W_\mu^+ + \tau^- W_\mu^-) + \frac{ig}{2} \tau^3 W_\mu^3 + \frac{ig'}{2} Y B_\mu \mathbf{1} \right] \psi_L \\ &= \left[\partial_\mu + \frac{ig}{2} (\tau^+ W_\mu^+ + \tau^- W_\mu^-) + ieQ A_\mu + \frac{ig}{\cos \theta_W} (T^3 - Q \sin^2 \theta_W) Z_\mu \right] \psi_L \end{aligned} \quad (3.27a)$$

and

$$D_\mu \psi_R = \left[\partial_\mu + \frac{ig}{2} \tau^3 W_\mu^3 + \frac{ig'}{2} Y B_\mu \right] \psi_R = [\partial_\mu + ieQ (A_\mu - \tan \theta_W Z_\mu)] \psi_R. \quad (3.27b)$$

Here, T^3 , Y and Q are the weak isospin, hypercharge and electromagnetic charge of the fermions, respectively. These quantum numbers are shown for the SM scalars and fermions in Table 3.1.

In order to generate masses for the fermions, we include Yukawa couplings between the fermions and Higgs multiplet,

$$\mathcal{L}_{\text{Yukawa}} = -Y_l^{ij} \left(\bar{L}^i \Phi e_R^j + \bar{e}_R^i \Phi^\dagger L^j \right) - Y_d^{ij} \left(\bar{Q}^i \Phi d_R^j + \bar{d}_R^i \Phi^\dagger Q^j \right), \quad (3.28)$$

where a sum over generations i, j is implied, and Y_l and Y_d are complex 3×3 matrices of Yukawa coupling constants. Note that all terms written down in Eq. (3.28) are $SU(2)_L$ and $U(1)_Y$ invariant. This however, introduces only mass terms for the fermions in the lower components of the doublets in Eq. (3.24). To get masses for the up-like quarks we must use the charge conjugated Higgs multiplet,

$$\Phi^c \equiv i\tau^2 \Phi^* = \frac{1}{\sqrt{2}} \begin{pmatrix} \varphi_3 + i\varphi^Z \\ -\varphi_1 + i\varphi_2 \end{pmatrix} \equiv \begin{pmatrix} \varphi^0 \\ -\varphi^- \end{pmatrix}. \quad (3.29)$$

Thus, we have²

$$\mathcal{L}_{\text{Yukawa}} = -Y_l^{ij} \bar{L}^i \Phi e_R^j - Y_d^{ij} \bar{Q}^i \Phi d_R^j - Y_u^{ij} \bar{Q}^i \Phi^c d_R^j + \text{h.c.} \quad (3.30)$$

The Y -couplings are arbitrary complex 3×3 matrices. They can be diagonalized by a bi-unitary transformation, and the fields can be transformed by the unitary transformations into mass eigenstates (see e.g. Ref. [2, sec. 29.3]). The new eigenstates are not diagonal in the interactions, which yields flavour mixing in weak, charged current. We will only consider one generation in this text, and therefore we do not go into details on flavour mixing. Writing the coupling in terms of masses, we have for instance

$$y_u \equiv Y_u^{11} = \sqrt{2} \frac{m_u}{v} = \frac{g}{\sqrt{2}} \frac{m_u}{m_W}. \quad (3.31)$$

R_ξ gauges

In Eq. (3.17), we removed the Goldstone fields by a gauge transformation, corresponding to the unitary gauge which gives the mass spectrum of physical particles. Although this gauge is suitable for showing how the gauge bosons acquire mass through the Higgs mechanism, it is often convenient to work in another gauge when performing calculations. In this section we will keep the Goldstone fields and fix the gauge by the Faddeev-Popov prescription [74].

We go back to the introduction of a vev to the Higgs potential, and the shift of the lower component in the Higgs doublet after SSB in Eq. (3.16). The doublet became

$$\Phi = \frac{1}{\sqrt{2}} \begin{pmatrix} \varphi^+ \\ v + h(x) + i\varphi^Z \end{pmatrix}. \quad (3.32)$$

²We do not discuss neutrino masses here, a discussion on the matter can be found in e.g. Ref. [2, p. 600-602].

Expanding the kinetic Higgs term, we find the following terms quadratic in the fields:

$$\begin{aligned} \mathcal{L}_{\text{Higgs}} = \dots + \frac{v^2 g^2}{8} & \left[(W_\mu^1)^2 + (W_\mu^2)^2 + \left(\frac{g'}{g} B_\mu + W_\mu^3 \right)^2 \right] \\ & + \frac{vg}{2} \left(\frac{g'}{g} B_\mu - W_\mu^3 \right) \partial^\mu \varphi^Z + \frac{ivg}{2} W_\mu^+ \partial^\mu \varphi^- - \frac{ivg}{2} W_\mu^- \partial^\mu \varphi^+. \end{aligned} \quad (3.33)$$

Performing the diagonalization in Eq. (3.19) and using $m_W = vg/2$ and $m_Z = m_W \cos \theta_W$, we get

$$\begin{aligned} \mathcal{L}_{\text{Higgs}} = \dots + \frac{1}{2} m_Z^2 Z_\mu Z^\mu + \frac{1}{2} m_W^2 W_\mu^+ W^{\mu-} \\ - m_Z Z_\mu \partial^\mu \varphi^Z - im_W \left(W_\mu^- \partial^\mu \varphi^+ - W_\mu^+ \partial^\mu \varphi^- \right). \end{aligned} \quad (3.34)$$

The last terms complicate the propagator definitions. In addition, the mass spectrum is the same as in the unitary gauge, but at the same time the Goldstone bosons have not disappeared. This means that the degrees of freedom before and after SSB do not match. We fix both issues by employing the Faddeev-Popov gauge-fixing procedure.

First, we define four gauge-fixing functions $G_A(A_\mu)$, $G_Z(Z_\mu)$, $G_+(W_\mu^+)$ and $G_-(W_\mu^-)$, with four corresponding gauge-fixing conditions: $G_A(A_\mu) = 0$, $G_Z(Z_\mu) = 0$ etc. Following [78, sec. 9.4], we introduce the constraint $\delta(G(x) - \omega(x))$ in the path integral and integrate over $\omega(x)$ with a Gaussian weight (for all four gauge-fixing functions). Effectively, this adds the following terms to the Lagrangian:

$$\mathcal{L}_{\text{GF}} = -\frac{1}{2\xi_A} G_A^2 - \frac{1}{2\xi_Z} G_Z^2 - \frac{1}{\xi_W} G_+ G_-. \quad (3.35)$$

We can use the arbitrary gauge-fixing functions to cancel the last terms in Eq. (3.34), let

$$G_A = \partial^\mu A_\mu, \quad (3.36a)$$

$$G_Z = \partial^\mu Z_\mu + \xi_Z m_Z \varphi^Z, \quad (3.36b)$$

$$G_+ = \partial^\mu W_\mu^+ + i\xi_W m_W \varphi^+, \quad (3.36c)$$

$$G_- = \partial^\mu W_\mu^- - i\xi_W m_W \varphi^-. \quad (3.36d)$$

These gauge-fixing conditions define the R_ξ gauge for the GSW model, and choosing different values for the ξ parameters corresponds to working in different gauges. Usual choices are the Landau gauge, $\xi = 0$, and the Feynman-'t Hooft gauge, $\xi = 1$. From e.g. $\varphi^Z = \partial^\mu Z_\mu / (\xi_Z m_Z)$ we see that the unitary gauge corresponds to $\xi \rightarrow \infty$. Calculating for example the square of G_Z , we have

$$G_Z^2 = (\partial_\mu Z^\mu)^2 + 2\xi_Z m_Z \varphi^Z \partial_\mu Z^\mu + \xi_Z^2 m_Z^2 (\varphi^Z)^2.$$

Performing a partial integration of the cross terms, we obtain

$$\frac{1}{2\xi_Z}G_Z^2 = \frac{1}{2\xi_Z}(\partial_\mu Z^\mu)^2 - m_Z Z^\mu \partial_\mu \varphi^Z + \frac{1}{2}\xi_Z m_Z^2 (\varphi^Z)^2, \quad (3.37)$$

which cancels out the third term in Eq. (3.34). One can similarly verify that the definitions of G_+ and G_- cancel the last term.

The introduction of the gauge-fixing constraint in the Lagrangian is accompanied by a Jacobian determinant $\det(\delta G/\delta\alpha)$, which correctly accommodates for the variable shift in the Dirac delta function. Here, α is the expansion parameter of an infinitesimal gauge transformation. The determinant can be represented by a functional integral over anticommuting scalar fields. Thus additional particles called Faddeev-Popov ghosts are added to the generating functional, and consequently to the Feynman rules. The part of the Lagrangian containing the ghost fields becomes

$$\mathcal{L}_{\text{Ghost}} = \sum_{i=1}^4 \left[\bar{c}_A \frac{\delta G_A}{\delta\alpha^i} + \bar{c}_Z \frac{\delta G_Z}{\delta\alpha^i} + \bar{c}_+ \frac{\delta G_+}{\delta\alpha^i} + \bar{c}_- \frac{\delta G_-}{\delta\alpha^i} \right] c_i. \quad (3.38)$$

In Appendix B, we present a selection of the Feynman rules (those used in this thesis) for the GSW model in the R_ξ gauge.

3.3 Goldstone boson equivalence theorem

The breaking of the $SU(2)_L \otimes U(1)_Y$ gauge symmetry in the GSW model involves a conservation of degrees of freedom. In the unbroken theory, the gauge bosons have only two (transverse) degrees of freedom. After SSB, the W^\pm and Z bosons have acquired a longitudinal component, while the Goldstone bosons φ^\pm and φ^Z have disappeared from the physical mass spectrum. Thus the physical degrees of freedom are the same before and after symmetry breaking.

We might suspect that in a physical sense, the Goldstone bosons have become the longitudinal components of the gauge bosons. The polarisation states of a massive gauge boson at rest are completely equivalent, but when the boson is moving at relativistic speed the longitudinal polarisation is easily distinguishable. Thus, at high energies a longitudinal polarised gauge boson might show its root as a Goldstone boson. Our suspicion is made precise by the Goldstone boson equivalence theorem (EQT), first proven by Cornwall et al. [24]. The theorem states that an amplitude involving longitudinal gauge bosons is equal to one with unphysical Goldstone bosons up to corrections of $\mathcal{O}(m_W/E)$, i.e.

$$\mathcal{M}(W_L^+, W_L^-, Z_L, \dots) = \mathcal{M}(\varphi^+, \varphi^-, \varphi^Z, \dots) \times \left(1 + \mathcal{O}\left(\frac{m_W}{E}\right) \right). \quad (3.39)$$

We do not prove the equivalence theorem here, but we follow Ref. [79] and argue why it holds in the special case of the Feynman-'t Hooft gauge. The complete proof is based on the Ward identities of the broken theory, and it is given in Ref. [80].

Consider a massive vector boson travelling in the z direction with momentum $k^\mu = (E, 0, 0, k_z)$. We choose the transverse polarisation vectors to be

$$\epsilon_1^\mu = (0, 1, 0, 0) \quad \text{and} \quad \epsilon_2^\mu = (0, 0, 1, 0)$$

which satisfies the conditions $(\epsilon_i^*)^\mu (\epsilon_j)_\mu = -\delta_{ij}$ and $\epsilon_i^\mu k_\mu = 0$ for $i = 1, 2$. The longitudinal polarisation vector is the third vector satisfying these conditions:

$$\epsilon_L^\mu = \frac{1}{m}(k_z, 0, 0, E). \quad (3.40)$$

For high energies, we have

$$\begin{aligned} k_z &= \sqrt{E^2 - m^2} \simeq E \left(1 - \frac{m^2}{2E^2} \right) = E \left(1 + \mathcal{O}(m^2/E^2) \right), \\ E &= \sqrt{k_z^2 + m^2} \simeq k_z \left(1 + \frac{m^2}{2k_z^2} \right) = k_z \left(1 + \mathcal{O}(m^2/E^2) \right), \end{aligned}$$

and thus

$$\epsilon_L^\mu = \frac{k^\mu}{m} + \mathcal{O}(m/E). \quad (3.41)$$

We defined the Feynman-'t Hooft gauge for the W^+ bosons, $\xi_W = 1$, in Eq. (3.36d) as

$$\partial^\mu W_\mu^+(x) + im_W \varphi^+(x) = 0,$$

which in momentum space implies

$$\frac{k^\mu}{m_W} W_\mu^+(k) = \varphi^+(k). \quad (3.42)$$

We can write a longitudinal polarised W^+ boson as $W_L^+ = \epsilon_L^\mu W_\mu^+$, which combined with Eqs. (3.41) and (3.42) yields

$$W_L^+ = \frac{k^\mu}{m_W} W_\mu^+ + \mathcal{O}(m_W/E) = \varphi^+ + \mathcal{O}(m_W/E). \quad (3.43)$$

Similar expressions are found for the W^- and Z gauge bosons, with the Goldstone bosons φ^- and φ^Z . Hence, we have verified the EQT in the Feynman-'t Hooft gauge.

The theorem comes in particularly useful when one computes cross sections with massive, high-energy gauge bosons in the initial or final state. We can then use transverse polarisation vectors in the polarisation sum, while we additionally compute diagrams with absorption or emission of the corresponding Goldstone bosons. This usually simplifies the calculations, and by the EQT we know that this approach is valid up to $\mathcal{O}(m_W/E)$ corrections. We will make use of this method in Chapter 6.

3.4 Polarisation sums

We will frequently need to sum matrix elements over possible spin configurations for incoming and outgoing particles in a given scattering process. In a typical experiment, it is difficult to prepare incoming particles in definite spin states, and also complicated to analyze the spin of outgoing particles. Therefore, one usually uses beams of unpolarised particles and the particle detectors are mostly blind to spin orientation. In addition, when considering final states consisting of quarks and gluons, the particles undergo hadronisation before they can be detected in an experiment. To compute such processes using perturbation theory, we must define inclusive observables which typically include summation over spin polarisations. We will discuss this in more detail in Chapter 4.

For these reasons, cross sections computed in this thesis are averaged over initial state spins and summed over final state spins. In this section, we will obtain expressions for polarisation sums for massive and massless spin-1 particles, which will be used in subsequent chapters.

Massive spin-1 fields

We can always boost a massive spin-1 field to its rest frame, where total angular momentum reduces to spin and non-relativistic quantum mechanics is valid. Thus, we know that a massive field with spin $s = 1$ has $2s + 1 = 3$ spin degrees of freedom. To describe a relativistic particle with three degrees of freedom, we need a four-vector and a constraint to eliminate the additional degree of freedom. Each component must satisfy the Klein-Gordon equation, and the only linear, Lorentz invariant constraint is $\partial_\mu A^\mu = 0$. The two equations can be combined into one equation that governs a vector field A^μ with mass m :

$$(\eta^{\mu\nu}\square - \partial^\mu\partial^\nu) A_\nu + m^2 A^\mu = 0. \quad (3.44)$$

This equation is called the Proca equation. Going to Fourier space, we find the general solutions of this equation to be

$$A^\mu(x) = \sum_s \int \frac{d^3k}{\sqrt{(2\pi)^3 2\omega_k}} \left[a_s(\mathbf{k}) \epsilon_s^\mu(k) e^{-i(\omega_k t - \mathbf{k}\cdot\mathbf{x})} + a_s^\dagger(\mathbf{k}) \epsilon_s^{\mu*}(k) e^{i(\omega_k t - \mathbf{k}\cdot\mathbf{x})} \right] \quad (3.45)$$

where the momenta of the Fourier modes are on-shell, $k^\mu = (\omega_k, \mathbf{k})$, and $a_s(\mathbf{k})$ and $a_s^\dagger(\mathbf{k})$ are ladder operators. For a fixed momentum k^μ , there are three independent solutions of Eq. (3.44) which we label by the *polarisation vectors* $\epsilon_s^\mu(k)$, with $s = 1, 2, 3$. These vectors are conventionally normalised as $\epsilon^{\mu*} \epsilon_\mu = -1$. Furthermore, the constraint $\partial_\mu A^\mu = 0$ implies in Fourier space that $k_\mu \epsilon^\mu = 0$.

The propagator of the massive vector field is the time-ordered product of two fields,

$$\begin{aligned}
 iD_F^{\mu\nu}(x) &= \langle 0|T\{A^\mu(x)A^{\nu*}(0)\}|0\rangle \\
 &= \sum_s \int \frac{d^3k}{(2\pi)^3 2\omega_k} \left[\epsilon_s^\mu(k)\epsilon_s^{\nu*}(k)e^{-ikx}\theta(x^0) + \epsilon_s^\mu(k)\epsilon_s^{\nu*}(k)e^{ikx}\theta(-x^0) \right] \\
 &= \int \frac{d^4k}{(2\pi)^4} \frac{\mathcal{P}^{\mu\nu} e^{-ikx}}{k^2 - m^2 + i\varepsilon}.
 \end{aligned} \tag{3.46}$$

Here, we defined the polarisation tensor $\mathcal{P}^{\mu\nu}$ as the sum of the polarisation states $\epsilon_s^\mu(k)\epsilon_s^{\nu*}(k)$. The result can be obtained by using the commutation relations of the ladder operators and the Feynman prescription for the k^0 contour integration. We can argue physically why the propagator $D_F^{\mu\nu}$ takes this form as follows: The amplitude for creation of a particle with momentum k and polarisation s is proportional to $\epsilon_s^{\mu*}(k)$, and similarly the amplitude for absorption is proportional to $\epsilon_s^\nu(k)$. The propagator describes the amplitude for propagation from source to sink, hence we multiply the individual amplitudes and sum over possible polarisations.

We want to obtain the polarisation sum $\mathcal{P}^{\mu\nu}$ for a massive spin-1 field in the R_ξ gauge. To do this, we will find the propagator in this gauge, and compare it with Eq. (3.46). Consider for example the Z_μ gauge boson from the GSW model discussed in the previous section, then we have the following quadratic terms in Z_μ ,

$$\mathcal{L}_{Z_\mu,2} = -\frac{1}{4}(\partial_\mu Z_\nu - \partial_\nu Z_\mu)^2 + \frac{1}{2}m_Z^2 Z_\mu Z^\mu - \frac{1}{2\xi_Z} G_Z^2, \tag{3.47}$$

where G_Z is the gauge-fixing function in the R_ξ gauge defined in Eq. (3.36b). Inserting only the term quadratic in Z_μ from Eq. (3.37), we get

$$\mathcal{L}_{Z_\mu,2} = -\frac{1}{4}(\partial_\mu Z_\nu - \partial_\nu Z_\mu)^2 + \frac{1}{2}m_Z^2 Z_\mu Z^\mu - \frac{1}{2\xi_Z}(\partial_\mu Z^\mu)^2. \tag{3.48}$$

Next, we integrate by parts to obtain

$$\begin{aligned}
 \mathcal{L}_{Z_\mu,2} &= \frac{1}{2}Z_\mu [\eta^{\mu\nu}\square - \partial^\mu\partial^\nu] Z_\nu + \frac{1}{2}Z_\mu \eta^{\mu\nu} m_Z^2 Z_\nu + \frac{1}{2\xi_Z} Z_\mu \partial^\mu \partial^\nu Z_\nu \\
 &= \frac{1}{2}Z_\mu \left[\eta^{\mu\nu}(\square + m_Z^2) - (1 - \xi_Z^{-1})\partial^\mu\partial^\nu \right] Z_\nu \\
 &\equiv \frac{1}{2}Z_\mu \Omega^{\mu\nu} Z_\nu
 \end{aligned} \tag{3.49}$$

where we defined $\Omega^{\mu\nu}$ as a shorthand for the terms in the bracket.

Varying the action of the Lagrangian in Eq. (3.49), one can show that the equations of motion are $\Omega^{\mu\nu} Z_\nu = 0$. Thus, the propagator $D_F^{\mu\nu}$ is the Green function of the differential operator $\Omega^{\mu\nu}$,

$$\Omega_{\mu\nu}(x) iD_F^{\nu\rho}(x-y) = \delta_\mu^\rho \delta^4(x-y), \tag{3.50}$$

$$\Omega_{\mu\nu}(k^2) iD_F^{\nu\rho}(k^2) = \delta_\mu^\rho, \tag{3.51}$$

where we went to momentum space in the second line. We have

$$\Omega^{\mu\nu}(k^2) = -(k^2 - m_Z^2)\eta^{\mu\nu} + (1 - \xi_Z^{-1})k^\mu k^\nu. \quad (3.52)$$

To invert this operator, it is convenient to write it in terms of projection operators. We define $P_L^{\mu\nu} \equiv k^\mu k^\nu / k^2$ which projects four-vectors on the subspace spanned by k^μ . The projection operator onto the complementary subspace becomes $P_T^{\mu\nu} = \eta^{\mu\nu} - P_L^{\mu\nu}$. These operators satisfy $P_L^2 = P_L$, $P_T^2 = P_T$, $P_L P_T = 0$ and $P_L^{\mu\nu} + P_T^{\mu\nu} = \eta^{\mu\nu}$. It follows that

$$\begin{aligned} \Omega^{\mu\nu}(k^2) &= -(k^2 - m_Z^2) \left(P_T^{\mu\nu} + \frac{k^\mu k^\nu}{k^2} \right) + (1 - \xi_Z^{-1})k^\mu k^\nu. \\ &= -(k^2 - m_Z^2)P_T^{\mu\nu} - \xi_Z^{-1}(k^2 - \xi_Z m_Z^2)P_L^{\mu\nu}. \end{aligned} \quad (3.53)$$

We can now invert the two prefactors to obtain

$$\begin{aligned} iD_F^{\mu\nu}(k^2) &= \frac{-iP_T^{\mu\nu}}{k^2 - m_Z^2 + i\epsilon} + \frac{-i\xi_Z P_L^{\mu\nu}}{k^2 - \xi_Z m_Z^2 + i\epsilon} \\ &= \frac{i}{k^2 - m_Z^2 + i\epsilon} \left[-\eta^{\mu\nu} + (1 - \xi_Z) \frac{k^\mu k^\nu}{k^2 - \xi_Z m_Z^2 + i\epsilon} \right]. \end{aligned} \quad (3.54)$$

By inserting this into Eq. (3.51) and using the projection operator properties, one can show that this is indeed the inverse of Ω . Hence, we have obtained the polarisation sum

$$\sum_s \epsilon_s^{\mu*} \epsilon_s^\nu = \mathcal{P}^{\mu\nu} = -\eta^{\mu\nu} + (1 - \xi_Z) \frac{k^\mu k^\nu}{k^2 - \xi_Z m_Z^2}. \quad (3.55)$$

By performing analogous manipulations to the Lagrangian, one can show that the propagators of the Higgs boson, the Goldstone bosons and the Faddeev-Popov ghosts becomes

$$\text{-----} \overset{h}{\quad} \text{-----} = \frac{i}{p^2 - m_h^2 + i\epsilon}, \quad (3.56)$$

$$\text{-----} \overset{\varphi^Z}{\quad} \text{-----} = \frac{i}{p^2 - \xi_Z m_Z^2 + i\epsilon}, \quad (3.57)$$

$$\text{.....} \overset{c_Z}{\quad} \text{.....} = \frac{i}{p^2 - \xi_Z m_Z^2 + i\epsilon}. \quad (3.58)$$

Moreover, similar results to Eqs. (3.55), (3.57) and (3.58) are found for the W bosons, the φ^\pm bosons and the c^\pm ghosts, only with m_W and ξ_W . The Goldstone bosons and the Faddeev-Popov ghosts have mass terms which depend on the gauge fixing parameter, e.g. $m_{\varphi^Z} = \sqrt{\xi_Z} m_Z$, indicating that these fields are not physical. Thus, the unitary gauge corresponds to the physical mass spectrum.

Massless spin-1

Massless spin-1 fields are described by Maxwell's equations, which correspond to the $m = 0$ limit of the Proca equation:

$$\partial_\mu F^{\mu\nu} = \square A^\nu - \partial_\nu \partial^\mu A^\mu = 0. \quad (3.59)$$

This equation and the corresponding Lagrangian, $\mathcal{L} = -F_{\mu\nu}^2/4$, are invariant under the gauge transformation

$$A^\mu(x) \rightarrow A^\mu(x) + \partial^\mu \Lambda(x), \quad (3.60)$$

for some function $\Lambda(x)$, a significant property the massive Lagrangian did not have. Massless spin-1 fields have two spin degrees of freedom, and we can use the gauge freedom to eliminate the unphysical degrees of freedom. For example, we may impose the *Lorenz gauge* condition $\partial_\mu A^\mu = 0$ (which is not automatically satisfied as it was in the Proca equation). This only eliminates one degree of freedom, so we can e.g. additionally set $\partial_i A_i = 0$ (*Coulomb gauge*) or $n_\mu A^\mu = 0$ for some arbitrary four-vector n (*physical gauges*). Note that the last two conditions are not Lorentz covariant, while the Lorenz condition is.

The solution of Eq. (3.59) can be expanded in Fourier components as in Eq. (3.45), with summation over two spin degrees of freedom instead of three. The gauge conditions translate into constraints on the polarisation vectors ϵ_s^μ , and consequently alter the polarisation sum. In this section, we present the polarisation sums for the *generalised Feynman gauges* and the physical gauges.

If we employ the Faddeev-Popov gauge-fixing prescription, the propagator for a massless spin-1 particle becomes

$$iD_F^{\mu\nu}(k^2) = \frac{i}{k^2 + i\epsilon} \left[-\eta^{\mu\nu} + (1 - \xi_\gamma) \frac{k^\mu k^\nu}{k^2} \right]. \quad (3.61)$$

This is called the generalised Feynman gauge, and it is similar to the R_ξ gauge of electroweak theory which we presented earlier. We can read off the polarisation sum:

$$\sum_s \epsilon_s^{\mu*} \epsilon_s^\nu = -\eta^{\mu\nu} + (1 - \xi_\gamma) \frac{k^\mu k^\nu}{k^2}. \quad (3.62)$$

As in Eq. (3.36), ξ_γ parametrises the gauge; $\xi_\gamma = 0$ corresponds for example to the Lorenz gauge. This gauge-fixing procedure has the virtue of being Lorentz covariant, but on the other hand, all unphysical degrees are not eliminated.

Alternatively, we can fix the gauge by imposing the Lorenz and physical gauge conditions: $k_\mu \epsilon_s^\mu = 0$ and $n_\mu \epsilon_s^\mu = 0$. Considering the available quantities carrying Lorentz indices, we can write down the following ansatz for the polarisation sum:

$$\sum_s \epsilon_s^{\mu*} \epsilon_s^\nu = A\eta^{\mu\nu} + Bk^\mu k^\nu + Cn^\mu n^\nu + Dk^\mu n^\nu + En^\mu k^\nu. \quad (3.63)$$

Applying the gauge conditions, as well as the normalisation $\epsilon^{\mu*}\epsilon_\mu = -1$, we obtain

$$\sum_s \epsilon_s^{\mu*} \epsilon_s^\nu = -\eta^{\mu\nu} + \frac{k^\mu n^\nu + k^\nu n^\mu}{k \cdot n}. \quad (3.64)$$

Here, we used our freedom in choosing n to set $n^2 = 0$. In this gauge-fixing scheme, all unphysical degrees of freedom are eliminated, but it came at the expense of Lorentz covariance. This is a general feature of gauge theories: we have to choose between a covariant gauge with unphysical degrees of freedom or a gauge with only physical degrees of freedom but in a selected frame [81].

In this text, we will in general operate in the middle ground and use the covariant propagator in Eq. (3.61) for virtual particles while using the polarisation sum in Eq. (3.64) for external particles.

4 Electron-positron annihilation

In this chapter, we calculate the total cross section for electron-positron annihilation to hadrons. First, we argue why this process can be calculated via perturbative methods. Then we compute the leading order process $e^+e^- \rightarrow q\bar{q}$, and introduce a convenient formalism for the computation of total cross sections of s-channel processes. We go on to the leading order corrections and calculate the Feynman diagrams with real gluon emission and virtual gluon exchange. The corrections contain infrared (IR) divergences, and we show how these divergences cancel at next-to-leading order using dimensional regularization (DR). The presentation follows partly Ref. [82, Sec. 3.5].

4.1 Hadronisation

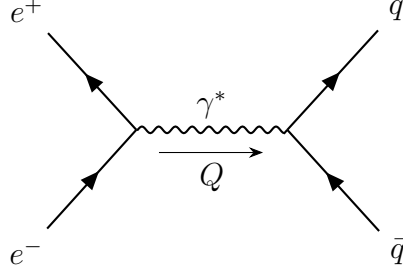
As discussed in Section 3.1, the asymptotic freedom of QCD means that we can only employ perturbative methods at the short-distance scale. It is, however, in the long-distance, low-energy processes where the formation of hadrons from quarks and gluons occurs. This process is called *hadronisation*. Due to *colour confinement*, the phenomenon that colour charged particles cannot be isolated, we can only detect hadrons in an experiment. Thus we need some method to connect perturbative QCD to experiment.

One approach to solve this issue is to define observables so that they are insensitive to the long-distance physics. In the case of e^+e^- -annihilation, the only process which involves hadronisation at leading order in both electroweak theory and QCD is $e^+e^- \rightarrow q\bar{q}$. Thus the cross section of this process is equal to the total cross section of $e^+e^- \rightarrow$ hadrons at leading order. This argument is repeated at any order in perturbation theory, when we include all partonic states subjected to hadronisation.

In the reasoning above, we have assumed that we can consider the partonic process and the hadronisation as independent processes. We argue why this assumption is valid as follows: The time scale in which the $e^+e^- \rightarrow \bar{q}q$ process takes place is $1/\sqrt{Q^2}$, where Q is the momentum transfer, while the time scale involved in the hadronisation is $1/\Lambda_{\text{QCD}}$. Thus we can view the quark creation and the hadronisation independently if we consider processes with $Q^2 \gg \Lambda_{\text{QCD}}^2$.

This brief, heuristic introduction of perturbative QCD can be made rigorous to greater extent, see e.g. Ref. [83].

The fact that we will consider processes in the limit $Q^2 \gg \Lambda_{\text{QCD}}^2$, lets us make some simplifications. If we take $\Lambda_{\text{QCD}} \sim 200$ MeV, then $Q^2 \gg \Lambda_{\text{QCD}}^2$ implies $Q^2 \gg m_q^2$ for


 Figure 4.1: Leading order diagram for $e^+e^- \rightarrow q\bar{q}$.

the quarks $q = u, d, s$. If we also take $4m_b^2 < Q^2 < 4m_t^2$, it is a good approximation to assume that all particles are massless (no top quark will be produced), which simplifies our calculations.

Next, we turn to the specific partonic processes at next-to-leading order. Splitting the total cross section according to partonic final state, we have

$$\sigma_{\text{hadrons}} = \sigma_{q\bar{q}} + \sigma_{q\bar{q}g} + \dots \quad (4.1)$$

We write the matrix elements in a perturbative series,

$$\sigma_{q\bar{q}} = \frac{1}{4I} \int d\Phi_2 |\mathcal{M}_{q\bar{q}}|^2 = \frac{1}{4I} \int d\Phi_2 \left[|\mathcal{M}_{q\bar{q}}^{(0)}|^2 + 2\alpha_s \Re \left\{ \mathcal{M}_{q\bar{q}}^{(0)*} \mathcal{M}_{q\bar{q}}^{(1)} \right\} + \dots \right], \quad (4.2a)$$

$$\sigma_{q\bar{q}g} = \frac{1}{4I} \int d\Phi_3 |\mathcal{M}_{q\bar{q}g}|^2 = \frac{1}{4I} \int d\Phi_3 \left[\alpha_s |\mathcal{M}_{q\bar{q}g}^{(0)}|^2 + \dots \right], \quad (4.2b)$$

where we expressly factored out the strong coupling. In this chapter, we will in general use subscripts like $q\bar{q}$ to denote the final state of the process the quantity belongs to. The only initial state considered is e^+e^- , so this notation unambiguously identifies the process in question. Additionally, a superscript (0) or (1) indicates the order in the perturbation expansion.

As we will see, the $\mathcal{M}_{q\bar{q}g}^{(0)}$ and the $\mathcal{M}_{q\bar{q}}^{(1)}$ diagrams contain IR divergences. Thus, a finite total cross section at order $\mathcal{O}(\alpha_s)$ requires

$$\int d\Phi_2 2\Re \left(\mathcal{M}_{q\bar{q}}^{(0)*} \mathcal{M}_{q\bar{q}}^{(1)} \right) + \int d\Phi_3 |\mathcal{M}_{q\bar{q}g}^{(0)}|^2 = \text{finite}. \quad (4.3)$$

In order to make our mathematical operations valid, we must employ an appropriate regularisation scheme for the IR divergences. We will use DR and work in $d = 4 - 2\epsilon$ dimensions. This scheme is particularly useful since gauge invariance is preserved.

4.2 Leading order process

We begin with the leading order process, which is given by the Feynman diagram in Fig. 4.1. There is also a diagram with the virtual photon replaced by a Z boson,

but it is strongly suppressed except around the $Q^2 = m_Z^2 \approx 90 \text{ GeV}$ pole of the Z propagator. We neglect the contribution in this calculation, thereby assuming a momentum transfer away from this resonance.

The diagram in Fig. 4.1 contains only QED vertices, and using the Feynman rules from Appendix B we get the amplitude

$$i\mathcal{M}_{q\bar{q}}^{(0)} = \bar{v}_{s'}(l^+)(-ie\gamma^\mu)u_s(l^-)iD_{\mu\nu}(Q)\bar{u}_r(q)(-iee_q\gamma^\nu)\delta_{ij}v_{r'}(\bar{q}) \quad (4.4)$$

where l^+ , l^- , q and \bar{q} are the four-momenta of the positron, electron, quark and antiquark, respectively. The momentum of the virtual photon is Q , which by energy-momentum conservation satisfies $l^+ + l^- = Q = q + \bar{q}$. We repeat the photon propagator from Eq. (B.2) for convenience,

$$iD^{\mu\nu}(Q^2) = \frac{i}{Q^2 + i\varepsilon} \left(-\eta^{\mu\nu} + (1 - \xi_\gamma) \frac{Q^\mu Q^\nu}{Q^2} \right), \quad (4.5)$$

where ξ_γ parametrises the gauge.

Furthermore, the subscripts s' , s , r and r' on the Dirac spinors \bar{v} , u , \bar{u} and v label the spin of the positron, electron, quark and antiquark respectively. The quarks have colour i and j , thus we enforce colour conservation with δ_{ij} , and finally, e_q is the electric charge of the quarks in units of e .¹

It is convenient to define lepton and hadron currents,

$$(J_L)^\mu = -ie\bar{v}_{s'}(l^+)\gamma^\mu u_s(l^-), \quad (4.6a)$$

$$(J_{q\bar{q}}^{(0)})^\nu = i\delta_{ij}ee_q\bar{u}_r(q)\gamma^\nu v_{r'}(\bar{q}), \quad (4.6b)$$

from which we can write

$$i\mathcal{M}_{q\bar{q}}^{(0)} = iD_{\mu\nu}(Q) (J_L)^\mu (J_{q\bar{q}}^{(0)})^\nu.$$

Contracting the currents with Q^μ , we have

$$Q^\mu (J_L)_\mu \propto \bar{v}_{s'}(l^+)(l^+ + l^-)u_s(l^-) = \bar{v}_{s'}(l^+)(-m_e + m_e)u_s(l^-) = 0, \quad (4.7a)$$

$$Q^\mu (J_{q\bar{q}}^{(0)})_\mu \propto \bar{u}_r(q)(\not{q} + \not{\bar{q}})v_{r'}(\bar{q}) = \bar{u}_r(q)(m_q - m_q)v_{r'}(\bar{q}) = 0, \quad (4.7b)$$

where we used that the spinors obey the Dirac equation. Hence, we can discard the $Q^\mu Q^\nu$ -part in the photon propagator. This is in accordance with the fact that the amplitude should be gauge invariant. It follows that

$$i\mathcal{M}_{q\bar{q}}^{(0)} = \frac{-i}{Q^2} (J_L)_\mu (J_{q\bar{q}}^{(0)})^\mu. \quad (4.8)$$

¹To avoid ambiguity with the momentum transfer, we use e_q instead of Q for the electric charge of the quarks here.

As discussed in Section 3.4, we are generally interested in cross sections where the initial and final spins are averaged and summed over, respectively. Moreover, we used the fact that the partonic state is completely inclusive in the hadronic state when we argued why perturbation theory is applicable to the process $e^+e^- \rightarrow \text{hadrons}$. It is the *total* cross section which is independent of the complicated physics of hadronisation, hence we must sum over spins and colours in the partonic state. We therefore write the squared amplitude as

$$\overline{|\mathcal{M}_{q\bar{q}}^{(0)}|^2} = \frac{1}{4} \sum_{s,s',r,r',i,j} |\mathcal{M}_{q\bar{q}}^{(0)}|^2 = \frac{1}{Q^4} L_{\mu\nu} \left(H_{q\bar{q}}^{(0)} \right)^{\mu\nu}, \quad (4.9)$$

where we defined the leptonic and hadronic tensors

$$L^{\mu\nu} = \frac{1}{4} \sum_{s,s'} (J_L)^\mu (J_L^*)^\nu, \quad (4.10a)$$

$$\left(H_{q\bar{q}}^{(0)} \right)^{\mu\nu} = \sum_{r,r',i,j} \left(J_{q\bar{q}}^{(0)} \right)^\mu \left(J_{q\bar{q}}^{(0)*} \right)^\nu. \quad (4.10b)$$

We can perform this factorisation at all orders in perturbative QCD, since the processes always have the same s-channel structure with the initial e^+e^- state. Furthermore, the factorisation is very useful since the leptonic tensor remains the same for all diagrams.

Total cross section

We can use the factorisation into leptonic and hadronic tensors to simplify the general expression for the total cross section. In the case of $e^+e^- \rightarrow X$, where X is some partonic state, we can write the total cross section as

$$\sigma_X = \frac{1}{2Q^2} L_{\mu\nu} \frac{1}{Q^4} \int d\Phi_X H_X^{\mu\nu}. \quad (4.11)$$

Here, we used the flux factor $4I = 4|\mathbf{1}^+|\sqrt{s} \simeq 2s = 2Q^2$, simplified using that $Q^2 \gg m_e^2$. After the phase space integration in Eq. (4.11), the momenta of the final state particles are integrated out, so the only free variable is Q . Thus the only quantities available carrying Lorentz indices are $\eta^{\mu\nu}$ and Q^μ , and we can use the ansatz

$$\int d\Phi H^{\mu\nu} = A\eta^{\mu\nu} + BQ^\mu Q^\nu. \quad (4.12)$$

Gauge invariance in QED implies that $Q_\mu L^{\mu\nu} = Q_\mu H^{\mu\nu} = 0$, such that the gauge-dependent $(1 - \xi_\gamma)Q^\mu Q^\nu$ -part of the photon propagator drops out. At leading order, we showed this explicitly with the currents in Eq. (4.6). Going to higher order, the cancellation is only guaranteed to happen when summing over all diagrams at a given

order. In our particular case, the leptonic tensor stays the same and will always cancel the gauge-dependent part of the propagator. However, since gauge invariance holds for all QED processes, the hadronic currents should also cancel gauge-dependent terms (consider for example a process $\mathcal{M} \propto H_{\mu\nu}H^{\mu\nu}$). Consequently, we contract Eq. (4.12) with Q_μ to get $A = -BQ^2$, which enables us to write

$$\int d\Phi H^{\mu\nu} = \frac{1}{d-1} \left(-\eta^{\mu\nu} + \frac{Q^\mu Q^\nu}{Q^2} \right) H(Q^2) \quad (4.13)$$

where

$$H(Q^2) = -\eta_{\mu\nu} \int d\Phi H^{\mu\nu}(Q^2) = -H^\mu{}_\mu(Q^2)\Phi. \quad (4.14)$$

The phase space integration in the last step is only valid if the hadronic tensor only depends on Q^2 . We can now express the total cross section of $e^+e^- \rightarrow X$ as

$$\sigma_X = \frac{1}{2(d-1)Q^6} (-L^\mu{}_\mu) H_X(Q^2). \quad (4.15)$$

Hence, the problem of computing the total cross section is reduced to computing the trace of the leptonic tensor and evaluating the hadron function $H_X(Q^2)$.

Trace evaluations

Writing out the leptonic and hadronic tensors from Eq. (4.10), we have

$$L^{\mu\nu} = \frac{e^2}{4} \sum_{s,s'} [\bar{v}_{s'}(l^+) \gamma^\mu u_s(l^-)] [\bar{v}_{s'}(l^+) \gamma^\nu u_s(l^-)]^* \quad (4.16a)$$

$$(H_{q\bar{q}}^{(0)})^{\mu\nu} = N_C (ee_q)^2 \sum_{r,r'} [\bar{u}_r(q) \gamma^\mu v_{r'}(\bar{q})] [\bar{u}_r(q) \gamma^\nu v_{r'}(\bar{q})]^* \quad (4.16b)$$

where we performed the quark colour sum, $\sum_{i,j} \delta_{ij} \delta_{ij} = N_C$. To evaluate the tensors, we first note that the brackets contain spinor-space scalars, so we can replace the complex conjugate with the Hermitian conjugate. We have e.g.

$$(\bar{u} \gamma^\mu v)^\dagger = v^\dagger (\gamma^\mu)^\dagger (\gamma^0)^\dagger u = v^\dagger \gamma^0 \gamma^0 (\gamma^\mu)^\dagger \gamma^0 u = \bar{v} \gamma^\mu u,$$

where we used the Dirac matrix properties $\gamma^0 \gamma^0 = 1$ and $(\gamma^0)^\dagger = \gamma^0$. Furthermore, we will use the following identities for Dirac spinors:²

$$\sum_s u_s(p) \bar{u}_s(p) = (\not{p} + m), \quad (4.17a)$$

$$\sum_s v_s(p) \bar{v}_s(p) = (\not{p} - m). \quad (4.17b)$$

²A derivation of these relations can be found in almost any book on quantum field theory (QFT), see e.g. Refs. [2, 78, 81].

We will from now on assume that the electrons and quarks are massless, $m_e = 0$, $m_q = 0$, as justified in Section 4.1. The leptonic tensor is evaluated to

$$\begin{aligned}
 L^{\mu\nu} &= \frac{e^2}{4} \sum_{s,s'} [\bar{v}_{s'} \gamma^\mu u_s] [\bar{v}_{s'} \gamma^\nu u_s]^\dagger \\
 &= \frac{e^2}{4} \sum_{s,s'} (\bar{v}_{s'})_a \gamma_{ab}^\mu (u_s)_b (\bar{u}_s)_c \gamma_{cd}^\nu (v_{s'})_d \\
 &= \frac{e^2}{4} l_{da}^+ \gamma_{ab}^\mu l_{bc}^- \gamma_{cd}^\nu = \frac{e^2}{4} \text{Tr} [l^+ \gamma^\mu l^- \gamma^\nu], \tag{4.18}
 \end{aligned}$$

where we used the relations in Eq. (4.17). The trace can be computed using results from Appendix A,

$$\begin{aligned}
 L^{\mu\nu} &= \frac{e^2}{4} \text{Tr} [l^+ \gamma^\mu l^- \gamma^\nu] = \frac{e^2}{4} l_\rho^+ l_\sigma^- \text{Tr} [\gamma^\rho \gamma^\mu \gamma^\sigma \gamma^\nu] \\
 &= e^2 l_\rho^+ l_\sigma^- [\eta^{\rho\mu} \eta^{\sigma\nu} + \eta^{\rho\nu} \eta^{\mu\sigma} - \eta^{\rho\sigma} \eta^{\mu\nu}] \\
 &= e^2 [l^{+\mu} l^{-\nu} + l^{+\nu} l^{-\mu} - (l^+ \cdot l^-) \eta^{\mu\nu}] \\
 &= e^2 [l^{+\mu} l^{-\nu} + l^{+\nu} l^{-\mu} - (Q^2/2) \eta^{\mu\nu}], \tag{4.19}
 \end{aligned}$$

where we in the last step used the energy-momentum relation

$$Q^2 = (l^+ + l^-)^2 = 2(l^+ \cdot l^-)$$

for massless particles. Using that $\eta_{\mu\nu} \eta^{\mu\nu} = d$ in d dimensions, the trace of $L^{\mu\nu}$ over Lorentz indices becomes

$$\eta_{\mu\nu} L^{\mu\nu} = \mu^{2\epsilon} e^2 Q^2 \frac{2-d}{2} = \mu^{2\epsilon} e^2 Q^2 (\epsilon - 1). \tag{4.20}$$

We supplied here a scale μ with mass dimension 1. The action should remain dimensionless in DR, where we have mass dimensions

$$[A_\mu] = \frac{d-2}{2} = 1 - \epsilon, \quad [\psi] = \frac{d-1}{2} = \frac{3}{2} - \epsilon, \quad [e] = \frac{4-d}{2} = \epsilon. \tag{4.21}$$

Thus the replacement $e \rightarrow \mu^\epsilon e$ ensures that the coupling remains dimensionless.

Similar manipulations for the hadronic tensor yield

$$\begin{aligned}
 (H_{q\bar{q}}^{(0)})^{\mu\nu} &= N_C \mu^{2\epsilon} (ee_q)^2 \text{Tr} [\not{q} \gamma^\mu \bar{\not{q}} \gamma^\nu] \\
 &= 4N_C \mu^{2\epsilon} (ee_q)^2 [q^\mu \bar{q}^\nu + q^\nu \bar{q}^\mu - (Q^2/2) \eta^{\mu\nu}]
 \end{aligned}$$

and consequently

$$\eta_{\mu\nu} (H_{q\bar{q}}^{(0)})^{\mu\nu} = 4N_C \mu^{2\epsilon} (ee_q)^2 Q^2 (\epsilon - 1). \tag{4.22}$$

This expression does not depend on the outgoing momenta, so we are allowed to move it outside the phase space integral.

The phase space integral in $d = 4 - 2\epsilon$ dimensions is derived in Appendix C, and repeated here:

$$\Phi = \int d\Phi_2^{(d)} = \frac{1}{4\pi} \frac{|\mathbf{q}|}{\sqrt{Q^2}} \left(\frac{\pi}{|\mathbf{q}|^2} \right)^\epsilon \frac{\Gamma(1-\epsilon)}{\Gamma(2-2\epsilon)} = \frac{1}{8\pi} \left(\frac{4\pi}{Q^2} \right)^\epsilon \frac{\Gamma(1-\epsilon)}{\Gamma(2-2\epsilon)}, \quad (4.23)$$

where we in the last equality used $|\mathbf{q}| = \sqrt{E_q^2 - m_q^2} = E_q = \sqrt{Q^2}/2$. Inserting Eqs. (4.20), (4.22) and (4.23) into Eq. (4.15), we conclude that

$$\sigma_{q\bar{q}}^{(0)} = \frac{1}{4I} \int d\Phi_2 |\mathcal{M}_{q\bar{q}}^{(0)}|^2 = \frac{4\pi N_C e_q^2 \mu^{2\epsilon} \alpha_{\text{em}}^2}{Q^2} \left(\frac{4\pi\mu^2}{Q^2} \right)^\epsilon \frac{(1-\epsilon)^2}{3-2\epsilon} \frac{\Gamma(1-\epsilon)}{\Gamma(2-2\epsilon)}. \quad (4.24)$$

Here, $\alpha_{\text{em}} = e^2/4\pi$. The result does not contain any IR divergences, so the $\epsilon \rightarrow 0$ limit is straightforward:

$$\sigma_{q\bar{q}}^{(0)} = \frac{4\pi\alpha_{\text{em}}^2}{3Q^2} e_q^2 N_C. \quad (4.25)$$

This formula reproduces the standard result, see e.g. Eq. (17.4) in Ref. [78]. Although it was not strictly necessary to use DR in the calculation of this process, it conveniently allows us to sum the result with IR divergent contributions at higher order later.

4.3 Real gluon emission

In this section we consider the process $e^+e^- \rightarrow q\bar{q}g$. The Feynman diagrams are shown in Fig. 4.2, where the e^+e^- -part is omitted. As discussed in the previous section, we only need to compute the Lorentz index trace of the hadronic tensor to evaluate the total cross section (the leptonic tensor stays the same). Using the gluon-quark-antiquark vertex from Eq. (B.6), we find the sum of the hadron currents of the two diagrams to be

$$\left(J_{q\bar{q}g}^{(0)} \right)^\mu = -i\mu^{2\epsilon} e e_q g_s T_{ij}^a (\epsilon_t^*)_\sigma \bar{u}_r(q) \left[\gamma^\sigma \frac{\not{q} + \not{g}}{(q+g)^2} \gamma^\mu + \gamma^\mu \frac{-\not{\bar{q}} + \not{g}}{(\bar{q}+g)^2} \gamma^\sigma \right] v_{r'}(\bar{q}) \quad (4.26)$$

where g_s is the QCD coupling constant, and we use the same notation for the momenta and spin of the quarks as in Section 4.2. The emitted gluon has four-momentum g , colour a , and polarisation vector ϵ_t . Factoring out the polarisation vectors, and summing over the polarisation and colour of the gluon in addition to the quarks, the hadron tensor is given by

$$\left(H_{q\bar{q}g}^{(0)} \right)^{\mu\nu} = \sum_t (\epsilon_t^*)_\sigma (\epsilon_t)_\rho \sum_{r,r',i,j,a} \left(J_{q\bar{q}g}^{(0)} \right)^{\mu\sigma} \left(J_{q\bar{q}g}^{(0)*} \right)^{\nu\rho} \quad (4.27)$$

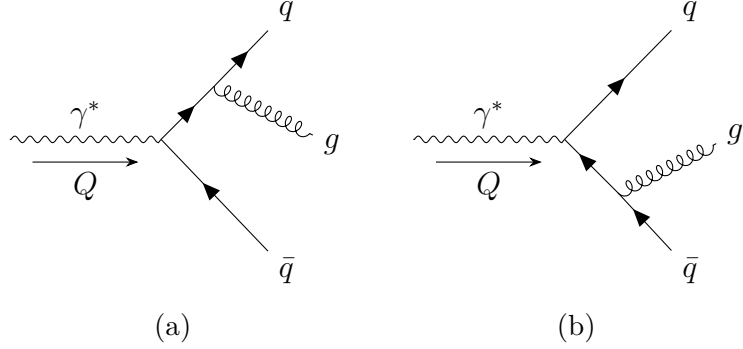


Figure 4.2: Leading order diagrams for $e^+e^- \rightarrow q\bar{q}g$. We have omitted the leptonic current part, which is identical to that in Fig. 4.1.

The polarisation sum for the massless gluon is given by Eq. (3.64). However, since there are only one external gluon, any part proportional to g^σ drops out in the Feynman amplitude [84]. Therefore, we can perform the replacement

$$\sum_t (\epsilon_t^*)_\sigma (\epsilon_t)_\rho \rightarrow -\eta_{\sigma\rho}.$$

It follows that

$$(H_{qqg}^{(0)})^{\mu\nu} = - \sum_{r,r',i,j,a} (J_{qqg}^{(0)})^{\mu\sigma} (J_{qqg}^{(0)*})_\sigma^\nu. \quad (4.28)$$

To evaluate the sum over quark and gluon colours, we use the results from Eqs. (3.5) and (3.6),

$$\sum_a T_{ij}^a (T_{ij}^a)^* = \sum_a T_{ij}^a T_{ji}^a = C_F \delta_{ii} = C_F N_C, \quad (4.29)$$

where we used that $SU(N)$ generators are Hermitian in the fundamental representation.

The remaining sum is that over spinor polarisations. We can use the same manipulations as in Section 4.2 to write it as a trace over Dirac matrices,

$$(H_{qqg}^{(0)})^{\mu\nu} \propto \text{Tr} \left[\not{q} \left(\gamma^\sigma \frac{\not{q} + \not{g}}{2q \cdot g} \gamma^\mu - \gamma^\mu \frac{\not{q} + \not{g}}{2\bar{q} \cdot g} \gamma^\sigma \right) \not{\bar{q}} \left(\gamma^\nu \frac{\not{q} + \not{g}}{2q \cdot g} \gamma_\sigma - \gamma_\sigma \frac{\not{q} + \not{g}}{2\bar{q} \cdot g} \gamma^\nu \right) \right]. \quad (4.30)$$

By the linearity of the trace, we can consider the terms in Eq. (4.30) one by one. We define

$$t_{qq} = \text{Tr} \left[\not{q} \gamma^\sigma (\not{q} + \not{g}) \gamma^\mu \not{\bar{q}} \gamma_\mu (\not{q} + \not{g}) \gamma_\sigma \right], \quad (4.31a)$$

$$t_{q\bar{q}} = \text{Tr} \left[\not{q} \gamma^\sigma (\not{q} + \not{g}) \gamma^\mu \not{\bar{q}} \gamma_\sigma (\not{q} + \not{g}) \gamma_\mu \right], \quad (4.31b)$$

$$t_{\bar{q}q} = \text{Tr} \left[\not{q} \gamma^\mu (\not{q} + \not{g}) \gamma^\sigma \not{\bar{q}} \gamma_\mu (\not{q} + \not{g}) \gamma_\sigma \right], \quad (4.31c)$$

$$t_{\bar{q}\bar{q}} = \text{Tr} \left[\not{q} \gamma^\mu (\not{q} + \not{g}) \gamma^\sigma \not{\bar{q}} \gamma_\sigma (\not{q} + \not{g}) \gamma_\mu \right], \quad (4.31d)$$

from which we can write

$$\eta_{\mu\nu} \left(H_{q\bar{q}g}^{(0)} \right)^{\mu\nu} = C_F N_C \mu^{4\epsilon} (e e_q g_s)^2 \left[-\frac{t_{qq}}{(2q \cdot g)^2} - \frac{t_{\bar{q}\bar{q}}}{(2\bar{q} \cdot g)^2} + \frac{t_{q\bar{q}} + t_{\bar{q}q}}{(2q \cdot g)(2\bar{q} \cdot g)} \right]. \quad (4.32)$$

Inspecting this expression, we see that it diverges for $q \cdot g \rightarrow 0$ and $\bar{q} \cdot g \rightarrow 0$. Writing

$$q \cdot g = E_q E_g (1 - \beta_q \cos \theta), \quad \beta_q = \sqrt{1 - \frac{m_q^2}{E_q^2}}, \quad (4.33)$$

it is apparent that the hadron tensor contains an IR divergence for $E_g \rightarrow 0$. A singularity at zero energy like this is called *soft*. Note that it appears even without assuming massless quarks. When we additionally set $m_q = 0$, we get $\beta_q = 1$ and $E_q \rightarrow 0$ becomes allowed. Then the expression diverges for both $\theta \rightarrow 0$ and $E_q \rightarrow 0$. The singularity at zero angle is called *collinear*.

Next, we evaluate the spinor-space traces in Eq. (4.31). We will make use of the computer algebra system FORM to compute traces like these [85]. Nonetheless, we include an explicit calculation of Eq. (4.31a) to show how one could do this manually.

We use the cyclic property of the trace to write

$$t_{qq} = \text{Tr} \left[\gamma_\sigma \not{q} \gamma^\sigma (\not{q} + \not{g}) \gamma^\mu \bar{\not{q}} \gamma_\mu (\not{q} + \not{g}) \right].$$

This expression is simplified using the second relation in Eq. (A.13), which we repeat for convenience:

$$\gamma^\mu \not{p} \gamma_\mu = p_\alpha (2\eta^{\mu\alpha} \gamma_\mu - \gamma^\alpha \gamma^\mu \gamma_\mu) = -2(1 - \epsilon) \not{p}.$$

We have therefore

$$\begin{aligned} t_{qq} &= 4(1 - \epsilon)^2 \text{Tr} \left[\not{q} (\not{q} + \not{g}) \bar{\not{q}} (\not{q} + \not{g}) \right] \\ &= 16(1 - \epsilon)^2 q_\mu (q + g)_\nu \bar{q}_\rho (q + g)_\sigma \text{Tr} \left[\eta^{\mu\nu} \eta^{\rho\sigma} + \eta^{\mu\sigma} \eta^{\nu\rho} - \eta^{\mu\rho} \eta^{\nu\sigma} \right] \\ &= 16(1 - \epsilon)^2 \left[2(q \cdot (q + g))(\bar{q} \cdot (q + g)) - q \cdot \bar{q} (q + g)^2 \right] \\ &= 32(1 - \epsilon)^2 (q \cdot g)(\bar{q} \cdot g), \end{aligned} \quad (4.34)$$

where we used that $q^2 = g^2 = 0$.

Using FORM, we also get $t_{\bar{q}\bar{q}} = t_{qq}$ and

$$t_{q\bar{q}} + t_{\bar{q}q} = -32(1 - \epsilon) \left[(q \cdot \bar{q}) Q^2 - 2\epsilon (q \cdot g)(\bar{q} \cdot g) \right]. \quad (4.35)$$

Thus, the Lorentz index trace of the hadron tensor becomes

$$\begin{aligned} \eta_{\mu\nu} \left(H_{q\bar{q}g}^{(0)} \right)^{\mu\nu} &= 8C_F N_C \mu^{4\epsilon} (e e_q g_s)^2 (1 - \epsilon) \\ &\quad \times \left[-(1 - \epsilon) \left(\frac{q \cdot g}{\bar{q} \cdot g} + \frac{\bar{q} \cdot g}{q \cdot g} \right) - \frac{(q \cdot \bar{q}) Q^2}{(q \cdot g)(\bar{q} \cdot g)} + 2\epsilon \right]. \end{aligned} \quad (4.36)$$

Phase space integration

The phase space integral for three outgoing particles is simplified considerably when the particles are massless. In the center-of-momentum (CoM) frame, it is convenient to define momentum fractions

$$x_i = \frac{2p_i \cdot Q}{Q^2}. \quad (4.37)$$

They satisfy $x_q + x_{\bar{q}} + x_g = 2$, as well as

$$1 - x_q = \frac{2\bar{q} \cdot g}{Q^2}, \quad 1 - x_{\bar{q}} = \frac{2q \cdot g}{Q^2} \quad \text{and} \quad 1 - x_g = \frac{2q \cdot \bar{q}}{Q^2}.$$

Writing the hadron tensor in terms of momentum fractions combined with the three-particle phase space from Eq. (C.24), we get

$$H_{q\bar{q}g}^{(0)}(Q^2) = -\eta_{\mu\nu} \int d\Phi_3^{(d)} (H_{q\bar{q}g}^{(0)})^{\mu\nu} = \frac{C_F N_C e_q^2 \alpha_{\text{em}} \alpha_s Q^2}{\pi} \left(\frac{4\pi\mu^2}{Q^2} \right)^{2\epsilon} \frac{1 - \epsilon}{\Gamma(2 - 2\epsilon)} I(\epsilon) \quad (4.38)$$

with $\alpha_s = g_s^2/4\pi$ and where

$$I(\epsilon) = \int_0^1 dx_q \int_{1-x_q}^1 dx_{\bar{q}} [(1-x_q)(1-x_{\bar{q}})(x_q+x_{\bar{q}}-1)]^{-\epsilon} \\ \times \left[(1-\epsilon) \left(\frac{1-x_{\bar{q}}}{1-x_q} + \frac{1-x_q}{1-x_{\bar{q}}} \right) + \frac{2(1-x_g)}{(1-x_q)(1-x_{\bar{q}})} - 2\epsilon \right]. \quad (4.39)$$

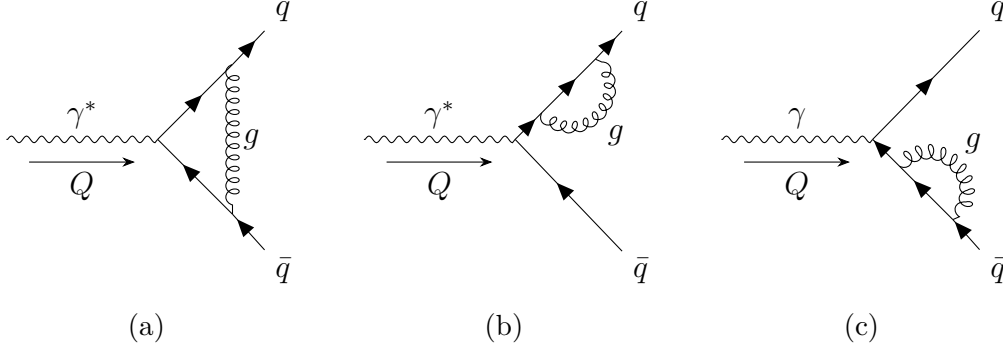
The collinear divergences now arise in the $x_q \rightarrow 1$ or $x_{\bar{q}} \rightarrow 1$ limit, while the soft gluon divergence corresponds to taking both limits simultaneously. Note that the interference term has a double pole in this limit. We simplify the integral by substituting $x_q = x$ and $x_{\bar{q}} = 1 - vx$. The Jacobian of this transformation is $|\det J| = x$, so we rewrite our integral as

$$I(\epsilon) = \int_0^1 dx \int_0^1 dv \frac{x}{[vx^2(1-x)(1-v)]^\epsilon} \left[(1-\epsilon) \left(\frac{vx}{1-x} + \frac{1-x}{vx} \right) + \frac{2(1-v)}{v(1-x)} - 2\epsilon \right].$$

We identify the integral of each term as two instances of Euler's Beta function, which can be expressed by Gamma functions using Eq. (A.6). Hence,

$$I(\epsilon) = 2(1-\epsilon) \frac{\Gamma(2-\epsilon)\Gamma(1-\epsilon)\Gamma(-\epsilon)}{\Gamma(3-3\epsilon)} + 2 \frac{\Gamma(2-\epsilon)\Gamma^2(-\epsilon)}{\Gamma(2-3\epsilon)} - 2\epsilon \frac{\Gamma^3(1-\epsilon)}{\Gamma(3-3\epsilon)} \\ = \frac{\Gamma^3(1-\epsilon)}{\Gamma(1-3\epsilon)} \left(\frac{2}{\epsilon^2} + \frac{3}{\epsilon} + \frac{19}{2} + \mathcal{O}(\epsilon) \right), \quad (4.40)$$

where we repeatedly used $\Gamma(z+1) = z\Gamma(z)$. The $1/\epsilon^2$ divergence comes from the interference term and is therefore associated with the combined soft gluon and collinear divergence. The other $1/\epsilon$ pole corresponds to collinear divergences.


 Figure 4.3: Hadronic part of $e^+e^- \rightarrow q\bar{q}$ at next-to-leading order.

Finally, combining Eqs. (4.38) and (4.40) as well as the leptonic tensor in Eq. (4.20), we find the total cross section of $e^+e^- \rightarrow q\bar{q}g$ at leading order to be

$$\begin{aligned} \sigma_{q\bar{q}g}^{(0)} &= \frac{2C_F N_C e_q^2 \mu^{2\epsilon} \alpha_{\text{em}}^2 \alpha_s}{Q^2} \left(\frac{4\pi\mu^2}{Q^2} \right)^{2\epsilon} \frac{(1-\epsilon)^2}{3-2\epsilon} \frac{\Gamma^3(1-\epsilon)}{\Gamma(2-2\epsilon)\Gamma(1-3\epsilon)} \\ &\quad \times \left(\frac{2}{\epsilon^2} + \frac{3}{\epsilon} + \frac{19}{2} + \mathcal{O}(\epsilon) \right) \\ &= \sigma_{q\bar{q}}^{(0)} \frac{C_F \alpha_s}{2\pi} \left(\frac{4\pi\mu^2}{Q^2} \right)^\epsilon \frac{\Gamma^2(1-\epsilon)}{\Gamma(1-3\epsilon)} \left(\frac{2}{\epsilon^2} + \frac{3}{\epsilon} + \frac{19}{2} + \mathcal{O}(\epsilon) \right). \end{aligned} \quad (4.41)$$

4.4 Virtual gluon exchange

The next-to-leading order corrections to $e^+e^- \rightarrow q\bar{q}$ are shown in Fig. 4.3. In our perturbative series of the matrix element in Eq. (4.2), the $\mathcal{O}(\alpha_s)$ -contribution to the cross section is the interference between $\mathcal{M}_{q\bar{q}}^{(0)}$ and $\mathcal{M}_{q\bar{q}}^{(1)}$. Writing the amplitudes in terms of leptonic and hadronic tensors, we have

$$|\mathcal{M}_{q\bar{q}}|^2 = |\mathcal{M}_{q\bar{q}}^{(0)}|^2 + 2\alpha_s \Re \left\{ \mathcal{M}_{q\bar{q}}^{(0)*} \mathcal{M}_{q\bar{q}}^{(1)} \right\} + \dots = \frac{1}{Q^4} L_{\mu\nu} \left[\left(H_{q\bar{q}}^{(0)} \right)^{\mu\nu} + \alpha_s \left(H_{q\bar{q}}^{(1)} \right)^{\mu\nu} + \dots \right]$$

where the strong coupling was explicitly factored out. Thus, the hadronic tensor we are looking for at order $\mathcal{O}(\alpha_s)$ is the interference term

$$\alpha_s \left(H_{q\bar{q}}^{(1)} \right)^{\mu\nu} = 2\Re \left\{ \sum_{i,j,r,r'} \left(J_{q\bar{q}}^{(0)*} \right)^\mu \left(J_{q\bar{q}}^{(1)} \right)^\nu \right\}. \quad (4.42)$$

The only new part we need to calculate is $J_{q\bar{q}}^{(1)}$, which is the sum of the diagrams in Fig. 4.3.

Self-energy diagrams

The diagrams in Figs. 4.3b and 4.3c involve the one-loop gluon contribution to the quark self-energy, which for massless quarks is

$$i\Sigma = (\mu^\epsilon g_s)^2 C_F \delta_{ij} \int \frac{d^d g}{(2\pi)^d} \frac{\gamma_\mu (\not{g} + \not{q}) \gamma_\nu}{[g^2 + 2g \cdot q]^2 g^2} \left[\eta^{\mu\nu} - (1 - \xi_G) \frac{g^\mu g^\nu}{g^2} \right]. \quad (4.43)$$

The denominator in the integrand can be simplified using Feynman parameters, in particular by utilising the following identity:

$$\frac{1}{ab} = \int_0^1 dx \frac{1}{[a(1-x) + bx]^2}. \quad (4.44)$$

We get

$$\frac{1}{[g^2 + 2g \cdot q]^2 g^2} = \int_0^1 dx \frac{1}{[(g^2 + 2g \cdot q)x + (1-x)g^2]^2} = \int_0^1 dx \frac{1}{(g^2 + qx)^4},$$

where $q^2 = 0$ was used. The next step is to shift the integration variable, $g \rightarrow g - qx$, which does not alter the integration measure. Performing the shift in the numerator, it is straightforward to show that the self-energy is proportional to

$$i\Sigma \propto \not{q} \int_0^1 dx f(x) \int \frac{d^d g}{(2\pi)^d} \frac{1}{g^4}, \quad (4.45)$$

where f is some function of the Feynman parameter. In this expression, terms linear or cubic in g were dropped, due to their antisymmetry under $g \rightarrow -g$ which implies that they vanish when integrated over all g .

The integral in Eq. (4.45) is not convergent for any value of d . Moreover, for $d = 4$ it is both ultraviolet (UV) and IR divergent. This is an example of a *scaleless* integral, a loop-integral where one can scale the momenta and the result is proportional to the original integral, i.e. $I(\alpha k) = \alpha I(k)$. In dimensional regularization, we *define* scaleless integrals to be zero. This can be justified as follows: We introduce a scale Λ to separate the UV and IR divergent regions of the integral:

$$\int \frac{d^d k_E}{k_E^4} = \Omega_d \int_0^\Lambda dk_E k_E^{d-5} + \Omega_d \int_\Lambda^\infty dk_E k_E^{d-5} = \Omega_d \left(\frac{\Lambda^{-2\epsilon_{\text{IR}}}}{-2\epsilon_{\text{IR}}} - \frac{\Lambda^{-2\epsilon_{\text{UV}}}}{-2\epsilon_{\text{UV}}} \right). \quad (4.46)$$

Here, we used $d = 4 - 2\epsilon_{\text{IR}}$ for the first integral, with $\epsilon_{\text{IR}} < 0$, and $d = 4 - 2\epsilon_{\text{UV}}$ for the second integral, assuming $\epsilon_{\text{UV}} > 0$. The subscript E indicates that the momentum is Euclidean. We know that ϵ_{IR} and ϵ_{UV} must vanish from physical quantities, thus we can set $\epsilon_{\text{IR}} = \epsilon_{\text{UV}} = \epsilon$. Then the integral is 0. More physically, we could argue that the integral has dimension $d - 4$, but there is no available quantity with non-zero mass dimension, so it must vanish in d dimensions.

Consequently, the quark self-energy diagrams do not contribute to the cross section.

Vertex correction

We are left with the vertex correction in Fig. 4.3a; the hadron current is given by

$$\left(J_{q\bar{q}}^{(1)}\right)^\mu = \mu^{3\epsilon} e e_q g_s^2 T_{ik}^a T_{kj}^a \int \frac{d^d g}{(2\pi)^d} \frac{\bar{u}_r(q) \Gamma^\mu v_{r'}(\bar{q})}{g^2 (q+g)^2 (\bar{q}-g)^2}, \quad (4.47)$$

where

$$\begin{aligned} \Gamma^\mu &= \gamma_\rho (\not{q} + \not{g}) \gamma^\mu (\not{q} - \not{\bar{q}}) \gamma_\sigma \left(-\eta^{\rho\sigma} + (1 - \xi_G) \frac{g^\rho g^\sigma}{g^2} \right) \\ &= -\gamma_\rho (\not{q} + \not{g}) \gamma^\mu (\not{q} - \not{\bar{q}}) \gamma^\rho + \frac{1 - \xi_G}{g^2} \not{g} (\not{q} + \not{g}) \gamma^\mu (\not{q} - \not{\bar{q}}) \not{g}. \end{aligned} \quad (4.48)$$

The summation over colours gives a factor $C_F N_C$, and the summation over spins introduces a trace over Dirac matrices. Thus, the Lorentz index trace of the hadronic tensor from Eq. (4.42) becomes

$$\begin{aligned} \alpha_s \eta_{\mu\nu} \left(H_{q\bar{q}}^{(1)} \right)^{\mu\nu} &= 2\Re \sum_{i,j,r,r'} \left(J_{q\bar{q}}^{(0)*} \right)_\mu \left(J_{q\bar{q}}^{(1)} \right)^\mu = -2i C_F N_C \mu^{4\epsilon} (e e_q g_s)^2 \\ &\quad \times \int \frac{d^d g}{(2\pi)^d} \frac{\text{Tr} \left[\gamma^\mu \not{q} \Gamma_\mu \bar{\not{q}} \right]}{g^2 (q+g)^2 (\bar{q}-g)^2}. \end{aligned} \quad (4.49)$$

We use FORM to compute the trace, the result is

$$\begin{aligned} \mathcal{N} \equiv \text{Tr} \left[\gamma^\mu \not{q} \Gamma_\mu \bar{\not{q}} \right] &= -8(1 - \epsilon) \left[Q^4 - 4(q \cdot g)(\bar{q} \cdot g) - 2g \cdot (q - \bar{q}) Q^2 + \epsilon g^2 Q^2 \right] \\ &\quad - 4(1 - \epsilon) \frac{1 - \xi_G}{g^2} Q^2 (q+g)^2 (\bar{q}-g)^2. \end{aligned} \quad (4.50)$$

The factors $(q+g)^2$ and $(\bar{q}-g)^2$ in the second line cancels against the same factors in the denominator in Eq. (4.49). This gauge-dependent term is consequently proportional to

$$\int \frac{d^d g}{(2\pi)^d} \frac{1}{g^4},$$

which is scaleless and vanishes in DR.

To compute the integral in Eq. (4.49), we use the method of Feynman parameters. For three factors in the denominator, the method is based on the following identity:

$$\frac{1}{abc} = \int_0^1 dx \int_0^{1-x} dy \frac{2}{[ax + by + c(1-x-y)]^3}. \quad (4.51)$$

Using this relation, we write the denominator in Eq. (4.49) as

$$\begin{aligned} \frac{1}{g^2 (q+g)^2 (\bar{q}-g)^2} &= \int_0^1 dx \int_0^{1-x} dy \frac{2}{[x(q+g)^2 + y(\bar{q}-g)^2 + (1-x-y)g^2]^3} \\ &= \int_0^1 dx \int_0^{1-x} dy \frac{2}{[(g+xq-y\bar{q})^2 - xyQ^2]^3}. \end{aligned} \quad (4.52)$$

Next, we shift integration variable in the momentum integral, $g \rightarrow g - xp + y\bar{q}$. Shifting the numerator given by Eq. (4.50) yields

$$\mathcal{N} = -8(1 - \epsilon) \left[(1 - x - y + xy(1 - \epsilon))Q^4 - 2g \cdot (q - \bar{q} - (1 - \epsilon)(xq - y\bar{q}))Q^2 + \epsilon g^2 Q^2 - 4(g \cdot q)(g \cdot \bar{q}) \right].$$

We can omit the term linear in g , since it vanishes under integration. Furthermore, we can simplify the $(g \cdot q)(g \cdot \bar{q})$ -term via the following trick: Consider

$$\int \frac{d^d g}{(2\pi)^d} g^\mu g^\nu = \eta^{\mu\nu} \int \frac{d^d g}{(2\pi)^d} f(g^2). \quad (4.53)$$

The integral transforms as a tensor under Lorentz transformations, but does not depend on any quantity carrying a Lorentz index (g is integrated out). Thus it must be proportional to the only tensor available, $\eta^{\mu\nu}$, with an unknown isotropic function $f(g^2)$ in the integrand. Contracting both sides of the equation with $\eta_{\mu\nu}$ shows that $f(g^2) = g^2/d$. Therefore we can replace $g^\mu g^\nu \rightarrow \eta^{\mu\nu} g^2/d$, which gives

$$\mathcal{N} = -8(1 - \epsilon)Q^2 \left[(1 - x - y + xy(1 - \epsilon))Q^2 - \frac{(1 - \epsilon)^2}{2 - \epsilon} g^2 \right]. \quad (4.54)$$

We compute the g -integrals using Eq. (A.7),

$$\int \frac{d^d g}{(2\pi)^d} \frac{1}{[g^2 + xyQ^2]^3} = \frac{i}{2(4\pi)^2} \left(-\frac{4\pi}{Q^2} \right)^\epsilon \frac{1}{(xy)^\epsilon} \frac{1}{xyQ^2} \Gamma(1 + \epsilon), \quad (4.55a)$$

$$\int \frac{d^d g}{(2\pi)^d} \frac{g^2}{[g^2 + xyQ^2]^3} = \frac{i}{2(4\pi)^2} \left(-\frac{4\pi}{Q^2} \right)^\epsilon \frac{1}{(xy)^\epsilon} \Gamma(1 + \epsilon) \frac{2 - \epsilon}{\epsilon}. \quad (4.55b)$$

Here, the relation $\Gamma(z + 1) = z\Gamma(z)$ was applied to make the expressions easily comparable.

Combining Eqs. (4.49), (4.52), (4.54) and (4.55), we obtain

$$\alpha_s \eta_{\mu\nu} \left(H_{q\bar{q}}^{(1)} \right)^{\mu\nu} = -8N_C C_F e_q^2 \mu^{2\epsilon} \alpha_{\text{em}} \alpha_s Q^2 \Re \left\{ \left(-\frac{4\pi\mu^2}{Q^2} \right)^\epsilon (1 - \epsilon) \Gamma(1 + \epsilon) I(\epsilon) \right\} \quad (4.56)$$

with

$$I(\epsilon) = \int_0^1 dx \int_0^{1-x} dy \frac{1}{(xy)^\epsilon} \left[\frac{1 - x - y + xy(1 - \epsilon)}{xy} - \frac{(1 - \epsilon)^2}{\epsilon} \right]. \quad (4.57)$$

The integral $I(\epsilon)$ over Feynman parameters is solved by the substitution $y = (1 - x)v$ as well as similar manipulations to those solving Eq. (4.39) in the previous section. The result is

$$I(\epsilon) = \frac{1}{2} \frac{\Gamma^2(1 - \epsilon)}{\Gamma(1 - 2\epsilon)} \left(\frac{2}{\epsilon^2} + \frac{3}{\epsilon} + \frac{8}{1 - 2\epsilon} \right). \quad (4.58)$$

There is no dependence on the quark momenta in Eq. (4.56), hence we can use the phase space integral from Eq. (4.23). It follows that the next-to-leading order correction to the cross section is

$$\begin{aligned}\sigma_{q\bar{q}}^{(1)} &= \frac{C_F N_C e_q^2 \mu^{2\epsilon} \alpha_{\text{em}}^2 \alpha_s}{Q^2} \left(\frac{4\pi\mu^2}{Q^2} \right)^{2\epsilon} \Re\{(-1)^\epsilon\} \frac{(1-\epsilon)^2}{3-2\epsilon} \frac{\Gamma^3(1-\epsilon)\Gamma(1+\epsilon)}{\Gamma(1-2\epsilon)\Gamma(2-2\epsilon)} \\ &\quad \times \left(\frac{2}{\epsilon^2} + \frac{3}{\epsilon} + 8 + \mathcal{O}(\epsilon) \right) \\ &= \sigma_{q\bar{q}}^{(0)} \frac{C_F \alpha_s}{2\pi} \left(\frac{4\pi\mu^2}{Q^2} \right)^\epsilon \Re\{(-1)^\epsilon\} \frac{\Gamma^2(1-\epsilon)\Gamma(1+\epsilon)}{\Gamma(1-2\epsilon)} \left(\frac{2}{\epsilon^2} + \frac{3}{\epsilon} + 8 + \mathcal{O}(\epsilon) \right).\end{aligned}\tag{4.59}$$

In Eq. (4.59), we have successfully moved the divergences to the last parenthesis. It is illuminating to investigate what types of divergences the terms in the parenthesis represent. First, if we carefully inspect the integration of $I(\epsilon)$, we find that the $1/\epsilon^2$ -term originates from the first term in $I(\epsilon)$, Eq. (4.57). The integral of this term is only convergent when $\epsilon < 0$, thus the $1/\epsilon^2$ -term represent IR divergences. Second, tracing the $1/\epsilon$ -term back reveals that it arose from the momentum space integration in Eq. (4.55b). This integral is UV divergent, and only convergent for $\epsilon > 0$. The result becomes the second term in the Feynman parameter integral $I(\epsilon)$, but this integration needs no further constrictions on ϵ to converge. Thus, the $1/\epsilon$ -term corresponds to an UV divergence.

Evidently, we should have used two separate dimension parameters, e.g. ϵ_{IR} and ϵ_{UV} , regulating the IR and UV divergences with the corresponding constraints, respectively. However, we will demonstrate that both divergent terms cancel when combined with the cross section for real gluon emission.

4.5 Combined $\mathcal{O}(\alpha_s)$ correction

Combining the result from the real gluon emission and the virtual correction, we obtain the complete cross section for electron-positron annihilation to hadrons at $\mathcal{O}(\alpha_s)$,

$$\begin{aligned}\sigma &= \sigma_{q\bar{q}}^{(0)} \left\{ 1 + \frac{C_F \alpha_s}{2\pi} \left(\frac{4\pi\mu^2}{Q^2} \right)^\epsilon \frac{\Gamma^2(1-\epsilon)}{\Gamma(1-3\epsilon)} \left[\left(\frac{2}{\epsilon^2} + \frac{3}{\epsilon} + \frac{19}{2} + \mathcal{O}(\epsilon) \right) \right. \right. \\ &\quad \left. \left. + \Re\{(-1)^\epsilon\} \frac{\Gamma(1+\epsilon)\Gamma(1-3\epsilon)}{\Gamma(1-2\epsilon)} \left(\frac{2}{\epsilon^2} + \frac{3}{\epsilon} + 8 + \mathcal{O}(\epsilon) \right) \right] \right\} + \mathcal{O}(\alpha_s^2).\end{aligned}\tag{4.60}$$

To combine the terms, we expand the prefactor in the second line. The prefactor must be equal to one up to $\mathcal{O}(\epsilon^3)$ -terms for a cancellation of the poles to occur. We

use the expansion in Eq. (A.4), repeated here for convenience:

$$\Gamma(1 + \epsilon) = 1 - \epsilon\gamma_E + \frac{1}{2} \left(\gamma_E^2 + \frac{\pi^2}{6} \right) \epsilon^2 + \mathcal{O}(\epsilon^3). \quad (4.61)$$

From $(1 + x)^{-1} = 1 - x + x^2 - x^3 + \dots$, we also have

$$\begin{aligned} \Gamma^{-1}(1 - 2\epsilon) &= \left[1 + 2\epsilon\gamma_E + 2 \left(\gamma_E^2 + \frac{\pi^2}{6} \right) \epsilon^2 + \mathcal{O}(\epsilon^3) \right]^{-1} \\ &= 1 - 2\epsilon\gamma_E + 2 \left(\gamma_E^2 + \frac{\pi^2}{6} \right) \epsilon^2 + 4\gamma_E^2 \epsilon^2 + \mathcal{O}(\epsilon^3). \end{aligned} \quad (4.62)$$

Combining the Gamma functions yields

$$\frac{\Gamma(1 + \epsilon)\Gamma(1 - 3\epsilon)}{\Gamma(1 - 2\epsilon)} = 1 + \frac{(\pi\epsilon)^2}{2} + \mathcal{O}(\epsilon^3), \quad (4.63)$$

and when multiplied with $\Re\{(-1)^\epsilon\} = \Re\{\exp(i\pi\epsilon)\} = 1 - (\pi\epsilon)^2/2 + \mathcal{O}(\epsilon^4)$, we see that the ϵ^2 -terms cancel. Thus we can safely take the $\epsilon \rightarrow 0$ limit:

$$\sigma = \sigma_{q\bar{q}}^{(0)} \left\{ 1 + \frac{3C_F\alpha_s}{4\pi} + \mathcal{O}(\alpha_s^2) \right\} = \frac{4\pi N_C e_q^2 \alpha_{\text{em}}^2}{3Q^2} \left\{ 1 + \frac{3C_F\alpha_s}{4\pi} + \mathcal{O}(\alpha_s^2) \right\}. \quad (4.64)$$

We have demonstrated that the total cross section of electron-positron annihilation to hadrons at order $\mathcal{O}(\alpha_s)$ is free of IR divergences. An argument for why this is the case can be made as follows: Compared to the rapid quark production, which occurs in a time scale $1/\sqrt{Q^2}$, the emission and virtual exchange of soft or collinear gluons are very slow processes. The virtuality of the virtual quark (or antiquark) is $2q \cdot g$, and hence it lives for a time $1/(2q \cdot g)$ before it decays. At arbitrary long time and distance scales, the emission or virtual exchange of a gluon becomes indistinguishable, which suggests that both processes must be taken into account when considering quantities including soft or collinear regions.

Another point of view is that of experimental reality. Physical observables have to be measurable, and since any experimental instrument has a finite energy and angular resolution, it is not possible to detect soft or collinear splitting below these resolution limits. From this perspective, only the detectable gluon momenta should have been integrated over in the computation of the gluon emission cross section. The soft or collinear gluon emission is to be regarded as part of the cross section without emission. Thus, the cross sections of unresolved processes must be summed up.

The discussion above is generalised and made precise by the Kinoshita-Lee-Nauenberg (KLN) theorem, which states that a fully inclusive observable is free of IR divergences to all orders in a general quantum field theory [86, 87]. In general, the observable requires a summation of initial states as well as final states. However, we were able to avoid this since the initial state did not participate in QCD interactions.

5 Four approaches to Higgs decay

In this chapter, we consider the decay of a Higgs boson into charged W bosons at leading order. The decay rate of this process is usually computed in the unitary gauge where only physical particles appear in the Feynman diagrams. In addition to repeating the calculation in the unitary gauge, we will here compute the amplitude using three different approaches:

- (i) with the Goldstone boson equivalence theorem,
- (ii) in the Feynman-'t Hooft gauge, and
- (iii) using the optical theorem on a W -boson loop.

The various approaches are illustrative of multiple features of electroweak theory. Firstly, gauge invariance lets us choose any gauge to work with. In the gauges where the gauge bosons have unphysical degrees of freedom, Goldstone bosons and Faddeev-Popov ghosts appear to cancel these degrees of freedom. Secondly, in the limit of high energy, the unbroken theory becomes a valid description, rigorously guaranteed by the EQT. Third, unitarity implies that the imaginary part of a loop diagram corresponds to cutting the diagram and putting the cut lines on-shell.

5.1 Unitary gauge

We start with the unitary gauge ($\xi = \infty$), defined in Section 3.2. In this gauge the only leading order diagram contributing to $h \rightarrow W^+W^-$ is the one shown in Fig. 5.1. Let the Higgs boson have four-momentum q , and let p and p' be the four-momenta of W^+ and W^- , respectively. Using the Feynman rule in Eq. (B.14), we can immediately write down the amplitude for this diagram,

$$i\mathcal{M} = igm_W\eta^{\mu\nu}(\epsilon_s^*)_\mu(\epsilon_r^*)_\nu \quad (5.1)$$

where g is the weak coupling constant and m_W is the mass of the W boson. Furthermore, $(\epsilon_s)_\mu$ and $(\epsilon_r)_\mu$ are the polarisation vectors of the positive and negative charged gauge boson, respectively. The squared amplitude is

$$|\mathcal{M}|^2 = g^2m_W^2\eta^{\mu\nu}\eta^{\alpha\beta}(\epsilon_s^*)_\mu(\epsilon_r^*)_\nu(\epsilon_s)_\alpha(\epsilon_r)_\beta = g^2m_W^2(\epsilon_s^*)_\mu(\epsilon_r^*)^\mu(\epsilon_s)_\alpha(\epsilon_r)^\alpha. \quad (5.2)$$

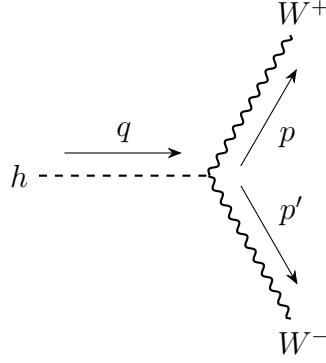


Figure 5.1: Leading order diagram for $h \rightarrow W^+W^-$ in the unitary gauge.

Since we are not interested in a particular polarisation of the final state gauge bosons, we sum over the different polarisations. From Eq. (3.55), we have that the polarisation sum in the unitary gauge for a gauge boson with mass m and momentum k is

$$\sum_t (\epsilon_t^*)_\mu (\epsilon_t)_\nu = -\eta_{\mu\nu} + \frac{k_\mu k_\nu}{m^2}. \quad (5.3)$$

Thus, we have

$$\begin{aligned} \overline{|\mathcal{M}|^2} &\equiv \sum_{s,r} |\mathcal{M}|^2 = g^2 m_W^2 \left(-\eta_{\mu\alpha} + \frac{p_\mu p_\alpha}{m_W^2} \right) \left(-\eta^{\mu\alpha} + \frac{p'^\mu p'^\alpha}{m_W^2} \right) \\ &= g^2 m_W^2 \left(2 + \frac{(p \cdot p')^2}{m_W^4} \right). \end{aligned} \quad (5.4)$$

We can use four-momentum conservation, $q = p + p'$, to write the scalar product in terms of particle masses.

$$\begin{aligned} q^2 &= p^2 + p'^2 + 2p \cdot p', \\ p \cdot p' &= \frac{1}{2}(m_h^2 - 2m_W^2) \equiv \frac{m_h^2}{2}(1 - 2z). \end{aligned} \quad (5.5)$$

Here we defined the mass ratio $z \equiv m_W^2/m_h^2$ for later convenience. The squared amplitude becomes

$$\overline{|\mathcal{M}|^2} = g^2 m_W^2 \left(2 + \frac{m_h^4}{4m_W^4}(1 - 2z)^2 \right) = \frac{g^2}{4} \left(\frac{m_h^2}{m_W} \right)^2 (1 - 4z + 12z^2). \quad (5.6)$$

Decay rate

The differential decay rate of a two-body decay in the CoM frame is given in Eq. (C.4), and repeated here for convenience:

$$d\Gamma = \frac{1}{32\pi^2} \frac{|\mathbf{p}|}{M^2} |\mathcal{M}|^2 d\Omega, \quad (5.7)$$

where M is the mass of the decaying particle, and \mathbf{p} is the momentum of either of the particles in the final state. To find the magnitude of the spacial momentum of the W -particle, we can calculate the scalar product $p \cdot p'$ in the CoM frame and compare with Eq. (5.5) (valid in any frame),

$$\frac{m_h^2}{2}(1 - 2z) = p \cdot p' = E^2 + |\mathbf{p}|^2 = m_W^2 + 2|\mathbf{p}|^2,$$

where we used that $E_{W^+} = E_{W^-}$ and $\mathbf{p} = -\mathbf{p}'$. Hence

$$|\mathbf{p}| = \frac{m_h^2}{2} \sqrt{1 - 4z}. \quad (5.8)$$

The Feynman amplitude in Eq. (5.6) has no angular dependence, we can therefore immediately integrate Eq. (5.7) over outgoing solid angles to obtain the total decay rate

$$\Gamma_{h \rightarrow W^+ W^-} = \frac{g^2}{64\pi} \frac{m_h^3}{m_W^2} \sqrt{1 - 4z} (1 - 4z + 12z^2). \quad (5.9)$$

This result agrees with e.g. Eq. (2.3) in Ref. [88, sec. XV].

5.2 Goldstone boson equivalence theorem

This section illustrates the EQT in the case of Higgs decay into charged gauge bosons. As explained in Section 3.3, the theorem states that in the limit of high energy, the amplitude of emission or absorption of a longitudinal gauge boson becomes equal to the amplitude of emission or absorption of the corresponding Goldstone boson. In the case of Higgs decay to W bosons, the high-energy limit corresponds to the Higgs mass being much larger than the W mass, $m_h \gg m_W$. We compute first the decay into longitudinal polarised W bosons, and compare the result in the high-energy limit to that of Higgs decay into Goldstone bosons.

The calculation of the amplitude of $h \rightarrow W_L^+ W_L^-$ mirrors the one in Section 5.1, except for the polarisation sum. We saw in Section 3.3 that the polarisation vectors for longitudinal vector bosons become proportional to k^μ at high energy, therefore the polarisation sum is

$$\sum_t (\epsilon_t^*)_\mu (\epsilon_t)_\nu = \frac{k_\mu k_\nu}{m_2}. \quad (5.10)$$

It follows that the squared amplitude summed over polarisations is given by

$$\begin{aligned} \overline{|\mathcal{M}_{W_L}|^2} &= g^2 m_W^2 \left(\frac{p_\mu p_\alpha}{m_W^2} \right) \left(\frac{p'^\mu p'^\alpha}{m_W^2} \right) = g^2 m_W^2 \frac{(p \cdot p')^2}{m_W^4} \\ &= \frac{g^2}{4} \left(\frac{m_h^2}{m_W} \right)^2 (1 - 4z + 4z^2) \end{aligned} \quad (5.11)$$

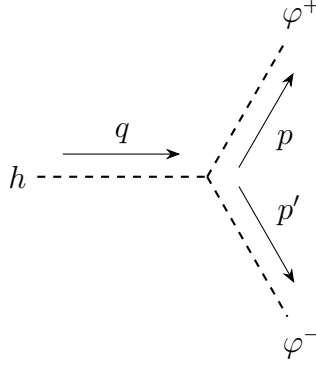


Figure 5.2: Leading order diagram for Higgs decay into Goldstone bosons.

where we used Eq. (5.5) and $z = m_W^2/m_h^2$. In the high-energy limit, z goes to zero, so

$$\overline{|\mathcal{M}_{W_L}|^2} \longrightarrow \frac{g^2}{4} \left(\frac{m_h^2}{m_W} \right)^2. \quad (5.12)$$

Comparing the result with Eq. (5.6), we note that the leading term of that result is associated with the longitudinal component.

Next, we consider Higgs decay into Goldstone bosons, see Fig. 5.2. Since all particles involved in this process are scalars, the squared amplitude is simply the square of the vertex factor in Eq. (B.15),

$$\overline{|\mathcal{M}_{\varphi^\pm}|^2} = \frac{g^2}{4} \left(\frac{m_h^2}{m_W} \right)^2. \quad (5.13)$$

This result is exactly equal to the high-energy limit in Eq. (5.12), as predicted by the EQT.

5.3 Feynman-'t Hooft gauge

We will now consider Higgs decay in the Feynman-'t Hooft gauge ($\xi = 1$). In this gauge, there are additional (unphysical) particles which couples to the Higgs particle: charged Goldstone bosons φ^+ and φ^- , and Faddeev-Popov ghosts c^+ and c^- from the W^\pm gauge fixing condition. At leading order, the diagrams contributing are shown in Fig. 5.3. In all diagrams we label q as the four-momentum of the Higgs boson, while p is the four momentum of W^+ , φ^+ and c^+ , and p' is the four-momentum of W^- , φ^- and c^- .

We begin with Fig. 5.3a and compute the amplitude of this process in the Feynman-'t Hooft gauge. The calculation follows closely that of Section 5.1, except that in this

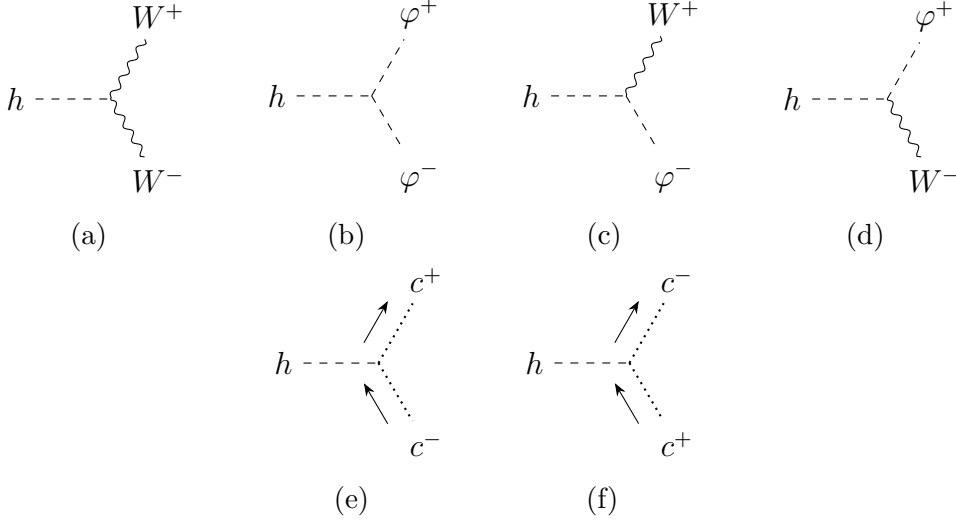


Figure 5.3: Diagrams contributing to Higgs decay into charged bosons in the Feynman-'t Hooft gauge. The arrows next to the ghost lines indicate if it is a particle or antiparticle.

gauge we replace the polarisation sum as follows:

$$\sum_t (\epsilon_t^*)_\mu (\epsilon_t)_\nu = -\eta_{\mu\nu}. \quad (5.14)$$

Thus, the squared amplitude summed over polarisations becomes

$$\overline{|\mathcal{M}_{WT}|^2} = g^2 m_W^2 (-\eta_{\mu\alpha})(-\eta^{\mu\alpha}) = 4g^2 m_W^2 = \frac{g^2}{4} \left(\frac{m_h^2}{m_W} \right)^2 (16z^2), \quad (5.15)$$

with $z = m_W^2/m_h^2$.

We already computed the amplitude of the diagram in Fig. 5.3b in Section 5.2, the matrix element is given in Eq. (5.13).

Third, we consider the diagrams in Figs. 5.3c and 5.3d. Their vertex factors are equal up to a change of sign (see Eq. (B.16)), so the squared Feynman amplitude is equal for the two diagrams. It is given by

$$|\mathcal{M}_{W\varphi}|^2 = \frac{g^2}{4} (q+p)^\mu (q+p)^\nu (\epsilon_s^*)_\mu (\epsilon_s^*)_\nu.$$

Using the polarisation sum in Eq. (5.14), we obtain

$$\overline{|\mathcal{M}_{W\varphi}|^2} = -\frac{g^2}{4} (q+p)^2. \quad (5.16)$$

As in Section 5.1, we use four-momentum conservation to express the scalar product:

$$\begin{aligned} m_W^2 = p^2 &= (q - p')^2 = m_h^2 + m_W^2 - 2q \cdot p' \\ 2q \cdot p' &= m_h^2, \end{aligned}$$

and consequently

$$(q + p') = 2m_h^2 + m_W^2. \quad (5.17)$$

The result becomes

$$\overline{|\mathcal{M}_{W\varphi}|^2} = \frac{g^2}{4} \left(\frac{m_h^2}{m_W} \right)^2 (-2z - z^2). \quad (5.18)$$

Finally, we compute the ghost diagrams in Figs. 5.3e and 5.3f. The amplitude for both diagrams is merely the vertex factor in Eq. (B.17),

$$i\mathcal{M} = -\frac{i}{2}gm_W.$$

For $2n$ external Faddeev-Popov ghosts, we must include a factor $(-1)^n$ in order to cancel the unphysical contributions to the squared amplitude in this gauge [81, sec. 10.3]. This follows from the fact that ghost fields are anticommuting scalars. Hence, we multiply the squared amplitude with (-1) ,

$$\overline{|\mathcal{M}_{W\varphi}|^2} = (-1) \frac{g^2 m_W^2}{4} = \frac{g^2}{4} \left(\frac{m_h^2}{m_W} \right)^2 (-z^2). \quad (5.19)$$

We are ready to sum the contributions from the diagrams in Fig. 5.3. Figures 5.3c and 5.3d and Figs. 5.3e and 5.3f have equal amplitudes, therefore we count the contributions from Eqs. (5.18) and (5.19) twice. The sum is

$$\overline{|\mathcal{M}|^2} = \frac{g^2}{4} \left(\frac{m_h^2}{m_W} \right)^2 (1 - 4z + 12z^2), \quad (5.20)$$

which is in agreement with the result in the unitary gauge, Eq. (5.6).

5.4 Charged boson loop

We consider a W boson loop correction to the Higgs self-energy, shown in Fig. 5.4. We will calculate this diagram in the unitary gauge, and show that the imaginary part equals the decay rate obtained in Eq. (5.9). This is a consequence of the optical theorem, as we will demonstrate in the first paragraph. The loop-diagram is UV divergent, i.e. it diverges for large momenta. We must therefore use a regularisation scheme to separate the result in a divergent and a finite part.

Optical theorem

In quantum field theory, the scattering matrix or S -matrix encodes all information about how initial states and final states evolve in time. It is defined in the Heisenberg picture, where states are stationary and all time-dependence is put into operators. Thus, a state $|i; t = -\infty\rangle$ evolves into $|f; t = \infty\rangle$ with amplitude given by the inner product

$$\langle f|S|i\rangle_{\text{H}} = \langle f; t = \infty|i; t = -\infty\rangle_{\text{S}}. \quad (5.21)$$

Here, the subscripts denote the Schrödinger and Heisenberg pictures. In this definition, it is assumed that all interactions happen in a finite time interval, so that the asymptotic states $|i\rangle$ and $|f\rangle$ are free of interactions. The probability of evolution from an initial state to a final state is given by the squared amplitude, $\langle f|S|i\rangle^2$. Conservation of probability then implies that the S -matrix must be unitary. One important consequence of this is the optical theorem.

We can split the S -matrix into a trivial and a transition part: $S = \mathbf{1} + iT$. Then unitarity implies

$$iT^\dagger T = T - T^\dagger. \quad (5.22)$$

Expressing the transition matrix as a matrix element times a momentum-conserving delta function, and putting the right hand side in between asymptotic states, one obtains

$$\langle f|T|i\rangle - \langle i|T|f\rangle^* = (2\pi)^4 \delta^4(p_i - p_f) [\mathcal{M}_{if} - \mathcal{M}_{fi}^*].$$

Inserting a complete set of states, the left hand side of Eq. (5.22) becomes

$$i\langle f|T^\dagger T|i\rangle = \sum_X \int d\Pi_X (2\pi)^8 \delta^4(p_i - p_X) \delta^4(p_f - p_X) \mathcal{M}_{iX} \mathcal{M}_{fX}^*,$$

where $d\Pi_X$ is the Lorentz invariant phase space for multi-particle state X (it equals $d\Phi_X$ defined in Eq. (C.2), except the delta function is factored out). Setting these expressions equal and cancelling the overall delta function gives the generalised optical theorem:

$$\mathcal{M}_{if} - \mathcal{M}_{fi}^* = i \sum_X \int d\Pi_X (2\pi)^4 \delta^4(p_i - p_X) \mathcal{M}_{iX} \mathcal{M}_{fX}^*. \quad (5.23)$$

One important special case of the generalised theorem is the forward scattering amplitude when $|i\rangle = |f\rangle = |A\rangle$. Then,

$$2i\Im \mathcal{M}_{AA} = i \sum_X \int d\Pi_X (2\pi)^4 \delta^4(p_A - p_X) |\mathcal{M}_{AX}|^2. \quad (5.24)$$

Comparing this to the decay rate of a one-particle state $|i\rangle$,

$$\Gamma_{A \rightarrow X} = \frac{1}{2m_A} \int d\Pi_X (2\pi)^4 \delta^4(p_A - p_X) |\mathcal{M}_{AX}|^2,$$

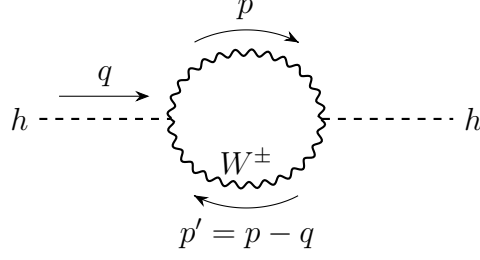


Figure 5.4: Charged gauge boson correction to the Higgs self-energy.

we obtain

$$\Im \mathcal{M}_{AA} = m_A \sum_X \Gamma_{A \rightarrow X}. \quad (5.25)$$

Thus, the imaginary part of the exact propagator equals the mass times the total decay rate. In our case of Higgs decay to W bosons, this equation tells us that

$$\Im \left\{ \text{---} \text{---} \text{---} \right\} = m_h \left| \text{---} \text{---} \right|^2, \quad (5.26)$$

which we will verify in this section.

Self-energy diagram

Let q be the four-momentum of the Higgs boson, and let p and $p' = p - q$ be the four-momenta of the bosons in the loop. The one-loop correction to the self-energy in Fig. 5.4 is

$$\begin{aligned} i\Pi &= (igm_W^2)^2 \\ &\times \int \frac{d^4 p}{(2\pi)^4} \left(-\eta_{\mu\nu} + \frac{p_\mu p_\nu}{m_W^2} \right) \left(-\eta^{\mu\nu} + \frac{p'_\mu p'_\nu}{m_W^2} \right) \frac{i}{p^2 - m_W^2 + i\epsilon} \frac{i}{(p')^2 - m_W^2 + i\epsilon}. \end{aligned} \quad (5.27)$$

This integral is UV divergent, so we will use DR and compute it in $d = 4 - 2\epsilon$ dimensions. Then we can separate the result in a divergent term and a finite remainder. As we will see, the imaginary part of the self-energy, which is what we are interested in, is finite.

We expand the parenthesis in Eq. (5.27), using that in d dimensions $\eta_{\mu\nu}\eta^{\mu\nu} = d$. To make the coupling constant stay dimensionless in DR, we supply a scale μ with mass dimension 1,

$$g \rightarrow \mu^{2-d/2} g = \mu^\epsilon g.$$

Thus, the matrix element becomes

$$\begin{aligned} i\Pi &= \frac{\mu^{2\epsilon} g^2}{m_W^2} \int \frac{d^d p}{(2\pi)^d} \frac{(p^2 - p \cdot q)^2 - m_W^2(2p^2 + q^2 - 2p \cdot q) + dm_W^4}{(p^2 - m_W^2 + i\epsilon)((p - q)^2 - m_W^2 + i\epsilon)} \\ &\equiv \frac{\mu^{2\epsilon} g^2}{m_W^2} \int \frac{d^d p}{(2\pi)^d} \frac{\mathcal{N}}{\mathcal{D}}, \end{aligned} \quad (5.28)$$

where we defined \mathcal{N} and \mathcal{D} as shorthands for the numerator and denominator.

The evaluation of this integral will proceed in the same manner as in Section 4.4. We will use Feynman parameters, and in particular utilise the following identity:

$$\frac{1}{ab} = \int_0^1 dx \frac{1}{[a(1-x) + bx]^2}. \quad (5.29)$$

The denominator \mathcal{D} becomes

$$\begin{aligned} \frac{1}{\mathcal{D}} &= \int_0^1 dx \frac{1}{[(p^2 - m_W^2 + i\epsilon)(1-x) + ((p-q)^2 - m_W^2 + i\epsilon)x]^2} \\ &= \int_0^1 dx \frac{1}{[(p-qx)^2 - \Delta]^2} \end{aligned}$$

with

$$\Delta \equiv -q^2 x(1-x) + m_W^2 - i\epsilon.$$

Having completed the square in the denominator, we can now shift $p \rightarrow p + qx$. This transformation does not affect the integral measure $d^d p$, since it is a linear shift.

Next, we evaluate the numerator after the integration variable shift. We discard terms which are linear or cubic in p , hence

$$\begin{aligned} \mathcal{N} &= (p^2)^2 + (p \cdot q)^2(1-2x)^2 - 2p^2 q^2 x(1-x) - 2p^2 m_W^2 \\ &\quad + (q^2)^2 x^2(1-x)^2 - q^2 m_W^2(1-2x+2x^2) + dm_W^4. \end{aligned} \quad (5.30)$$

We can perform the substitution $(p \cdot q)^2 \rightarrow p^2 q^2 / d$ by the argument below Eq. (4.53). The result is

$$\mathcal{N} = (p^2)^2 + p^2 \left(A + \frac{B}{d} \right) + C + dm_W^4, \quad (5.31)$$

where some simplifying definitions were made:

$$A = -2q^2 x(1-x) - 2m_W^2, \quad (5.32a)$$

$$B = q^2(1-2x)^2, \quad (5.32b)$$

$$C = (q^2)^2 x^2(1-x)^2 - q^2 m_W^2(1-2x+2x^2). \quad (5.32c)$$

We are now ready to perform the p -integral. The relevant integrals are special cases of Eq. (A.7), hence

$$\begin{aligned}
 i\Pi &= \frac{\mu^{2\epsilon} g^2}{m_W^2} \int_0^1 dx \int \frac{d^d p}{(2\pi)^d} \frac{(p^2)^2 + p^2 \left(A + \frac{B}{d}\right) + C + dm_W^4}{[p^2 - \Delta]^2}, \\
 &= \frac{\mu^{2\epsilon} g^2}{m_W^2} \int_0^1 dx \frac{i\Delta^{d/2}}{(4\pi)^{d/2}} \\
 &\quad \times \left\{ \frac{\Gamma(2 + d/2)\Gamma(-d/2)}{\Gamma(2)\Gamma(d/2)} - \frac{d\Gamma(1 - d/2)}{2\Delta} \left(A + \frac{B}{d}\right) + \frac{\Gamma(2 - d/2)}{\Delta^2} (C + dm_W^4) \right\}.
 \end{aligned} \tag{5.33}$$

To combine the terms in the curly bracket, we use the identity $\Gamma(z + 1) = z\Gamma(z)$, which yields that

$$\frac{\Gamma(2 + d/2)\Gamma(-d/2)}{\Gamma(2)\Gamma(d/2)} = \frac{2 + d}{d - 2} \Gamma(2 - d/2) \tag{5.34}$$

and

$$\frac{d}{2} \Gamma(1 - d/2) = \frac{d}{2 - d} \Gamma(2 - d/2). \tag{5.35}$$

We get

$$\begin{aligned}
 \Pi &= \frac{1}{(4\pi)^{d/2}} \frac{\mu^{2\epsilon} g^2}{m_W^2} \Gamma(2 - d/2) \int_0^1 dx \Delta^{d/2} \\
 &\quad \times \left\{ \frac{2 + d}{d - 2} - \frac{d}{2 - d} \frac{1}{\Delta} \left(A + \frac{B}{d}\right) + \frac{1}{\Delta^2} (C + dm_W^4) \right\}.
 \end{aligned} \tag{5.36}$$

The UV divergence is now isolated in $\Gamma(2 - d/2) = \Gamma(\epsilon)$. We take ϵ small, and Taylor expand to order $\mathcal{O}(\epsilon)$.

$$\begin{aligned}
 \Gamma(\epsilon) &= \frac{1}{\epsilon} - \gamma_E + \mathcal{O}(\epsilon), \\
 \mu^{2\epsilon} \left(\frac{\Delta}{4\pi}\right)^{d/2} &= \mu^{2\epsilon} \left(\frac{\Delta}{4\pi}\right)^{2-\epsilon} = \frac{\Delta^2}{(4\pi)^2} \left[1 + \epsilon \ln \left(\frac{4\pi\mu^2}{\Delta}\right) + \mathcal{O}(\epsilon) \right]
 \end{aligned}$$

so that

$$\mu^{2\epsilon} \left(\frac{\Delta}{4\pi}\right)^{2-\epsilon} \Gamma(\epsilon) = \frac{\Delta^2}{(4\pi)^2} \left[\frac{1}{\epsilon} + \ln \left(\frac{\tilde{\mu}^2}{\Delta}\right) + \mathcal{O}(\epsilon) \right], \tag{5.37}$$

with $\tilde{\mu}^2 \equiv 4\pi e^{-\gamma_E} \mu^2$. Furthermore, we expand the ϵ -dependent terms in the curly

bracket and discard terms of second or higher order. The result is

$$\begin{aligned}
 \Pi &= \frac{1}{(4\pi)^2} \frac{g^2}{m_W^2} \int_0^1 dx \left(\frac{1}{\epsilon} + \ln \left(\frac{\tilde{\mu}^2}{\Delta} \right) \right) \\
 &\quad \times \left\{ \Delta^2(3+2\epsilon) + \Delta(2+\epsilon)A + \frac{1}{2}\Delta(1+\epsilon)B + C + 2(2-\epsilon)m_W^4 \right\} \\
 &= \frac{1}{(4\pi)^2} \frac{g^2}{m_W^2} \int_0^1 dx \left\{ \frac{1}{\epsilon} \left(3\Delta^2 + 2\Delta A + \frac{1}{2}\Delta B + C + 4m_W^4 \right) \right. \\
 &\quad \left. + \left(2\Delta^2 + \Delta A + \frac{1}{2}\Delta B - 2m_W^4 \right) \right. \\
 &\quad \left. + \ln \left(\frac{\tilde{\mu}^2}{\Delta} \right) \left(3\Delta^2 + 2\Delta A + \frac{1}{2}\Delta B + C + 4m_W^4 \right) \right\}, \quad (5.38)
 \end{aligned}$$

where we excluded terms of order ϵ . The first term in the integrand contains the UV divergence, and it can be subtracted in an appropriate renormalisation scheme.

Imaginary part

The only part in Eq. (5.38) that develops an imaginary part is the logarithm for negative argument. The principal value of the complex logarithm is defined as

$$\text{Log}(z) = \ln|z| + i \text{Arg } z, \quad (5.39)$$

which implies that $\Im(\text{Log}(x \pm i\epsilon)) = \pm\pi$ for $x \in \mathbb{R}_-$. Here, ϵ is an infinitesimal shift into the complex plane due to the principal value being discontinuous for negative real numbers. We find the interval where Δ is negative by identifying its roots,

$$-q^2x(1-x) + m_W^2 = 0 \quad \implies \quad x_{\pm} = \frac{1}{2} \pm \frac{1}{2} \sqrt{1 - \frac{4m_W^2}{q^2}}. \quad (5.40)$$

Thus $\Delta < 0$ for $x \in (x_-, x_+)$. The $i\epsilon$ -term in the definition of Δ (which follows from the Feynman prescription in the propagator definition) tells us to approach the discontinuity in the complex plane from above, picking up a factor $+\pi$. Consequently, the imaginary part of the amplitude is given by

$$\begin{aligned}
 \Im(\Pi) &= \frac{\pi}{(4\pi)^2} \frac{g^2}{m_W^2} \int_{x_-}^{x_+} dx \left(3\Delta^2 + 2\Delta A + \frac{1}{2}\Delta B + C + 4m_W^4 \right) \\
 &= \frac{1}{64\pi} \frac{g^2}{m_W^2} \sqrt{1 - \frac{4m_W^2}{q^2}} \left(q^4 - 4q^2m_W^2 + 12m_W^4 \right). \quad (5.41)
 \end{aligned}$$

Introducing again the mass ratio $z = m_W^2/m_h^2$, we write the result as

$$\Im \left(\Pi(q^2 = m_h^2) \right) = \frac{g^2}{64\pi} \left(\frac{m_h}{m_W} \right)^2 \sqrt{1 - 4z} (1 - 4z + 12z^2). \quad (5.42)$$

Comparing with Eq. (5.9), we have a confirmation of the optical theorem,

$$\Im \left(\Pi(q^2 = m_h^2) \right) = m_h \Gamma_{h \rightarrow W^+ W^-}. \quad (5.43)$$

6 Electroweak bremsstrahlung corrections

In this chapter, we apply the Goldstone boson equivalence theorem to electroweak bremsstrahlung corrections to quark pair production. We restrict ourselves to s-channel processes where the mediator is a virtual photon, which means that we can perform the same tensor factorisation as we did in Chapter 4. Thus we effectively consider decay of a virtual photon. To combine our results with an explicit observable, we consider an electron-positron initial state, and compute the total cross section ratio of W bremsstrahlung to tree-level quark production. We include a calculation of unpolarised W emission for comparison. The longitudinal component have a unitarity-violating high-energy behaviour, but by the EQT it equals the corresponding Goldstone boson, and should be well-behaved. Hence, we conclude that when including all sub-processes at a given order, the leading, unitarity-violating terms cancel.

6.1 Explicit calculations

We compute in this section the process $\gamma^* \rightarrow u\bar{d}W^-$ for a transverse W^- boson, the corresponding Goldstone boson and finally, for an unpolarised W^- boson. In order to employ the EQT, we consider an energetic photon with four-momentum $Q^2 \gg m_W^2$. At this scale it is a reasonable approximation to assume that the light quarks are massless, which simplifies our calculations.

We will use similar notation to that in Chapter 4, so $H^{\mu\nu}$ denotes a squared current analogous to the hadron tensor and $H(Q^2)$ is the Lorentz index trace of the squared current integrated over phase space, as defined in Section 4.2. The quark and antiquark spins are labeled r and r' , respectively, and e_u is the electric charge of the u quark in units of e .

Transverse W boson emission

The Feynman diagram for $\gamma^* \rightarrow u\bar{d}W^-$ is shown in Fig. 6.1. Applying relevant Feynman rules from Appendix B, we find the current to be

$$J_W^\mu = -i \frac{eg}{\sqrt{2}} e_u (\epsilon_t^*)_\rho \bar{u}_r(p_u) \left[\gamma^\mu \frac{-\not{p}_d + \not{k} + m_d}{(p_d + k)^2 - m_d^2} \gamma^\rho P_L \right] v_{r'}(p_d) \quad (6.1)$$

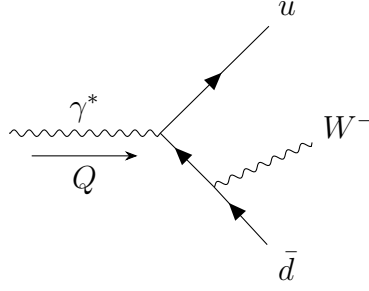


Figure 6.1: Electroweak bremsstrahlung correction to quark production.

where p_u , p_d and k are the momenta of the u quark, d quark and the W^- boson, respectively. The polarisation vector of the gauge boson is ϵ_t , and $P_L = (1 - \gamma^5)/2$ is the left-chiral projection operator. The weak coupling constant is denoted by g .

We construct the tensor $H_W^{\mu\nu}$ by squaring the current and summing over polarisations:

$$H_W^{\mu\nu} = \sum_t (\epsilon_t^*)_\rho (\epsilon_t)_\sigma \sum_{r,r'} (J_W)^{\mu\rho} (J_W^*)^{\nu\sigma}. \quad (6.2)$$

Here, we also factored out the polarisation vectors. In the unitary gauge, the polarisation sum for unpolarised weak gauge bosons is

$$\mathcal{P}^{\rho\sigma} \equiv \sum_t \epsilon_t^{*\rho} \epsilon_t^\sigma = -\eta^{\rho\sigma} + \frac{k^\rho k^\sigma}{m^2}. \quad (6.3)$$

We found in Section 3.3 that $\epsilon_L^\rho = k^\rho/m$ in the high-energy limit. Thus, in this limit, the first and second term in Eq. (6.3) come from the transverse and longitudinal degrees of freedom, respectively, so that we can replace

$$\sum_t (\epsilon_t^*)_\rho (\epsilon_t)_\sigma \rightarrow -\eta_{\rho\sigma}. \quad (6.4)$$

Furthermore, we will eventually contract $H_W^{\mu\nu}$ with $\eta_{\mu\nu}$, doing it right away simplifies calculations,

$$\eta_{\mu\nu} H_W^{\mu\nu} = - \sum_{r,r'} (J_W)^{\mu\rho} (J_W^*)_{\mu\rho}. \quad (6.5)$$

The spinor index sum can once again be expressed as a trace over Dirac matrices. We neglect the quark masses, hence

$$\eta_{\mu\nu} H_W^{\mu\nu} = - \frac{N_C e_u^2 (eg)^2}{8} \frac{1}{[2(p_d \cdot k) + m_W^2]^2} \text{Tr} \left\{ \not{p}_u \Gamma^{\mu\rho} \not{p}_d \bar{\Gamma}_{\mu\rho} \right\}, \quad (6.6)$$

where we defined

$$\Gamma^{\mu\rho} = \gamma^\mu (-\not{p}_d - \not{k}) \gamma^\rho (1 - \gamma^5), \quad (6.7a)$$

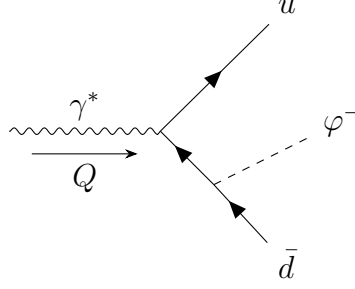


Figure 6.2: Emission of a Goldstone boson from the quark current.

and consequently

$$\bar{\Gamma}_{\mu\rho} = (1 + \gamma^5)\gamma_\rho(-\not{p}_d - \not{k})\gamma_\mu. \quad (6.7b)$$

The sign of γ^5 changed in the last line due to the anticommutation property $\{\gamma^5, \gamma^\mu\} = 0$. The trace is computed by FORM, with the following result:

$$\text{Tr} \left\{ \not{p}_u \Gamma^{\mu\rho} \not{p}_d \bar{\Gamma}_{\mu\rho} \right\} = 64(p_u \cdot k)(p_d \cdot k) - 32m_W^2(p_u \cdot p_d). \quad (6.8)$$

It follows that the squared current is given by

$$\eta_{\mu\nu} H_W^{\mu\nu} = \frac{4N_C e_u^2 (eg)^2}{[2(p_d \cdot k) + m_W^2]^2} \left[m_W^2(p_u \cdot p_d) - 2(p_u \cdot k)(p_d \cdot k) \right]. \quad (6.9)$$

Goldstone boson emission

We go on to the emission of the corresponding Goldstone boson from the d quark. The Feynman diagram is shown in Fig. 6.2. We use the Feynman rule in Eq. (B.12), and get the following expression for the current:

$$J_\varphi^\mu = i \frac{e_u eg}{\sqrt{2}} \bar{u}_r(p_u) \left[\gamma^\mu \frac{-(\not{p}_d + \not{p}_\varphi) + m_d}{(p_d + p_\varphi)^2 - m_d^2} (g_u P_L - g_d P_R) \right] v_{r'}(p_d). \quad (6.10)$$

Here, we defined the coupling constants $g_u \equiv m_u/m_W$ and $g_d \equiv m_d/m_W$ for Goldstone boson interaction with a pair of right-left- and left-right-chiral fermions, respectively. The quark masses are set to zero, but we keep the mass ratios g_u and g_d non-zero (if these are zero, the current is zero). The momentum of the Goldstone boson is denoted by p_φ . We obtain the following expression for the squared current summed over quark polarisation:

$$\eta_{\mu\nu} H_\varphi^{\mu\nu} = \frac{N_C e_u^2 (eg)^2}{8} \frac{1}{[2(p_d \cdot p_\varphi) + m_W^2]^2} \text{Tr} \left\{ \not{p}_u \Gamma^\mu \not{p}_d \bar{\Gamma}_\mu \right\}, \quad (6.11)$$

where

$$\Gamma^\mu = \gamma^\mu(-\not{p}_d - \not{p}_\varphi) [g_u(1 - \gamma^5) - g_d(1 + \gamma^5)], \quad (6.12a)$$

$$\bar{\Gamma}_\mu = [g_u(1 + \gamma^5) - g_d(1 - \gamma^5)] (-\not{p}_d - \not{p}_\varphi) \gamma_\mu. \quad (6.12b)$$

The trace evaluates to

$$\text{Tr} \{ \not{p}_u \Gamma^\mu \not{p}_d \bar{\Gamma}_\mu \} = (g_u^2 + g_d^2) [16m_W^2(p_u \cdot p_d) - 32(p_u \cdot p_\varphi)(p_d \cdot p_\varphi)], \quad (6.13)$$

from which it follows that

$$\eta_{\mu\nu} H_\varphi^{\mu\nu} = \frac{2N_C e_u^2 (eg)^2 (g_u^2 + g_d^2)}{[2(p_d \cdot p_\varphi) + m_W^2]^2} [m_W^2(p_u \cdot p_d) - 2(p_u \cdot p_\varphi)(p_d \cdot p_\varphi)]. \quad (6.14)$$

Comparing this expression to Eq. (6.9), we observe that the momentum dependence of the squared currents are equal. In particular, we have

$$2\eta_{\mu\nu} H_\varphi^{\mu\nu}(k) = (g_u^2 + g_d^2) \eta_{\mu\nu} H_W^{\mu\nu}(k), \quad (6.15)$$

where the H -tensors are written as functions of the emitted particle's momentum. The kinematic constraints for the momentum of the W boson and for the Goldstone boson are identical since the masses are equal. Therefore, the phase space integration for emission of a W boson and a Goldstone boson are equivalent, and we can sum the contributions straight away:

$$\eta_{\mu\nu} H^{\mu\nu} \equiv \eta_{\mu\nu} (H_W^{\mu\nu} + H_\varphi^{\mu\nu}) = \left(1 + \frac{g_u^2 + g_d^2}{2}\right) \eta_{\mu\nu} H_W^{\mu\nu}. \quad (6.16)$$

Phase space integration

The phase space integral for three outgoing particles is rather complicated, so we simplify it by additionally setting the mass of the emitted boson to zero in the kinematical constraints defining the available phase space. Then we can use the momentum fractions defined in Eq. (C.18). They satisfy $x_u + x_d + x_k = 2$, and we have

$$1 - x_u = \frac{2p_d \cdot k}{Q^2}, \quad 1 - x_d = \frac{2p_u \cdot k}{Q^2} \quad \text{and} \quad 1 - x_k = \frac{2p_u \cdot p_d}{Q^2}.$$

Inserting these definitions into Eq. (6.16) yields

$$\eta_{\mu\nu} H^{\mu\nu} = N_C e_u^2 (eg)^2 (2 + g_u^2 + g_d^2) \frac{(1 - x_k) \cdot 1/z - (1 - x_u)(1 - x_d)}{(1 - x_u + 1/z)^2}, \quad (6.17)$$

where we defined $z \equiv Q^2/m_W^2$. Next, we perform the phase space integration. Using the result from Eq. (C.25), we have

$$\begin{aligned} H(Q^2) &= -\eta_{\mu\nu} \int d\Phi_3 H^{\mu\nu} \\ &= \frac{Q^2}{(4\pi)^3} N_C e_u^2 (eg)^2 (2 + g_u^2 + g_d^2) \\ &\quad \times \int_0^1 dx_u \int_{1-x_u}^1 dx_d \left[\frac{(1-x_u)(1-x_d) - (x_u+x_d-1) \cdot 1/z}{(1-x_u+1/z)^2} \right]. \end{aligned} \quad (6.18)$$

This integral is similar to those we encountered in Chapter 4, hence we once again substitute $x_u = x$, $x_d = 1 - vx$, with Jacobian x . The integral evaluates to

$$H(Q^2) = \frac{1}{(4\pi)^3} N_C e_u^2 (eg)^2 (2 + g_u^2 + g_d^2) Q^2 \left[-\frac{7}{4} - \frac{5}{2z} + \left(\frac{1}{2} + \frac{3}{z} + \frac{5}{2z^2} \right) \ln(1+z) \right]. \quad (6.19)$$

This result can be interpreted as the decay rate of a virtual photon into an $u\bar{d}$ -quark pair and a W^- gauge boson (through the specific channel we have studied) times the energy of the photon. In order to consider a more definite observable, we connect our result to electron-positron annihilation using Eqs. (4.15), (4.20) and (4.22). The ratio of the bremsstrahlung correction to tree-level u quark production becomes

$$\begin{aligned} R_{\text{EQT}} &= \frac{\sigma(e^+e^- \rightarrow \gamma^* \rightarrow u\bar{d}W^-)}{\sigma(e^+e^- \rightarrow \gamma^* \rightarrow u\bar{u})} \\ &= \frac{\alpha_W}{2} (2 + g_u^2 + g_d^2) \left[-\frac{7}{4} - \frac{5}{2z} + \left(\frac{1}{2} + \frac{3}{z} + \frac{5}{2z^2} \right) \ln(1+z) \right], \end{aligned} \quad (6.20)$$

where $\alpha_W \equiv g^2/(4\pi)^2$. Since the EQT was used to obtain this result, it is only valid for large momentum transfer, in particular up to corrections of $\mathcal{O}(1/z)$. We note in passing that the same result as Eq. (6.19) is found if we consider W^+ -bremsstrahlung, where a transverse W^+ boson and the corresponding Goldstone boson is emitted from the u -quark, except for an exchange of e_u with e_d .

Unpolarised W boson

We include a calculation where the W boson has both transverse and longitudinal degrees of freedom for comparison. Figure 6.1 displays the Feynman diagram, and the calculation mirrors that for the transverse W boson except for the polarisation sum. We can copy the result from Eq. (6.6), while adding the appropriate polarisation tensor,

$$\eta_{\mu\nu} H_W^{\mu\nu} = -\frac{N_C e_u^2 (eg)^2}{8} \frac{1}{[2(p_d \cdot k) + m_W^2]^2} \text{Tr} \left\{ \not{p}_u \Gamma^{\mu\rho} \not{p}_d \bar{\Gamma}_\mu^\sigma \right\} \mathcal{P}_{\rho\sigma}, \quad (6.21)$$

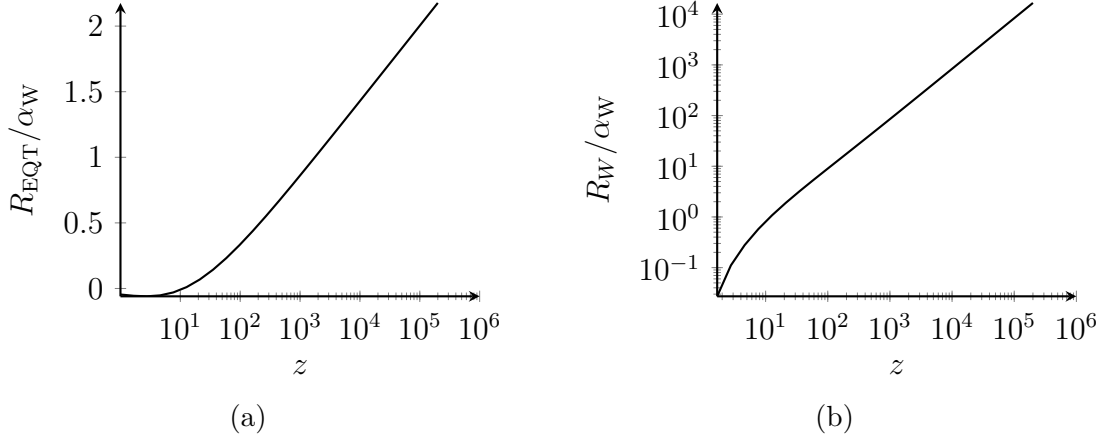


Figure 6.3: Ratio of W -bremsstrahlung correction to the tree-level process of electron-positron annihilation using (a) the EQT, (b) unpolarised W emission.

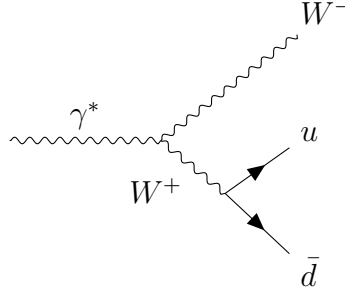


Figure 6.4: Internal bremsstrahlung contribution to $\gamma^* \rightarrow u\bar{d}W^-$ at order $\mathcal{O}(\alpha_W)$.

where $\mathcal{P}_{\rho\sigma}$ is given in Eq. (6.3). Evaluating the trace and contracting it with the polarisation tensor yields

$$\begin{aligned} \eta_{\mu\nu} H_W^{\mu\nu} &= \frac{2N_C e_u^2 (eg)^2}{[2(p_d \cdot k) + m_W^2]^2} \\ &\times \left[m_W^2 (p_u \cdot p_d) - 4(p_u \cdot k)(p_d \cdot k) - 4(p_u \cdot p_d)(p_d \cdot k) - \frac{4}{m_W^2} (p_u \cdot p_d)(p_d \cdot k)^2 \right]. \end{aligned} \quad (6.22)$$

We integrate this expression over available phase space in the same way as in the previous paragraph. The result is

$$H(Q^2) = \frac{1}{(4\pi)^3} N_C e_u^2 (eg)^2 Q^2 z \left[\frac{1}{6} - \frac{21}{6z} - \frac{5}{z^2} + \left(\frac{1}{z} + \frac{6}{z^2} + \frac{5}{z^3} \right) \ln(1+z) \right], \quad (6.23)$$

where $z = Q^2/m_W^2$. Hence, we find in this case the bremsstrahlung-to-tree-level ratio to be

$$R_W = \frac{\alpha_W}{2} z \left[\frac{1}{6} - \frac{21}{6z} - \frac{5}{z^2} + \left(\frac{1}{z} + \frac{6}{z^2} + \frac{5}{z^3} \right) \ln(1+z) \right]. \quad (6.24)$$

We note that the process studied in this section is similar to that examined in Ref. [29], indeed, a quick investigation shows that the momentum dependence in their Eq. (5) is equivalent to our Eq. (6.22). Our ratio has the same z -dependence in the high-energy limit as them, except for the overall factor which is attributed to the difference in the specific models considered.

6.2 Discussion

We end this chapter by comparing the results obtained using EQT with those found for unpolarised W emission, as well as discussing various properties of both results.

In Fig. 6.3, the ratios R_{EQT} (setting $g_u = g_d = 0$) and R_W are plotted as functions of the momentum transfer $z = Q^2/m_W^2$. It is apparent that the latter grows considerably faster; specifically we have $R_W \propto z$ while $R_{\text{EQT}} \propto \ln(z)$ for large z . Since the Goldstone couplings g_u and g_d to fermion lines are proportional to the vanishing masses of the light fermions, we have $g_u^2, g_d^2 \ll 1$ and the Goldstone contribution to R_{EQT} can be neglected. Thus, R_{EQT} incorporate the energy dependence of emission of a transverse gauge boson, and consequently the rapidly increasing cross section for an unpolarised gauge boson can be ascribed to its longitudinal component. The large dissimilarity between the emission of a longitudinal gauge boson and the corresponding Goldstone boson is ostensibly in violation of the EQT.

However, there is an issue with the total cross section $\sigma(e^+e^- \rightarrow u\bar{d}W^-)$ for the unpolarised W boson. For $z \gg 1$ it is constant, while unitarity demands a $1/z$ -dependence. The resolution to the problem is that we have ignored a diagram contributing to the process at order $\mathcal{O}(\alpha_W)$ — the internal bremsstrahlung sub-process displayed in Fig. 6.4, and the leading order contributions in both sub-processes cancel. In fact, this cancellation is required by the EQT. Using Eq. (6.19), we find that the cross section $\sigma(e^+e^- \rightarrow u\bar{d}\varphi^-)$ has the proper behaviour at large energies: It decreases as $1/z$ for increasing z , as expected for scalar emission. By the EQT, emission of a longitudinal massive gauge boson must have the same behaviour when all sub-processes are included. Moreover, the statement can be extended further: Theories including massive vector bosons which are renormalisable and have the appropriate high-energy behaviour required by unitarity, are equivalent to spontaneously broken gauge theories by field transformations. This is proven systematically for a large class of Lagrangians in Ref. [24].

It is also interesting to view the obtained ratios in terms of the infrared singularities we encountered in Chapter 4. If we let the mass of the emitted boson go to zero, $z \rightarrow \infty$ and the ratio R_{EQT} diverges logarithmically. Going back to Eq. (6.17), it is

apparent that the expression diverges for $x_u \rightarrow 1$ when $m_W = 0$, and we therefore associate the logarithmic factor with a soft divergence. One can also see this by considering splitting functions associated with the branching of a quark into a quark and a weak gauge boson, similar to the Altarelli-Parisi splitting functions of QCD [89]. The relevant splitting functions for the GSW model are derived in Ref. [90], which in the high-energy limit show a soft singularity for both transverse and longitudinal weak gauge bosons.

7 Summary and outlook

In this thesis, we have studied applications of the Goldstone boson equivalence theorem to decay rate and cross section computations. We have seen examples of how the broken gauge theory structure of electroweak interactions lead to substantial and consistent properties of physical observables. In addition to being interesting by itself, such considerations may be of value to indirect searches of dark matter, where the significance of electroweak corrections have widely been recognised.

After a brief review of the current knowledge of dark matter, we went on to introduce the theoretical foundation of our work. In particular, the equivalence theorem was presented. Following this, we reproduced the standard computation of the total cross section of electron-positron annihilation at next-to-leading order in QCD. By defining a sufficiently inclusive observable, and using dimensional regularization to safely manipulate the infrared infinities, we demonstrated how the singularities cancel out at that order in perturbation theory. The cancellation of infrared singularities is guaranteed by the Kinoshita-Lee-Nauenberg theorem for suitably defined observables in any quantum field theory.

We proceeded to the case of massive gauge bosons, and considered Higgs decay to W bosons. Four approaches were used, each illuminating noteworthy features of the underlying theory. In the unitary gauge, the degrees of freedom of the gauge boson as well as the particle spectrum are entirely physical, while in the Feynman-'t Hooft gauge, unphysical particles are introduced to cancel the unphysical degrees of freedom of the gauge boson. The equivalence of the two schemes are required by gauge invariance. In the high-energy limit, the equivalence theorem is applicable and shows that the longitudinal component is dominant. Finally, unitarity implies that the imaginary part of the self-energy correspond to the decay rate times the mass.

Next, we examined W bremsstrahlung in a specific process of quark production and computed the cross section ratio to the corresponding tree-level process. Performing the calculation using the equivalence theorem, we found that contribution from the emission of a Goldstone boson is negligible due to the coupling being proportional to the vanishing mass of the quark. However, a calculation of unpolarised emission yields a dominant, unitarity-violating contribution from the longitudinal component of the emitted gauge boson. The resolution of the apparent problem is that a cancellation of the leading contributions from all sub-processes at next-to-leading order must occur, necessiated by the equivalence theorem. The fact that the massive gauge bosons emerge in a broken gauge theory, implies that they have the appropriate high-energy behaviour, and this property is intrinsic of the scalar Goldstone bosons. Lastly, we

noted that the logarithmic enhancement of the total cross sections can be associated with soft divergences.

One may connect our last result to dark matter annihilation, if the initial state is replaced with a dark matter pair, and the virtual particle is exchanged with a Z boson, Higgs boson or some beyond-the-SM particle. The dark matter model may be specified carefully, for example within the framework of supersymmetry, or one may postulate a broader model to attempt to constrain the properties of the dark matter particle. Due to the generality of our considerations, they should still apply for such models.

Appendix A

Mathematical conventions and formulae

Mathematical conventions

We typically follow the common conventions of quantum field theory.

Four-vectors are denoted in italics, while spatial vectors are typeset in roman with boldface. For example, we have $k = (k^0, \mathbf{k})$. We use the Feynman slash for contraction of a four-vector and a Dirac matrix, $\not{A} = A_\mu \gamma^\mu$. For s-channel processes, we use Q for the momentum transfer, with $Q^2 = s$. Complex and Hermitian (adjoint) conjugation of operators are denoted A^* and A^\dagger , respectively. We also use the abbreviation h.c. for Hermitian conjugate.

Spacetime indices are labeled by Greek letters: μ, ν etc. Indices a, b, c typically refer to different generators of a gauge symmetry group, while i, j, k are usually indices in colour or isospin space. We use a Minkowski metric with signature

$$\eta^{\mu\nu} = \text{diag}(1, -1, -1, -1). \quad (\text{A.1})$$

Repeated indices are summed over. Finally, we use natural units, $c = \hbar = 1$.

Euler's Gamma and Beta functions

The Euler Gamma function is defined by the integral

$$\Gamma(z) = \int_0^\infty dt t^{z-1} e^{-t}, \quad \Re\{z\} > 0, \quad (\text{A.2})$$

which converges absolutely. Using integration by parts, one can confirm the identity

$$\Gamma(z+1) = z\Gamma(z), \quad (\text{A.3})$$

and hence we have $\Gamma(z) = (z-1)!$ for integer z . By analytic continuation, the Gamma function can be extended to all complex numbers, except for $z = 0, -1, -2, \dots$ where it has simple poles. Expanding the function around 1 yields

$$\Gamma(1+\epsilon) = 1 - \gamma_E \epsilon + \left(\frac{\pi^2}{12} + \frac{\gamma_E^2}{2} \right) \epsilon^2 + \mathcal{O}(\epsilon^3), \quad (\text{A.4})$$

where $\gamma_E = 0.577\,215\,664\dots$ is the Euler-Mascheroni constant.

The related Beta function is defined as

$$B(a, b) = \int_0^1 dt t^{a-1}(1-t)^{b-1}, \quad \Re\{a, b\} > 0. \quad (\text{A.5})$$

It can be shown (see e.g. Ref. [81, App. A3]) that

$$B(a, b) = \frac{\Gamma(a)\Gamma(b)}{\Gamma(a+b)}, \quad (\text{A.6})$$

which we use frequently.

Scalar integrals. We need a particular class of d -dimensional integrals when working in DR. The following result is not derived here, but cited from Ref. [2, p. 827]:

$$\int \frac{d^d k}{(2\pi)^d} \frac{k^{2a}}{(k^2 - \Delta)^b} = i \frac{(-1)^{a-b}}{(4\pi)^{d/2}} \frac{1}{\Delta^{b-a-d/2}} \frac{\Gamma(a+d/2)\Gamma(b-a-d/2)}{\Gamma(b)\Gamma(d/2)}. \quad (\text{A.7})$$

Diracology

The Dirac matrices γ^μ are defined by the Clifford algebra

$$\{\gamma^\mu, \gamma^\nu\} = 2\eta^{\mu\nu} \mathbf{1}. \quad (\text{A.8})$$

We impose the conditions $(\gamma^0)^\dagger = \gamma^0$ and $(\gamma^i)^\dagger = -\gamma^i$, which can be combined to read $(\gamma^\mu)^\dagger = \gamma^0 \gamma^\mu \gamma^0$. One additionally defines the fifth Dirac matrix,

$$\gamma^5 \equiv i\gamma^0 \gamma^1 \gamma^2 \gamma^3 \quad (\text{A.9})$$

which is Hermitian, anticommutes with the other Dirac matrices and satisfies $(\gamma^5)^2 = \mathbf{1}$.

Traces for $d = 4$. We list some useful trace relations in four dimensions:

- Traces over an odd number of Dirac matrices vanish, and also

$$\text{Tr} \{\gamma^5\} = \text{Tr} \{\gamma^\mu \gamma^\nu \gamma^5\} = 0. \quad (\text{A.10})$$

- The simplest non-zero traces are

$$\text{Tr} \{\gamma^\mu \gamma^\nu\} = 4\eta^{\mu\nu}, \quad (\text{A.11a})$$

$$\text{Tr} \{\gamma^\mu \gamma^\nu \gamma^\rho \gamma^\sigma\} = 4[\eta^{\mu\nu}\eta^{\rho\sigma} + \eta^{\mu\sigma}\eta^{\nu\rho} - \eta^{\mu\rho}\eta^{\nu\sigma}], \quad (\text{A.11b})$$

$$\text{Tr} \{\gamma^5 \gamma^\mu \gamma^\nu \gamma^\rho \gamma^\sigma\} = 4i\epsilon^{\mu\nu\rho\sigma}, \quad (\text{A.11c})$$

where the antisymmetric tensor is defined such that $\epsilon_{0123} = -\epsilon^{0123} = 1$.

- Some contraction identities are

$$\gamma^\mu \gamma_\mu = 4, \quad \gamma^\mu \not{a} \gamma_\mu = -2\not{a} \quad \gamma^\mu \not{a} \not{b} \gamma_\mu = 4(a \cdot b). \quad (\text{A.12})$$

Traces for arbitrary d . In the general case of d dimensions, the same Clifford algebra $\{\gamma^\mu, \gamma^\nu\} = 2\eta^{\mu\nu}\mathbf{1}_d$, and linearity and cyclicity of the trace hold. We have $\eta^\mu{}_\mu = d$, and the trace of the identity can be defined as any well-behaved function satisfying $f(4) = 4$. The simplest choice is $\text{Tr}\{\mathbf{1}_d\} = f(d) = 4$, then the relations in Eqs. (A.11a) and (A.11b) remain unchanged. The contraction identities in Eq. (A.12) become in $d = 4 - 2\epsilon$ dimensions

$$\gamma^\mu\gamma_\mu = d = 4 - 2\epsilon, \quad \gamma^\mu\cancel{\not{a}}\gamma_\mu = -2(1 - \epsilon)\cancel{a}, \quad \gamma^\mu\cancel{\not{a}}\cancel{\not{b}}\gamma_\mu = 4(a \cdot b)\mathbf{1}_d + 2\epsilon\cancel{a}\cancel{b}. \quad (\text{A.13})$$

The generalisation of γ^5 to d dimensions is not obvious, and since we do not encounter the fifth Dirac matrix when using dimensional regularization in this text, we do not discuss it.

Appendix B

Feynman rules

We present a selection of the Feynman rules of the Standard Model (SM), including Goldstone bosons and ghosts. Only the vertices used in calculations in the text are included, a full review of all the Feynman rules of the SM can be found in e.g. Ref. [91].

We will label the momenta of scalars and fermions as p , while k labels the momentum of gauge bosons. The electric charge (in units of e) and weak isospin of fermions are denoted Q and T^3 , respectively. Furthermore, $P_L = (1 - \gamma^5)/2$ and $P_R = (1 + \gamma^5)/2$ are the spinor projection operators.

Propagators.

$$\text{---}\xrightarrow{f}\text{---} = iS_F(p) = \frac{i(\not{p} + m)}{p^2 - m^2 + i\epsilon} \quad (\text{B.1})$$

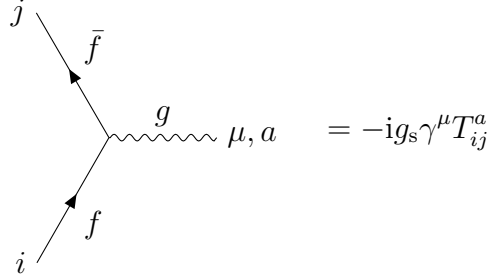
$$\mu \text{---}\overset{\gamma}{\text{---}}\nu = \frac{i}{k^2 + i\epsilon} \left(-\eta^{\mu\nu} + (1 - \xi_\gamma) \frac{k^\mu k^\nu}{k^2} \right) \quad (\text{B.2})$$

$$\mu, a \text{---}\overset{g}{\text{---}}\nu, b = \frac{i\delta_{ab}}{k^2 + i\epsilon} \left(-\eta^{\mu\nu} + (1 - \xi_G) \frac{k^\mu k^\nu}{k^2} \right) \quad (\text{B.3})$$

$$\mu \text{---}\overset{W^\pm}{\text{---}}\nu = \frac{i}{k^2 - m_W^2 + i\epsilon} \left(-\eta^{\mu\nu} + (1 - \xi_W) \frac{k^\mu k^\nu}{k^2 - \xi_W m_W^2} \right) \quad (\text{B.4})$$

$$\mu \text{---}\overset{Z}{\text{---}}\nu = \frac{i}{k^2 - m_Z^2 + i\epsilon} \left(-\eta^{\mu\nu} + (1 - \xi_Z) \frac{k^\mu k^\nu}{k^2 - \xi_Z m_Z^2} \right) \quad (\text{B.5})$$

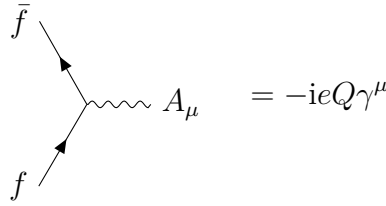
Fermion-gluon interaction.



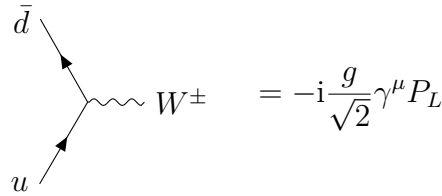
$$= -ig_s \gamma^\mu T_{ij}^a, \quad (\text{B.6})$$

where T^a are the generators of the SU(3) gauge group in QCD.

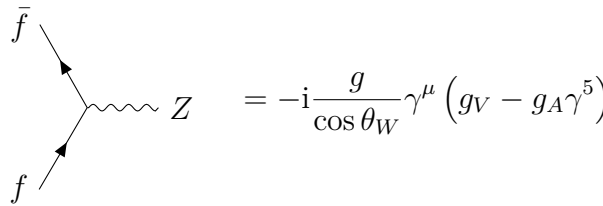
Fermion-electroweak gauge boson interactions.



$$= -ieQ\gamma^\mu \quad (\text{B.7})$$



$$= -i\frac{g}{\sqrt{2}}\gamma^\mu P_L \quad (\text{B.8})$$



$$= -i\frac{g}{\cos\theta_W}\gamma^\mu (g_V - g_A\gamma^5) \quad (\text{B.9})$$

Here, we have defined

$$g_V = \frac{1}{2}T^3 - Q\sin^2\theta_W \quad \text{and} \quad g_A = \frac{1}{2}T^3. \quad (\text{B.10})$$

Ghost-Higgs interaction.

$$\begin{array}{c}
 c_{\mp} \\
 \text{---} \nearrow \\
 \text{---} \\
 \text{---} \searrow \\
 c_{\pm}
 \end{array}
 h = -i \frac{g}{2} \xi_W m_W \quad (\text{B.17})$$

Here, the arrows indicate particle/antiparticle.

Appendix C

Kinematics of scattering and decay

Cross sections from scattering events and decay rates are natural quantities to measure in experiments. In this appendix, we relate matrix elements to cross sections and decay rates. The general expressions for these quantities are presented, and we derive phase space integrals in dimensional regularization for two and three outgoing particles.

Particle decays

Consider a particle with mass M decaying into n particles in the rest frame of the decaying particle. The decay rate is given by [92]

$$d\Gamma = \frac{1}{2M} |\mathcal{M}|^2 d\Phi_n, \quad (\text{C.1})$$

where \mathcal{M} is the Feynman amplitude and $d\Phi_n$ is an infinitesimal element of n -body phase space:

$$d\Phi_n = (2\pi)^4 \delta^{(4)}\left(Q - \sum_{i=1}^n p_i\right) \prod_{i=1}^n \frac{d^3 p_i}{(2\pi)^3} \frac{1}{2E_i}. \quad (\text{C.2})$$

In this expression, Q is the four-momentum of the decaying particle, while p_i is the four-momentum of outgoing particle i . The overall delta function establishes momentum conservation.

An important special case is decay into two particles. It can be shown that the 2-body phase space in the CoM frame is [78, App. 5]

$$d\Phi_2 = \frac{1}{16\pi^2} \frac{|\mathbf{p}|}{E_{\text{CM}}} d\Omega, \quad (\text{C.3})$$

where $|\mathbf{p}|$ is the magnitude of the spacial momentum of either outgoing particle. Thus, the decay rate into two particles is

$$d\Gamma = \frac{1}{32\pi^2} \frac{|\mathbf{p}|}{M^2} |\mathcal{M}|^2 d\Omega \quad (\text{C.4})$$

in the rest frame of the decaying particle.

Cross sections

The differential cross section for scattering into a differential volume in n -body phase space $d\Phi_n$ is given by [92]

$$d\sigma = \frac{1}{4I} |\mathcal{M}|^2 d\Phi_n, \quad (\text{C.5})$$

where \mathcal{M} is the Feynman amplitude, and I is the incoming flux factor:

$$I = \sqrt{(p_1 \cdot p_2)^2 - m_1^2 m_2^2}. \quad (\text{C.6})$$

Here, p_1 and p_2 are the momenta of the two scattering particles. In the CoM frame, the flux factor is

$$I = |\mathbf{p}_1| \sqrt{s}, \quad (\text{C.7})$$

where $s \equiv (p_1 + p_2)^2$ is a Mandelstam invariant [92]. Note that $|\mathbf{p}_1| = |\mathbf{p}_2|$ in this frame.

Using Eqs. (C.3) and (C.7), we find the differential cross section for $2 \rightarrow 2$ scattering processes,

$$d\sigma = \frac{1}{64\pi^2 s} \frac{|\mathbf{p}_f|}{|\mathbf{p}_i|} |\mathcal{M}|^2 d\Omega. \quad (\text{C.8})$$

Phase space in d dimensions

The generalisation of Eq. (C.2) to d dimensions is

$$d\Phi_n^{(d)} = (2\pi)^d \delta^{(d)} \left(Q - \sum_{i=1}^n p_i \right) \prod_{i=1}^n \frac{d^{d-1} p_i}{(2\pi)^{d-1}} \frac{1}{2E_i}. \quad (\text{C.9})$$

We derive specific expressions for the integrated phase spaces in the case of $n = 2$ and $n = 3$ in the following paragraphs.

Two-body phase space. For the case of two outgoing particles, the differential phase space is

$$d\Phi_2^{(d)} = (2\pi)^{(d)} \delta^{(d)}(Q - p_1 - p_2) \frac{d^{d-1} p_1}{(2\pi)^{d-1}} \frac{1}{2E_1} \frac{d^{d-1} p_2}{(2\pi)^{d-1}} \frac{1}{2E_2}. \quad (\text{C.10})$$

We consider the phase space integral over some function $f(\mathbf{p}_1, \mathbf{p}_2)$,

$$I = \int d\Phi_2^{(d)} f(\mathbf{p}_1, \mathbf{p}_2) = \frac{1}{4(2\pi)^{d-2}} \int \frac{d^{d-1} p_1}{E_1} \frac{d^{d-1} p_2}{E_2} \delta^{(d)}(Q - p_1 - p_2) f(\mathbf{p}_1, \mathbf{p}_2). \quad (\text{C.11})$$

First, we integrate over $d^{d-1} p_2$ using the momentum delta function, and obtain

$$I = \frac{1}{4(2\pi)^{d-2}} \int d^{d-1} p_1 \frac{f(\mathbf{p}_1, \mathbf{Q} - \mathbf{p}_1)}{E_1 E_2} \delta(Q^0 - E_1 - E_2)$$

where now E_2 is a function of \mathbf{p}_1 : $E_2^2 = (\mathbf{Q} - \mathbf{p}_1)^2 + m_2^2$. To proceed, we must make assumptions about the dependence of the function f on \mathbf{p}_1 . If the function is isotropic (for example after averaging over spins), we may perform the angular integration right away. Additionally, we specialise to the CoM frame where $\mathbf{Q} = 0$ and $Q^0 = \sqrt{Q^2} = \sqrt{s}$. Define $p = |\mathbf{p}_1|$, then

$$I = \frac{\Omega_{d-1}}{4(2\pi)^{d-2}} \int_0^\infty dp p^{d-2} \frac{f(p)}{E_1 E_2} \delta(\sqrt{s} - E_1 - E_2), \quad (\text{C.12})$$

where

$$\Omega_d = \frac{2\pi^{\frac{d}{2}}}{\Gamma\left(\frac{d}{2}\right)} \quad (\text{C.13})$$

is the surface area of the $(d-1)$ -sphere embedded in d dimensions [2]. Let the argument of the delta function be $g(p)$, then

$$g(p) = \sqrt{s} - E_1(p) - E_2(p), \quad (\text{C.14a})$$

$$g'(p) = -\frac{p}{E_1} - \frac{p}{E_2} = -p \left(\frac{\sqrt{s}}{E_1 E_2} \right). \quad (\text{C.14b})$$

Using that

$$\delta[g(p)] = \sum_i \frac{\delta(p - p_i^*)}{|g'(p_i^*)|}, \quad (\text{C.15})$$

where p_i^* are the solutions to $g(p) = 0$, we find

$$I = \frac{\Omega_{d-1}(p^*)^{d-3}}{4(2\pi)^{d-2}\sqrt{s}} f(p^*). \quad (\text{C.16})$$

Here, p^* is the positive solution to $g(p) = 0$. The constraint also has a negative solution, but it does not contribute since the integration is over positive p . Inserting Eq. (C.13) for the surface area, we obtain

$$I = \frac{1}{4\pi} \left(\frac{\pi}{p^2} \right)^\epsilon \frac{p}{\sqrt{s}} \frac{\Gamma(1-\epsilon)}{\Gamma(2-2\epsilon)} f(p) \quad (\text{C.17})$$

where $d = 4 - 2\epsilon$ and p is understood to be subject to constraints from energy-momentum conservation.

Three-body phase space. The phase space integral for three massive particles is rather complicated, so we simplify matters by considering massless particles. We follow Ref. [2, Sec. 20.A.3] and introduce momentum fractions

$$x_i = \frac{2p_i \cdot Q}{Q^2} \quad (\text{C.18})$$

where Q is the momentum transfer and $i = 1, 2, 3$. For massless particles, the fractions satisfy $\sum_i x_i = 2$ by four-momentum conservation. Moreover, in the CoM frame, we have $x_i = 2E_i/\sqrt{s} = 2|\mathbf{p}_i|/\sqrt{s}$. We consider the three-particle phase space integral over some function f :

$$I = \int d\Phi_3^{(d)} f(x_1, x_2, x_3). \quad (\text{C.19})$$

Inserting the momentum fractions into Eq. (C.9), and integrating over x_3 we get that

$$I = \left(\frac{\sqrt{s}}{4\pi}\right)^{2d-3} \frac{1}{(\sqrt{s})^3} \times \int dx_1 x_1^{d-2} d\Omega_{d-1} \int dx_2 x_2^{d-2} d\Omega_{d-1} \frac{\delta(x_1 + x_2 + x_3 - 2)}{x_1 x_2 x_3} f(x_1, x_2, x_3), \quad (\text{C.20})$$

where $d\Omega_{d-1}$ denotes the differential solid angle of the sphere in $d - 1$ dimensions. We cannot immediately perform the integral over the delta function, since x_3 has an implicit dependence on \mathbf{p}_1 and \mathbf{p}_2 :

$$x_3 = \frac{2E_3}{\sqrt{s}} = \frac{2}{\sqrt{s}} \sqrt{(\mathbf{p}_1 + \mathbf{p}_2)^2} = \sqrt{x_1^2 + x_2^2 - 2x_1 x_2 \cos \theta} \quad (\text{C.21})$$

where θ is the angle between \mathbf{p}_1 and \mathbf{p}_2 in the CoM frame. Hence, there is a θ -dependence in the integrand, and we must write out the differential solid angle related to one of the particles,

$$d\Omega_{d-1} = d\Omega_{d-2} \sin^{d-3} \theta d\theta = -d\Omega_{d-2} (1 - \cos^2 \theta)^{\frac{d-4}{2}} d(\cos \theta).$$

The remaining angular integration is trivial, so we have

$$I = \left(\frac{\sqrt{s}}{4\pi}\right)^{2d-3} \frac{\Omega_{d-2} \Omega_{d-1}}{(\sqrt{s})^3} \int dx_1 x_1^{d-3} \int dx_2 x_2^{d-3} \times \int_{-1}^1 d(\cos \theta) (1 - \cos^2 \theta)^{\frac{d-4}{2}} \frac{\delta(x_1 + x_2 + x_3 - 2)}{x_3} f(x_1, x_2, x_3). \quad (\text{C.22})$$

Having expressly collected the θ -dependence, we write it in terms of x_3 using Eq. (C.21),

$$\cos \theta = \frac{x_1^2 + x_2^2 - x_3^2}{2x_1 x_2}. \quad (\text{C.23a})$$

and

$$1 - \cos^2 \theta = \frac{4(1 - x_1)(1 - x_2)(1 - x_3)}{x_1^2 x_2^2} \quad (\text{C.23b})$$

where $\sum_i x_i = 2$ was used. Inserting this and the definition of the surface area in Eq. (C.13), we obtain

$$I = \frac{s}{2(4\pi)^3} \left(\frac{4\pi}{s}\right)^\epsilon \frac{1}{\Gamma(2-2\epsilon)} \times \int_0^1 dx_1 \int_{1-x_1}^1 dx_2 [(1-x_1)(1-x_2)(1-x_3)]^\epsilon f(x_1, x_2, x_3). \quad (\text{C.24})$$

The four-momentum conservation $x_3 = 2 - x_1 - x_2$ is understood. Combined with $0 < x_i < 1$, the integration limits were determined. Furthermore, the dimension is parametrised as $d = 4 - 2\epsilon$. We note the four-dimensional ($\epsilon = 0$) limit of this result:

$$I_{d=4} = \frac{s}{2(4\pi)^3} \int_0^1 dx_1 \int_{1-x_1}^1 dx_2 f(x_1, x_2, x_3). \quad (\text{C.25})$$

Bibliography

- [1] Cosimo Bambi and Alexandre D. Dolgov. *Introduction to Particle Cosmology*. Springer, 2015. ISBN: 9783662480779.
- [2] Matthew D. Schwartz. *Quantum Field Theory and the Standard Model*. Cambridge University Press, 2014. ISBN: 9781107034730.
- [3] Tatsumi Aoyama et al. “Tenth-Order QED Contribution to the Electron $g-2$ and an Improved Value of the Fine Structure Constant”. In: *Phys. Rev. Lett.* 109 (2012), p. 111807.
- [4] D. Hanneke, S. Fogwell, and G. Gabrielse. “New Measurement of the Electron Magnetic Moment and the Fine Structure Constant”. In: *Phys. Rev. Lett.* 100 (2008), p. 120801.
- [5] G. Arnison et al. “Experimental Observation of Isolated Large Transverse Energy Electrons with Associated Missing Energy at $s^{*}(1/2) = 540\text{-GeV}$ ”. In: *Phys. Lett.* B122 (1983). [611(1983)], pp. 103–116.
- [6] G. Arnison et al. “Experimental Observation of Lepton Pairs of Invariant Mass Around $95\text{-GeV}/c^{*2}$ at the CERN SPS Collider”. In: *Phys. Lett.* B126 (1983). [7.55(1983)], pp. 398–410.
- [7] Georges Aad et al. “Observation of a new particle in the search for the Standard Model Higgs boson with the ATLAS detector at the LHC”. In: *Phys. Lett.* B716 (2012), pp. 1–29.
- [8] P. A. R. Ade et al. “Planck 2015 results. XIII. Cosmological parameters”. In: *Astron. Astrophys.* 594 (2016), A13.
- [9] Gerard Jungman, Marc Kamionkowski, and Kim Griest. “Supersymmetric dark matter”. In: *Phys. Rept.* 267 (1996), pp. 195–373.
- [10] Lars Bergström. “Nonbaryonic dark matter: Observational evidence and detection methods”. In: *Rept. Prog. Phys.* 63 (2000), p. 793.
- [11] Gianfranco Bertone, Dan Hooper, and Joseph Silk. “Particle dark matter: Evidence, candidates and constraints”. In: *Phys. Rept.* 405 (2005), pp. 279–390.
- [12] Jonathan L. Feng. “Dark Matter Candidates from Particle Physics and Methods of Detection”. In: *Ann. Rev. Astron. Astrophys.* 48 (2010), pp. 495–545.
- [13] Edmund J. Copeland, M. Sami, and Shinji Tsujikawa. “Dynamics of dark energy”. In: *Int. J. Mod. Phys.* D15 (2006), pp. 1753–1936.

- [14] Y. Fukuda et al. “Evidence for oscillation of atmospheric neutrinos”. In: *Phys. Rev. Lett.* 81 (1998), pp. 1562–1567.
- [15] Q. R. Ahmad et al. “Direct evidence for neutrino flavor transformation from neutral current interactions in the Sudbury Neutrino Observatory”. In: *Phys. Rev. Lett.* 89 (2002), p. 011301.
- [16] Eldad Gildener. “Gauge Symmetry Hierarchies”. In: *Phys. Rev.* D14 (1976), p. 1667.
- [17] Chen-Ning Yang and Robert L. Mills. “Conservation of Isotopic Spin and Isotopic Gauge Invariance”. In: *Phys. Rev.* 96 (1954). [,150(1954)], pp. 191–195.
- [18] S. L. Glashow. “Partial Symmetries of Weak Interactions”. In: *Nucl. Phys.* 22 (1961), pp. 579–588.
- [19] Abdus Salam and John Clive Ward. “Electromagnetic and weak interactions”. In: *Phys. Lett.* 13 (1964), pp. 168–171.
- [20] Steven Weinberg. “A Model of Leptons”. In: *Phys. Rev. Lett.* 19 (1967), pp. 1264–1266.
- [21] Peter W. Higgs. “Broken Symmetries and the Masses of Gauge Bosons”. In: *Phys. Rev. Lett.* 13 (1964). [,160(1964)], pp. 508–509.
- [22] F. Englert and R. Brout. “Broken Symmetry and the Mass of Gauge Vector Mesons”. In: *Phys. Rev. Lett.* 13 (1964). [,157(1964)], pp. 321–323.
- [23] G. S. Guralnik, C. R. Hagen, and T. W. B. Kibble. “Global Conservation Laws and Massless Particles”. In: *Phys. Rev. Lett.* 13 (1964). [,162(1964)], pp. 585–587.
- [24] John M. Cornwall, David N. Levin, and George Tiktopoulos. “Derivation of Gauge Invariance from High-Energy Unitarity Bounds on the S Matrix”. In: *Phys. Rev.* D10 (1974). [Erratum: *Phys. Rev.* D11,972(1975)], p. 1145.
- [25] Xue-lei Chen and Marc Kamionkowski. “Three body annihilation of neutralinos below two-body thresholds”. In: *JHEP* 07 (1998), p. 001.
- [26] V. Berezhinsky, M. Kachelriess, and S. Ostapchenko. “Electroweak jet cascading in the decay of superheavy particles”. In: *Phys. Rev. Lett.* 89 (2002), p. 171802.
- [27] M. Kachelriess and P. D. Serpico. “Model-independent dark matter annihilation bound from the diffuse γ ray flux”. In: *Phys. Rev.* D76 (2007), p. 063516.
- [28] Nicole F. Bell et al. “Electroweak Bremsstrahlung in Dark Matter Annihilation”. In: *Phys. Rev.* D78 (2008), p. 083540.
- [29] M. Kachelriess, P. D. Serpico, and M. Aa. Solberg. “On the role of electroweak bremsstrahlung for indirect dark matter signatures”. In: *Phys. Rev.* D80 (2009), p. 123533.

-
- [30] Nicole F. Bell et al. “Dark Matter Annihilation Signatures from Electroweak Bremsstrahlung”. In: *Phys. Rev.* D84 (2011), p. 103517.
- [31] Nicole F. Bell et al. “W/Z Bremsstrahlung as the Dominant Annihilation Channel for Dark Matter, Revisited”. In: *Phys. Lett.* B706 (2011), pp. 6–12.
- [32] Mathias Garny, Alejandro Ibarra, and Stefan Vogl. “Antiproton constraints on dark matter annihilations from internal electroweak bremsstrahlung”. In: *JCAP* 1107 (2011), p. 028.
- [33] Mathias Garny, Alejandro Ibarra, and Stefan Vogl. “Dark matter annihilations into two light fermions and one gauge boson: General analysis and antiproton constraints”. In: *JCAP* 1204 (2012), p. 033.
- [34] Torsten Bringmann et al. “Fermi LAT Search for Internal Bremsstrahlung Signatures from Dark Matter Annihilation”. In: *JCAP* 1207 (2012), p. 054.
- [35] Torsten Bringmann et al. “Electroweak and Higgs Boson Internal Bremsstrahlung: General considerations for Majorana dark matter annihilation and application to MSSM neutralinos”. In: *JHEP* 09 (2017), p. 041.
- [36] Paolo Ciafaloni et al. “Weak Corrections are Relevant for Dark Matter Indirect Detection”. In: *JCAP* 1103 (2011), p. 019.
- [37] Massimo Persic, Paolo Salucci, and Fulvio Stel. “The Universal rotation curve of spiral galaxies: 1. The Dark matter connection”. In: *Mon. Not. Roy. Astron. Soc.* 281 (1996), p. 27.
- [38] Matthias Bartelmann and Peter Schneider. “Weak gravitational lensing”. In: *Phys. Rept.* 340 (2001), pp. 291–472.
- [39] P. Schneider. “Introduction to Gravitational Lensing and Cosmology”. In: *Gravitational Lensing: Strong, Weak and Micro*. Berlin, Heidelberg: Springer Berlin Heidelberg, 2006, pp. 1–89. ISBN: 978-3-540-30310-7.
- [40] Douglas Clowe et al. “A direct empirical proof of the existence of dark matter”. In: *Astrophys. J.* 648 (2006), pp. L109–L113.
- [41] F. Zwicky. “Die Rotverschiebung von extragalaktischen Nebeln”. In: *Helv. Phys. Acta* 6 (1933). [Gen. Rel. Grav.41,207(2009)], pp. 110–127.
- [42] Wayne Hu and Scott Dodelson. “Cosmic microwave background anisotropies”. In: *Ann. Rev. Astron. Astrophys.* 40 (2002), pp. 171–216.
- [43] M. Milgrom. “A Modification of the Newtonian dynamics as a possible alternative to the hidden mass hypothesis”. In: *Astrophys. J.* 270 (1983), pp. 365–370.
- [44] C. Alcock et al. “The MACHO project: Microlensing results from 5.7 years of LMC observations”. In: *Astrophys. J.* 542 (2000), pp. 281–307.

- [45] P. Tisserand et al. “Limits on the Macho Content of the Galactic Halo from the EROS-2 Survey of the Magellanic Clouds”. In: *Astron. Astrophys.* 469 (2007), pp. 387–404.
- [46] Stephen P. Martin. “A Supersymmetry primer”. In: (1997). [Adv. Ser. Direct. High Energy Phys.18,1(1998)], pp. 1–98.
- [47] Scott Dodelson and Lawrence M. Widrow. “Sterile-neutrinos as dark matter”. In: *Phys. Rev. Lett.* 72 (1994), pp. 17–20.
- [48] Kalliopi Petraki and Alexander Kusenko. “Dark-matter sterile neutrinos in models with a gauge singlet in the Higgs sector”. In: *Phys. Rev.* D77 (2008), p. 065014.
- [49] Xiang-Dong Shi and George M. Fuller. “A New dark matter candidate: Non-thermal sterile neutrinos”. In: *Phys. Rev. Lett.* 82 (1999), pp. 2832–2835.
- [50] C. A. Baker et al. “An Improved experimental limit on the electric dipole moment of the neutron”. In: *Phys. Rev. Lett.* 97 (2006), p. 131801.
- [51] R. D. Peccei and Helen R. Quinn. “CP Conservation in the Presence of Instantons”. In: *Phys. Rev. Lett.* 38 (1977). [,328(1977)], pp. 1440–1443.
- [52] Frank Wilczek. “Problem of Strong p and t Invariance in the Presence of Instantons”. In: *Phys. Rev. Lett.* 40 (1978), pp. 279–282.
- [53] Steven Weinberg. “A New Light Boson?” In: *Phys. Rev. Lett.* 40 (1978), pp. 223–226.
- [54] Georg G. Raffelt. “Astrophysical Axion Bounds”. In: *Axions: Theory, Cosmology, and Experimental Searches*. Ed. by Markus Kuster, Georg Raffelt, and Berta Beltrán. Berlin, Heidelberg: Springer Berlin Heidelberg, 2008, pp. 51–71. ISBN: 978-3-540-73518-2.
- [55] Max Tegmark et al. “Dimensionless constants, cosmology and other dark matters”. In: *Phys. Rev.* D73 (2006), p. 023505.
- [56] Aous A. Abdo et al. “Measurement of the Cosmic Ray e+ plus e- spectrum from 20 GeV to 1 TeV with the Fermi Large Area Telescope”. In: *Phys. Rev. Lett.* 102 (2009), p. 181101.
- [57] Oscar Adriani et al. “An anomalous positron abundance in cosmic rays with energies 1.5-100 GeV”. In: *Nature* 458 (2009), pp. 607–609.
- [58] Brian Feldstein et al. “Neutrinos at IceCube from Heavy Decaying Dark Matter”. In: *Phys. Rev.* D88.1 (2013), p. 015004.
- [59] David N. Spergel. “The Motion of the Earth and the Detection of Wimps”. In: *Phys. Rev.* D37 (1988), p. 1353.
- [60] E. Aprile et al. “First Dark Matter Search Results from the XENON1T Experiment”. In: *Phys. Rev. Lett.* 119.18 (2017), p. 181301.

-
- [61] E. Armengaud et al. “Final results of the EDELWEISS-II WIMP search using a 4-kg array of cryogenic germanium detectors with interleaved electrodes”. In: *Phys. Lett.* B702 (2011), pp. 329–335.
- [62] R. Agnese et al. “Search for Low-Mass Weakly Interacting Massive Particles with SuperCDMS”. In: *Phys. Rev. Lett.* 112.24 (2014), p. 241302.
- [63] R. Bernabei et al. “First results from DAMA/LIBRA and the combined results with DAMA/NaI”. In: *Eur. Phys. J.* C56 (2008), pp. 333–355.
- [64] John F. Beacom, Nicole F. Bell, and Gianfranco Bertone. “Gamma-ray constraint on Galactic positron production by MeV dark matter”. In: *Phys. Rev. Lett.* 94 (2005), p. 171301.
- [65] Lars Bergstrom et al. “Gamma rays from Kaluza-Klein dark matter”. In: *Phys. Rev. Lett.* 94 (2005), p. 131301.
- [66] Torsten Bringmann, Lars Bergstrom, and Joakim Edsjo. “New Gamma-Ray Contributions to Supersymmetric Dark Matter Annihilation”. In: *JHEP* 01 (2008), p. 049.
- [67] Nima Arkani-Hamed et al. “A Theory of Dark Matter”. In: *Phys. Rev.* D79 (2009), p. 015014.
- [68] Marco Cirelli et al. “Model-independent implications of the e^+ -, anti-proton cosmic ray spectra on properties of Dark Matter”. In: *Nucl. Phys.* B813 (2009). [Addendum: *Nucl. Phys.*B873,530(2013)], pp. 1–21.
- [69] Paolo Gondolo and Graciela Gelmini. “Cosmic abundances of stable particles: Improved analysis”. In: *Nucl. Phys.* B360 (1991), pp. 145–179.
- [70] Lars Bergstrom. “Radiative Processes in Dark Matter Photino Annihilation”. In: *Phys. Lett.* B225 (1989), pp. 372–380.
- [71] H. Fritzsch, Murray Gell-Mann, and H. Leutwyler. “Advantages of the Color Octet Gluon Picture”. In: *Phys. Lett.* 47B (1973), pp. 365–368.
- [72] D. J. Gross and Frank Wilczek. “Asymptotically Free Gauge Theories - I”. In: *Phys. Rev.* D8 (1973), pp. 3633–3652.
- [73] Steven Weinberg. “Nonabelian Gauge Theories of the Strong Interactions”. In: *Phys. Rev. Lett.* 31 (1973), pp. 494–497.
- [74] L. D. Faddeev and V. N. Popov. “Feynman Diagrams for the Yang-Mills Field”. In: *Phys. Lett.* B25 (1967). [325(1967)], pp. 29–30.
- [75] C. S. Wu et al. “Experimental Test of Parity Conservation in Beta Decay”. In: *Phys. Rev.* 105 (1957), pp. 1413–1414.
- [76] T. Nakano and K. Nishijima. “Charge Independence for V-particles”. In: *Prog. Theor. Phys.* 10 (1953), pp. 581–582.

- [77] M. Gell-Mann. “[The interpretation of the new particles as displaced charge multiplets](#)”. In: *Nuovo Cim.* 4.S2 (1956), pp. 848–866.
- [78] Michael E. Peskin and Daniel V. Schroeder. *An Introduction to quantum field theory*. Reading, USA: Addison-Wesley, 1995. ISBN: 9780201503975.
- [79] Benjamin W. Lee, C. Quigg, and H. B. Thacker. “[Weak Interactions at Very High-Energies: The Role of the Higgs Boson Mass](#)”. In: *Phys. Rev.* D16 (1977), p. 1519.
- [80] Michael S. Chanowitz and Mary K. Gaillard. “[The TeV Physics of Strongly Interacting W’s and Z’s](#)”. In: *Nucl. Phys.* B261 (1985), pp. 379–431.
- [81] Michael Kachelriess. *Quantum Fields*. Oxford Graduate Texts. Oxford University Press, 2017. ISBN: 9780198802877.
- [82] Günther Dissertori, I. G. Knowles, and Michael Schmelling. *Quantum Chromodynamics : High Energy Experiments and Theory*. International Series of Monographs on Physics Vol. 115. Clarendon Press, 2009. ISBN: 9780198505723.
- [83] Raymond Brock et al. “[Handbook of perturbative QCD: Version 1.0](#)”. In: *Rev. Mod. Phys.* 67 (1995), pp. 157–248.
- [84] Elliot Leader and Enrico Predazzi. “[A note on the implications of gauge invariance in QCD](#)”. In: *J. Phys.* G40 (2013), p. 075001.
- [85] Jan Kuipers et al. “FORM version 4.0”. In: *CoRR* abs/1203.6543 (2012).
- [86] T. Kinoshita. “[Mass singularities of Feynman amplitudes](#)”. In: *J. Math. Phys.* 3 (1962), pp. 650–677.
- [87] T. D. Lee and M. Nauenberg. “[Degenerate Systems and Mass Singularities](#)”. In: *Phys. Rev.* 133 (1964). [,25(1964)], B1549–B1562.
- [88] John F. Donoghue, Eugene Golowich, and Barry R. Holstein. *Dynamics of the Standard Model*. 2nd ed. Cambridge Monographs on Particle Physics, Nuclear Physics and Cosmology. Cambridge University Press, 2014.
- [89] Guido Altarelli and G. Parisi. “[Asymptotic Freedom in Parton Language](#)”. In: *Nucl. Phys.* B126 (1977), pp. 298–318.
- [90] Sally Dawson. “[The Effective W Approximation](#)”. In: *Nucl. Phys.* B249 (1985), pp. 42–60.
- [91] Jorge C. Romao and Joao P. Silva. “[A resource for signs and Feynman diagrams of the Standard Model](#)”. In: *Int. J. Mod. Phys.* A27 (2012), p. 1230025.
- [92] K. A. Olive et al. “[Review of Particle Physics](#)”. In: *Chin. Phys.* C38 (2014), p. 090001.